Institut für Nutzpflanzenwissenschaften und Ressourcenschutz (INRES)

der

Rheinischen Friedrich-Wilhelms-Universität Bonn

Molecular characterization of the maize (*Zea mays* L.) *AUXIN/INDOLE-3-ACETIC ACID* (*Aux/IAA*) gene family

Inaugural – Dissertation

zur

Erlangung des Grades

Doktorin der Agrarwissenschaften

(Dr. agr.)

der

Landwirtschaftlichen Fakultät

der

Rheinischen Friedrich-Wilhelms-Universität Bonn

von

Yvonne Ludwig

aus

Werder/Havel, Deutschland

2014

Referent: Prof. Dr. Frank Hochholdinger

Koreferent: Prof. Dr. Andreas Meyer

Tag der mündlichen Prüfung: 06.10.2014

Erscheinungsjahr: 2014

Content

Abbreviations

α-NAA	1-Naphthaleneacetic acid
AFB	Auxin signaling F-box protein
ARF	Auxin response factor
ASK1	Arabidopsis SKP1-like
Aux/IAA	*AUXIN/INDOLE-3-ACETIC ACID*
AuxRE	Auxin-responsive elements
BAR	BARWIN protein
bdl	*bodenlos*
BiFC	Bimolecular fluorescence complementation
BP1	Type I/II Phox and Bem1p
CoGe	Comparative Genomics software
CTD	C-terminal dimerization domain
CUL1	CULLIN1
DAPI	4,6-diamidino-2-phenylindole
EAR	ERF-associated amphiphilic repression motif
GAL4-DBD	GAL4-DNA binding domain
GFP	Green fluorescence protein
GH3	GRETCHEN HAGEN3
LSD1	LESIONS SIMULATING DISEASE RESISTANCE1
LUC	Luciferase
MCS	Multiple cloning site
MES	2-(N-Morpholino)ethanesulfonic acid
NLS	Nuclear localization signal
ocs	octopine synthase gene
ON	Overnight
Os	*Oryza sativa*
PEG	Polyethylene glycol
PKL	PICKLE
RT	Room temperature
RUB	RELATED TO UBIQUITIN protein
rul1	*rum1*-like
rum1	*rootless with undetectable meristem 1*
SAUR	SMALL AUXIN-UP RNA
Sb	*Sorghum bicolor*
SD	Standard deviation
Sl	*Solarium lycopersicum*
TIR1	TRANSPORT INHIBITOR RESPONSE1
TMV	Tobacco mosaic virus
TPL	TOPLESS
TPR	TPL-related protein
YFP	Yellow fluorescence protein

1 Zusammenfassung/Summary

1.1 Zusammenfassung

Dem Phytohormon Auxin ist ein wichtige Komponente der pflanzlichen Signaltransduktion. Als endogener Signalstoff steuert Auxin vielfältige Aspekte der pflanzlichen Entwicklung. Mitglieder der *AUXIN/INDOLE-3-ACETIC ACID* (*Aux/IAA*) Genfamilie spielen eine zentrale Rolle in der Auxin-Signaltransduktion.
In Mais kodiert das Gen *rum1* (*rootless with undetectable meristem 1*) das Aux/IAA Protein ZmIAA29, dem bislang als einzigem Aux/IAA Protein eine Rolle in der Entwicklung zugeschrieben werden konnte. Es kontrolliert die Initiation der embryonalen Seminalwurzeln und der postembryonalen Lateralwurzeln der Primärwurzel. Ausgehend von diesem Befund wurde in dieser Arbeit die *Aux/IAA* Genfamilie von Mais genauer charakterisiert.
Zu Beginn dieser Arbeit waren 31 *Aux/IAA* Gene im Maisgenom beschrieben. Eine Homologiesuche in der aktuellsten Annotation des Maisgenoms führte zur Identifizierung von drei weiteren *Aux*/*IAA* Genen (*ZmIAA32* – GRMZM2G366373, *ZmIAA33* – GRMZM2G359924 und *ZmIAA34* – GRMZM2G031615). Phylogenetische Analysen aller 34 Aux/IAA Proteine ergaben eine strukturelle Aufspaltung des Stammbaums in zwei Klassen aufgrund von Unterschieden der Aminosäuresequenz in der konservierten Domäne III. Insgesamt konnten durch Syntänievergleiche sieben paraloge *Aux/IAA* Paare bestimmt werden. Die *Aux*/*IAA* Gene zeigten unterschiedliche Expressionsmuster in verschiedenen Wurzeltypen. Im Durchschnitt war das Expressionsniveau der *Aux/IAA* Gene in den Kronwurzeln am höchsten, gefolgt von den Seminal- und Primärwurzeln. Die geringste Expression wurde in den Lateralwurzeln der Primärwurzel gemessen. Basierend auf den Ergebnissen der phylogenetischen Untersuchungen und der Expressionsanalysen wurden die *Aux*/*IAA* Gene *ZmIAA2*, *ZmIAA11*, *ZmIAA15*, *ZmIAA20* und *ZmIAA33* für die weitere funktionelle Charakterisierung ausgewählt. Alternative Varianten dieser Proteine wurden durch zielgerichtete Punktmutationen erzeugt, die dazu führten, dass in den Degron-Sequenzen der fünf Aux/IAA Proteine das primäre Prolin durch Serin und das sekundäre Prolin durch Leuzin ersetzt wurden. *Aux*/*IAA* Gene kodieren für kurzlebige Proteine, welche im Kern lokalisiert sind. Die gemessenen Halbwertszeiten der untersuchten wildtypischen Aux/IAA Proteine betrugen zwischen ~11 Minuten (ZmIAA2) und ~120 Minuten (ZmIAA15). Die Punktmutationen führten zu einer deutlichen Stabilisierung der Aux/IAA Proteine im Vergleich zu den Wildtypvarianten. Die Wildtyp- sowie die mutierten Proteine von ZmIAA2, ZmIAA11 und ZmIAA15 wurden ausschließlich im Kern nachgewiesen. Dagegen waren die Proteine ZmIAA20 und ZmIAA33 in Kern und Zytoplasma lokalisiert. Außerdem konnte gezeigt werden, dass alle *Aux/IAA* Kandidatengene als aktive Repressoren fungieren. Weiterhin konnte eine Wechselwirkung der fünf untersuchten Aux/IAA Proteine mit RUM1 gezeigt werden, jedoch interagierten nur ZmIAA15 und ZmIAA33 mit dessen Paralog RUL1.
Zusammenfassend konnte nachgewiesen werden, dass die untersuchten *Aux/IAA* Gene wurzel-, gewebe- und entwicklungsspezifische Expressionsmuster aufwiesen, darüber hinaus zeigten die von diesen Genen kodierten Proteine unterschiedliche Stabilitäten sowie eine unterschiedlich starke Repressoraktivität. Während alle fünf Aux/IAA Proteine im Kern lokalisiert waren, zeigten *ZmIAA20* und *ZmIAA33* zusätzlich Expression im Zytoplasma. Schließlich wurden spezifische Protein-Protein-Interaktionen der Aux/IAA Proteine mit RUM1 und RUL1 identifiziert.

1.2 Summary

The phytohormone auxin is an important molecular component in plant signal transduction. As an endogenous signaling molecule, auxin controls many aspects of plant development. Members of the *AUXIN/INDOLE-3-ACETIC ACID* (*Aux/IAA*) gene family play an important role in auxin signal transduction.

The *rum1* (*rootless with undetectable meristem 1*) gene encodes the Aux/IAA protein ZmIAA29, which is to date the only Aux/IAA member with an assigned function in plant development in maize. It controls the initiation of the embryonic seminal roots and post-embryonic lateral roots of the primary root. Based on the function of *rum1* in root development a comprehensive characterization of the *Aux/IAA* gene family was initiated in this study.

At the beginning of this study 31 *Aux/IAA* genes were known. A homology search for novel Aux/IAA sequences in the latest maize genome assembly version identified three unknown *Aux/IAA* genes (*ZmIAA32* - GRMZM2G366373, *ZmIAA33* – GRMZM2G359924, *ZmIAA34* – GRMZM2G031615). Phylogenetic reconstructions of the 34 Aux/IAA proteins revealed two classes of Aux/IAA proteins that can be distinguished by alterations in their domain III. Moreover, seven pairs of paralogous maize Aux/IAA proteins were discovered via syntenic comparisons. Comprehensive root-type and tissue-specific expression profiling revealed unique expression patterns of the diverse members of the gene family. The *Aux/IAA* genes displayed their highest expression in crown roots followed by seminal and primary roots. Lateral roots of the primary root displayed the lowest *Aux/IAA* expression level. Based on the results of the phylogenetic and expression studies five members of the maize *Aux/IAA* gene family, *ZmIAA2*, *ZmIAA11*, *ZmIAA15*, *ZmIAA20* and *ZmIAA33,* were functionally characterized. Alternative protein variants were generated via the introduction of specific point mutations in the degron sequence by substituting the first proline by serine or the second proline by leucine. In general, Aux/IAA proteins are short-lived and localized in the nucleus. The five Aux/IAA protein half-life times ranged between ~11 min (ZmIAA2) to ~120 min (ZmIAA15) while the mutated forms were more stable. Subcellular localization studies revealed that ZmIAA2, ZmIAA11 and ZmIAA15 and their mutated forms were exclusively localized in the nucleus, whereas ZmIAA20 and ZmIAA33 were detected in nucleus and cytoplasm. Furthermore, all five maize Aux/IAA proteins were acting as active repressors. In addition, interaction of RUM1 with all five Aux/IAA proteins was detected, but only ZmIAA15 and ZmIAA33 interacted with the RUM1 paralog RUL1.

In summary, the analyzed *Aux/IAA* genes displayed root-, tissue- and development specific expression patterns. Furthermore, the selected Aux/IAA proteins revealed different half-life times together with various activity of their repressor function. All five Aux/IAA proteins were localized in the nucleus; ZmIAA20 and ZmIAA33 were additionally expressed in the cytoplasm. Finally, specific protein interactions were identified between the selected Aux/IAA proteins with RUM1 and RUL1.

The results of this PhD thesis were published or are submitted for publication in the following articles:

Ludwig, Y., Zhang, Y., and Hochholdinger, F. (2013) The Maize (*Zea mays* L.) *AUXIN/INDOLE-3-ACETIC ACID* Gene Family: Phylogeny, Synteny, and Unique Root-Type and Tissue-Specific Expression Patterns during Development. *PLoS ONE* **8**, e78859

Own contribution: All experiments of this study were performed and interpreted by myself except the auxin treatment of primary roots which was performed by Dr. Yanxiang Zhang. Prof. Dr. Frank Hochholdinger conceived and coordinated the study and participated in drafting the manuscript.

Ludwig, Y., Berendzen, K. W., Xu, C., Piepho, H. P., Hochholdinger, F. (2014) Diversity of stability, localization, interaction and control of downstream gene activity in the maize Aux/IAA protein family. Submitted.

Own contribution: All experiments of this study were performed and interpreted by myself except the cloning of the Aux/IAA gene ZmIAA20 by Eva Husáková. Prof. Dr. Hans-Peter Piepho helped with the statistical analysis of the interaction experiments. Dr. Kenneth Berendzen supported cell sorting with the flow cytometer. Prof. Dr. Frank Hochholdinger conceived and coordinated the study and participated in drafting the manuscript.

2 Introduction

2.1 Maize as a model plant

While more than 50,000 plants are edible for humans, only three of them, wheat (*Triticum aestivum*), rice (*Oryza sativa*) and maize (*Zea mays*), provide around 60% of the human food energy intake (Food and Agriculture Organization of the United Nations, FAO, www.fao.org). Among those, maize provides the highest grain yield of all plants with ~870 million tons in 2012 (FAO). In addition to food and feed production, around 28% of the produced maize is used in the industrial sector (Deutsches Maiskomitee, www.maiskomitee.de). In particular maize starch is a valuable product, which is utilized to produce chemicals, drugs, paper and biogas (Deutsches Maiskomitee, www.maiskomitee.de). Besides its agronomic and industrial importance, maize is an important model for monocotyledonous plants. Its monoecious floral development with female (pistillate) and male (staminate) flowers situated on separate parts of the plant, made maize easily accessible for genetic analyses (Strable and Scanlon, 2009). Furthermore, transposable elements allow effective mutagenesis of the maize genes (McClintock, 1950). A vast collection of maize mutants was assembled over decades (Neuffer et al., 1997) and high-throughput mutagenesis programs such as TILLING (Targeting Induced Local Lesions IN Genomes) (Till et al., 2004) and maize-targeted mutagenesis (MTM) projects (Slotkin et al., 2003) continued generating new mutant phenotypes. Finally, the sequencing of the genome of the maize reference inbred line B73 (Schnable et al., 2009) facilitated cloning of genes identified by mutants and enabled functional genomic analyses.

2.2 Architecture of the maize root system

The unique architecture of the maize root system ensures nutrient and water uptake and anchorage of the plant in soil (Lynch, 1995; Aiken and Smucker, 1996). The structure of the maize root stock is determined by an endogenous genetic program (Hochholdinger et al., 2004a; Hochholdinger et al., 2005). However, this regulation is also influenced by flexible adaptations to environmental changes (Drew and Saker, 1975; McCully, 1999) and by interactions with the rhizosphere (Bais et al., 2006; Watt et al., 2006) which determine the plasticity of the maize root system. Morphology of the complex monocot maize root system is different from that of the dicot model plant *Arabidopsis thaliana*, displaying a simpler root system. The root system of maize is generally structured into embryonic primary and seminal roots and post-embryonic shoot borne roots (Hochholdinger et al., 2004a).

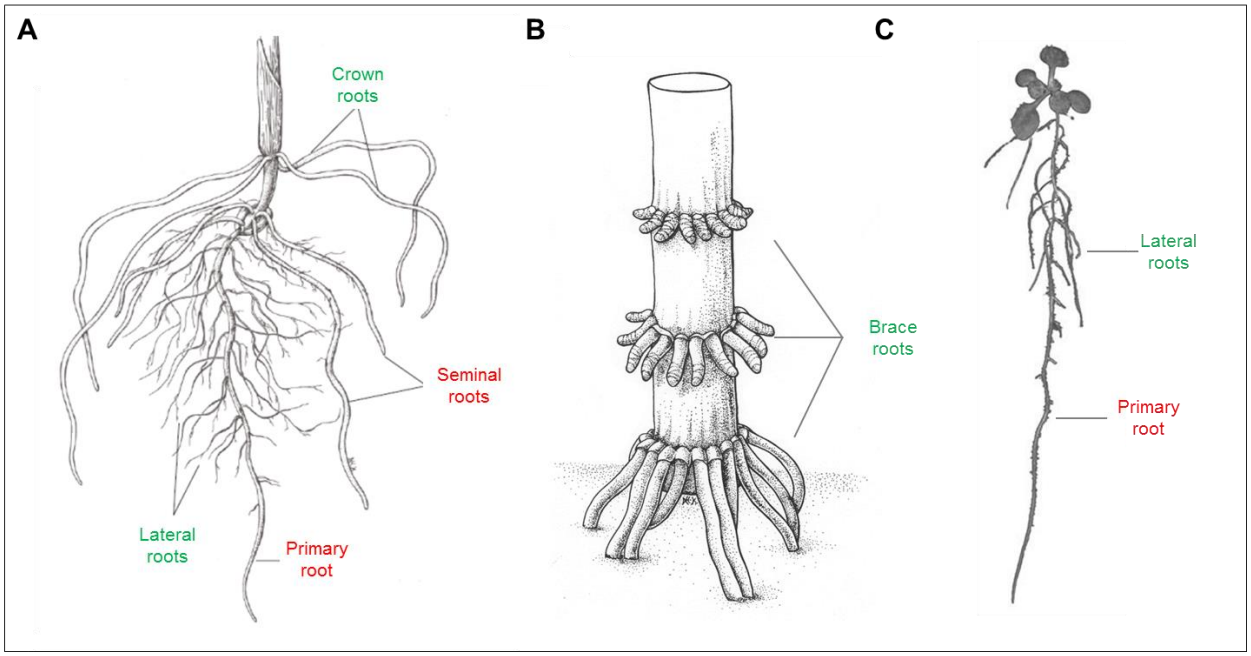

Figure 2.1 Architecture of the maize and *Arabidopsis* root systems (modified after Hochholdinger (2009) and http://www.bio.sci.osaka-u.ac.jp/~hirokazu.tanaka/toppage-EN.html). (A) Underground root structure of approximately 14-day-old seedling with embryonic primary and seminal roots, early post-embryonic crown root and late post-embryonic lateral root. (B) Aboveground shoot borne brace roots of around six weeks old plant which belongs to early embryonic root system. (C) Primary and lateral roots of a 14-day-old *Arabidopsis*. Red: embryonic roots, green: post-embryonic roots.

2.2.1 The embryonic root system of maize

The embryonic root system of a maize seedling consists of primary and seminal roots (Figure 2.1 A). As early as 10 to 15 days after pollination the primary root is visible in the embryo (Erdelska and Vidovencova, 1993). During the penetration of different tissues by the developing primary root the coleorhiza is generated at the proximal end of the newly formed primary root (Hochholdinger, 2009). At the basal pole of the seedling, the primary root emerges two to three days after germination (Hochholdinger et al., 2005). In contrast to the single primary root, a variable number of 0 to 13 seminal roots develop at the scutellar node of the maize seedling depending on its genetic background (Hochholdinger, 2009). Seminal roots develop in the embryo endogenously 22 to 40 days after pollination (Erdelska and Vidovencova, 1993). Around one week after germination, seminal roots appear at the scutellar node which is a differentiated structure that can be easily penetrated by the evolving seminal roots. Therefore seminal roots do not establish a coleorhiza (Hochholdinger et al., 2004a). In contrast, only a single primary root with its lateral roots (Figure 2.1 C), defines the root architecture of *Arabidopsis* which is established during the embryogenesis (Schiefelbein et al., 1997). In contrast to most maize genotypes, the embryonic

primary root of *Arabidopsis* plays an important role during the whole life cycle (Feldman, 1994). In some maize inbred lines the embryonic roots remain active during the whole life span of the plant and maintain and stabilize the adult plant, However, in other maize inbred lines the embryonic roots are functionally substituted by the shoot borne roots (Hochholdinger et al., 2004b).

2.2.2 The post-embryonic root system of maize

The main root types of adult maize plants are the shoot borne roots which are differentiated into underground crown roots (Figure 2.1 A) and aboveground brace roots (Figure 2.1 B) (Hochholdinger, 2009). Already 10 days after germination crown roots become visible, whereas brace roots only develop around six weeks after germination (Hochholdinger et al., 2004a). Shoot borne roots are organized in approximately six whorls of crown roots and two to three whorls of brace roots. The number of shoot borne roots per node increases at higher nodes (Hoppe et al., 1986). Similar to the embryonic root system, shoot borne roots are endogenously formed. The primordia of shoot-borne roots are located opposite to the collateral vascular bundles (Martin and Harris, 1976). Only the brace roots growing at the first two whorls are penetrating the soil and form lateral roots (Feldman, 1994). These lateral roots are also responsible for water and nutrient uptake and can interact with the soil surface (Hochholdinger et al., 2004a). Maize lateral roots (Figure 2.1 A) are defined as all roots that emerge from other roots. Therefore, lateral roots are formed at primary, seminal and shoot borne crown and brace roots (Esau, 1965). Lateral roots in maize are initiated from the pericycle and endodermal cells opposite of the phloem poles (Bell and McCully, 1970). In contrast, *Arabidopsis* lateral roots are initiated exclusively from pericycle cells (Péret et al., 2009). Based on their branching capacity (McCully and Canny, 1988; Varney and Canny, 1993) and the open late metaxylem the lateral roots mainly determine the water and nutrient uptake capacity of maize (Wang et al., 1994).

2.3 The phytohormone auxin

The phytohormone auxin is involved in various aspects of plant growth and development (Abel et al., 1995; Abel and Theologis, 1996). Major developmental process such as specification of apical cells or establishment of the root pole in embryogenesis are marked by dynamic patterns of auxin accumulation (Vanneste and Friml, 2009). Moreover, post-embryonic development of flowers, leaves or lateral roots are tightly regulated by auxin activity (Benková et al., 2003).

Precisely coordinated auxin maxima within the plant tissue are an important prerequisite for the auxin action (Tanaka et al., 2006). The regulation of auxin accumulation within single cells, cell complexes and its depletion is pivotal for auxin-mediated development (Sorefan et al., 2009).

Differential auxin distribution in organs, as a response to environmental stimuli such as light or gravity, can lead to differential growth resulting in bended organs like root or shoot (Vanneste and Friml, 2009). Increasing auxin accumulation at the lower side of roots or shoots is a result of gravistimulation and results in organ bending (Tanaka et al., 2006). In general, auxin accumulation inhibits root elongation, whereas it stimulates growth in shoots (Vanneste and Friml, 2009).

Auxin also plays an important role in shade avoidance. Neighboring plants are competing for sunlight whereby shade-induced stimuli trigger local auxin biosynthesis that results into stem elongation (Tao et al., 2008). Moreover, auxin is able to control the expression of genes (Estelle, 1992) which can trigger auxin-mediated transcription (Rogg et al., 2001).

2.4 Auxin Signaling

Interactions between *cis*-acting DNA sequence elements and *trans*-acting transcriptional regulators are necessary for the expression of hormone-responsive genes (Chapman and Estelle, 2009). Auxin-responsive promoter domains such as auxin-responsive elements (AuxRE) contain DNA-binding motifs which are required to bind transcription factors. Initially, a major auxin-responsive region was identified in the upstream regulatory section of the PsIAA4/5 promoter. The region is located between the nucleotides -150 and -325 relative to the transcriptional start site ATG in which auxin inducibility was attributed to two domains. Domain A has the motif 5´-(T/A)GTCCTA–3´ while domain B is located upstream of A, and contains the sequence 5´-ACATGGN -3´ upstream of motif 5´- TTCTC-3´ (Ulmasov et al., 1995; Ulmasov et al., 1997b). These motifs can repress an adjacent constitutive element which was demonstrated by analyses of native and synthetic promoters containing these sequence motifs (Ulmasov et al., 1995; Ulmasov et al., 1997b). Probably the variance of the canonical TGTCTC and its inverted sequence function as AuxRE and furthermore the variations of its derivatives may act to recruit different transcriptional factors (Chapman and Estelle, 2009).

The characterization of AuxRE resulted in the identification of auxin response factor 1 (ARF1) and other members of the ARF family, which can bind to tandem repeat AuxRE sequences and form dimers with other ARFs or dimers with repressive Aux/IAA proteins (Figure 2.3 and Ulmasov et al., 1997a, 1999). ARFs are nuclear proteins and consist of three domains. The first domain is the amino-terminal DNA-binding domain (DBD) which is embedded in a plant-specific B3-type transcription factor domain. The middle region of the ARF protein can either be glutamine rich and associated with transcriptional activation or proline rich and be associated with repression (Ulmasov et al., 1997a, 1999; Vert et al., 2008). The third domain is the C-terminal dimerization domain (CTD) which is required for auxin response and for the interaction with Aux/IAA proteins.

Moreover, the activity of ARFs is partly regulated through the interaction with Aux/IAA repressors (Chapman and Estelle, 2009). In various analyses it was demonstrated that Aux/IAA proteins block the ARF-mediated activation of AuxRE containing promoters (Kim et al., 1997; Ulmasov et al., 1999; Tiwari et al., 2003; Weijers et al., 2005).

After expressing the chimeric IAA17-based transcriptional activator in *Arabidopsis* an ectopic expression of auxin-responsive genes was detected in the absence of exogenous auxin application (Li et al., 2009). These results suggested that IAA17 interacts in the chromatin with auxin-responsive genes. The direct binding of Aux/IAA proteins was not demonstrated which led to the conclusion that Aux/IAA protein-binding to chromatin is mediated by the interaction with ARF proteins (Chapman and Estelle, 2009). In the *Arabidopsis* Aux/IAA mutant *slr1* a constitutive repression of the auxin response required the protein PICKLE (PKL) (Fukaki et al., 2006). PKL is a homolog of the animal chromatin remodeling factor CHD3/Mi-2 and represses the transcription together with histone deacetylases (Ogas et al., 1999). Moreover, in the *bodenlos* (*bdl*) mutant, plant embryo polarity defects are revealed by mutations of the TOPLESS (TPL) family of transcriptional co-repressors (Szemenyei et al., 2008). BDL interacts with TPL through the conserved ERF-associated amphiphilic repression motif (EAR) motif in domain I which is required for transcriptional repression (Ikeda and Ohme-Takagi, 2009). In yeast-two-hybrid assays the interaction of TPL with many Aux/IAA proteins was identified. However, no interaction was demonstrated for TPL with AXR2/IAA7 or MSG2/IAA19 which possibly interact with other members of the TPL family (Szemenyei et al., 2008).

Moreover, transcriptional co-regulators may interact directly with ARF proteins to regulate auxin responses. The protein ETT/ARF3 can interact with SEUSS, a protein associated with transcriptional repression through LEUNING (Pfluger and Zambryski, 2004; Sridhar et al., 2004). It can act as transcriptional co-repressor although the DNA binding activity is missing (Sridhar et al., 2006).

A critical event in signaling is the degradation of Aux/IAA proteins (Figure 2.3). The transcriptional Aux/IAA repressors dissociate from the ARF proteins, which interact with the promoter of auxin-responsive genes and regulate the auxin response of the downstream gene.

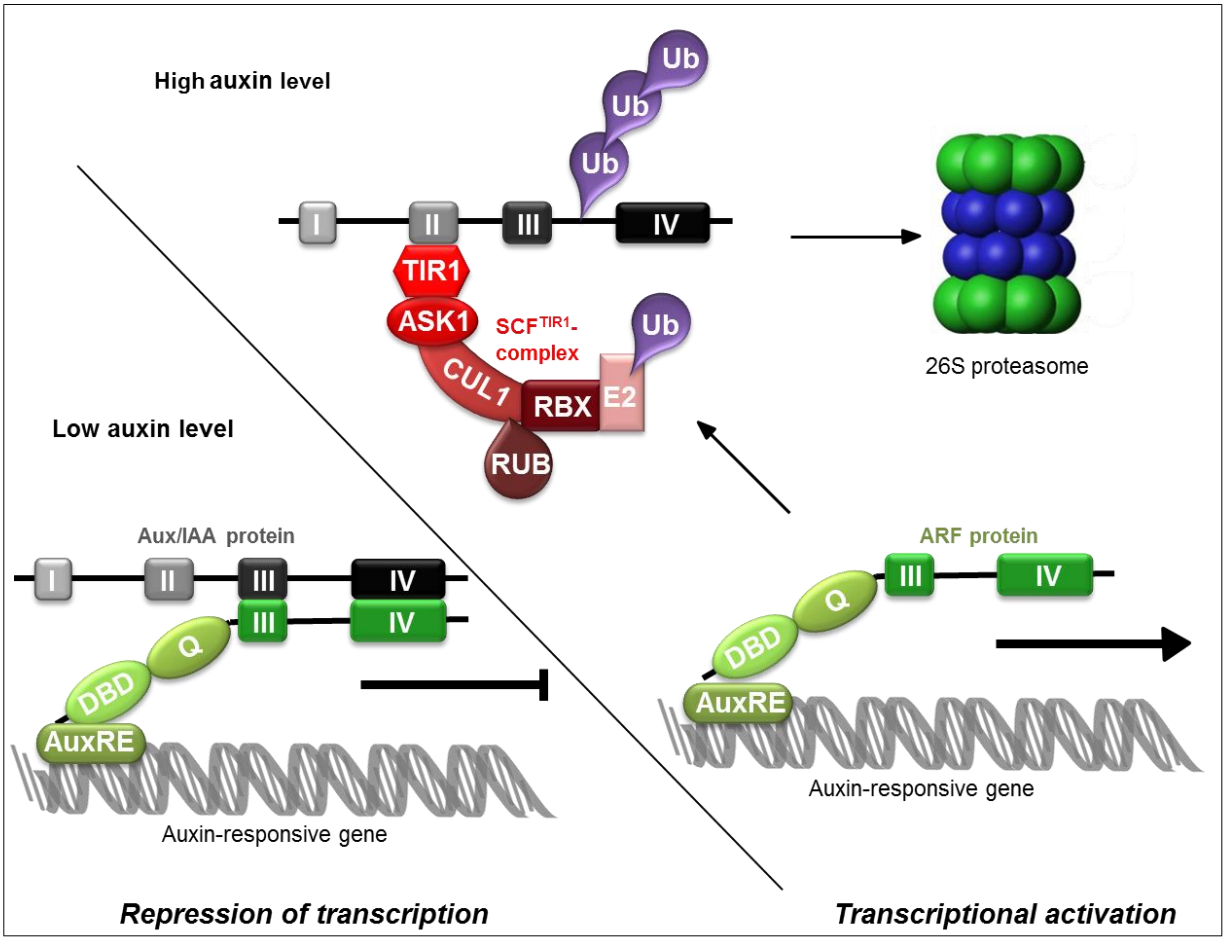

Figure 2.3 Auxin signaling and ubiquitination (modified after Woodward and Bartel (2005) and Santner et al. (2009)). At low auxin concentration the transcription of downstream auxin responsive genes is repressed via the protein complex of Aux/IAA and ARF. The ubiquitination of the Aux/IAA protein is promoted after auxin binds to the TIR1 which is followed by degradation in the 26S proteasome. Ub - ubiquitin; TIR1 – TRANSPORT INHIBITOR RESPONSE 1, ASK1 - ARABIDOPSIS SKP1-LIKE; CUL1 - CULLIN1; RBX – small RING protein; RUB - RELATED TO UBIQUITIN protein; DBD – DNA binding domain.

A crucial regulator of auxin signaling is the SCF^{TIR1}-complex (Woodward and Bartel, 2005).This complex consists of ARABIDOPSIS SKP1-LIKE (ASK1), CULLIN1 (CUL1), F-box protein (TIR1) and small RING protein RBX1 (Figure 2.3). The SCF E3 ligase belongs to the largest family of ubiquitin ligases in plants. The gene *TRANSPORT INHIBITOR RESPONSE* (*TIR1*) encodes for a nuclear protein of the F-box protein family including AUXIN SIGNALING F-BOX PROTEIN 1 (AFB1), AFB2, AFB3, AFB4 and AFB5 (Dharmasiri et al., 2005a; Dharmasiri et al., 2005b; Mockaitis and Estelle, 2008), and furthermore interacts with the core SCF subunit (Gray et al., 1999; Gray et al., 2002). CUL1 binds ASK1 at its N-terminus and RBX1 at its C-terminus and thereby acts as a backbone of the complex. A covalent modification of CUL1 by conjugation of RELATED TO UBIQUITIN protein (RUB) is required to function properly. The RUB conjugation

needs RUB-specific E1 and E2 enzymes together with RBX1, which functions as RUB E3 ligase (del Pozo and Estelle, 1999; Gray et al., 2001; Gray et al., 2002; Dharmasiri et al., 2003). ASK1 interacts with the F-box protein which functions as substrate-specific adaptor and mobilizes proteins to the complex for ubiquitination (Zheng et al., 2002; Petroski and Deshaies, 2005). The conjugation of ubiquitin to the Aux/IAA protein is catalyzed by E3 ubiquitin ligases. After ubiquitination of the substrate protein it is targeted to the 26S proteasome for proteasomal degradation (Woodward and Bartel, 2005).

2.5 The maize *AUXIN/INDOLE-3-ACETIC ACID* (*Aux/IAA*) gene family

Three primary auxin-responsive gene families have been identified and characterized including *GRETCHEN HAGEN 3* (*GH3*), *SMALL AUXIN-UP RNA* (*SAUR*) and *AUXIN/INDOLE-3-ACETIC ACID* (*Aux/IAA*) (Abel and Theologis, 1996). At the beginning of this work the maize *Aux*/*IAA* gene family comprised 31 members (Wang et al., 2010).

2.5.1 Aux/IAA protein structure and function

In general, canonical Aux/IAA proteins share four conserved sequence motifs named domain I, II, III and IV (Ainley et al., 1988; Abel et al., 1995; Hagen and Guilfoyle, 2002). Domain I of Aux/IAA proteins functions as transcriptional repressor by interacting in a complex with auxin response factors (ARF) with the promoters of downstream genes (Tiwari et al., 2001; Tiwari et al., 2004). The conserved ERF-associated amphiphilic repression motif (EAR) in domain I (Figure 2.2) permits the interaction with co-repressor protein TOPLESS (TPL) and TPL-related proteins (TPR) (Szemenyei et al., 2008). The degron sequence (GWPPV) is embedded in domain II which confers stability to the protein (Tiwari et al., 2004). The interaction of domain II with the F-box protein TIR1 leads to rapid degradation (Dharmasiri et al., 2005a). However, specific point-mutations can stabilize the short-lived protein (Worley et al., 2000) which can affect the plant phenotype (Reed, 2001; Liscum and Reed, 2002). The Aux/IAA domains III and IV can form homo- and heterodimers with themselves and heterodimers with ARF proteins (Kim et al., 1997; Ulmasov et al., 1997b). Originally, it was reported that domain III contains the putative βαα secondary structure which is similar to the prokaryotic β-ribbon DNA binding domain (Abel et al., 1994; Morgan et al., 1999) together with domain IV containing an acidic region. Nevertheless, recent studies revealed that the domain complex III/IV may form a type I/II Phox and Bem1p (BP1) protein-protein interaction domain (Guilfoyle and Hagen, 2012; Korasick et al., 2014). The predicted secondary structure of domain region III/IV has the following $\beta_1\beta_2\alpha_1\beta_3\beta_4\alpha_2\beta_5$ motif (Guilfoyle and Hagen, 2012 and Figure 2.2). Aux/IAA proteins contain two nuclear localization signals (NLS) which target the protein to the nucleus. The bipartite NLS composed of an KR sequence between domain I and II and a six

amino acid sequence in domain II. The second NLS is located in domain IV at the carboxyl terminus (Abel et al., 1994). Thus far, only one Aux/IAA protein, AtIAA8, is described to be localized in both the nucleus and cytosol in *Arabidopsis* (Arase et al., 2012).

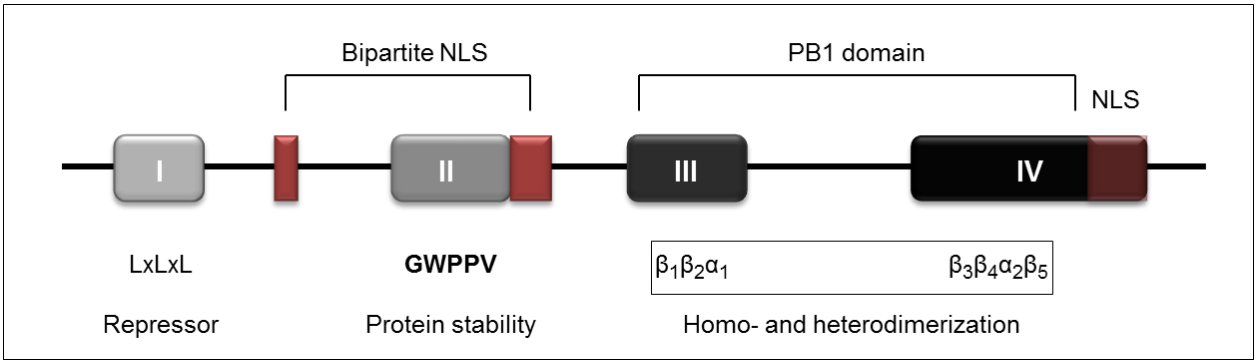

Figure 2.2 Canonical Aux/IAA protein structure including the four conserved domains (I-IV). Domain I functions as transcriptional repressor via the LxLxL motif (Tiwari et al., 2001). Domain II, including the degron-sequence GWPPV, is related to the instability of the protein (Tiwari et al., 2004). Homo- and heterodimerization of Aux/IAA proteins among themselves or with an auxin response factor (ARF) are conferred by domain III and IV which form a type I/II Phox and Bem1p (PB1) domain (Guilfoyle and Hagen, 2012; Korasick et al., 2014). Aux/IAA proteins contain two nuclear localization signals (NLS).

2.5.2 *Aux/IAA* mutants defective in root formation

Several *Aux/IAA* mutants (Table 2.1) with a defect in root formation were identified in *Arabidopsis*, rice and maize. These gain-of-function mutants share a common feature: a specific mutation in the degron sequence of domain II. A substitution of an amino acid by a point mutation (Worley et al., 2000) or a deletion (von Behrens et al., 2011) in this particular sequence stabilizes the protein which can result in specific developmental phenotypes (Reed, 2001; Liscum and Reed, 2002)

Table 2.1 Summary of Aux/IAA gene mutants in different species. Indicated in bold letter is the specific point mutation in the degron sequence.

Aux/IAA gene	*Mutant*	*Point-mutation*	*Root phenotype*	*Reference*
Arabidopsis thaliana				
AXR2/IAA7	*axr2-1*	GW**S**PV	No root hairs, agravitropic root	Nagpal et al. (2000)
AXR3/IAA17	*axr3-1*	GWP**L**C	Reduced root elongation, increased adventitious rooting	Rouse et al. (1998)
SLR1/IAA14	*slr1-1*	GWP**S**V	No lateral roots, few root hairs	Fukaki et al. (2002)
SHY2/IAA3	*shy2-2*	GW**S**PV	Few lateral roots	Tian and Reed (1999)
IAA12	*bdl*	GW**S**PI	No embryonic roots	Hamann et al. (1999)
IAA1	*iaa1-GR*	GW**L**PV	Curtailed lateral root formation	Park et al. (2002)
IAA16	*iaa16-1*	GW**L**PV	Reduced lateral root number	Rinaldi et al. (2012)
IAA28	*iaa28-1*	GW**L**PV	Few lateral roots	Rogg et al. (2001)
IAA18	*crane-1* *crane-2/iaa18-1*	**R**WPPV **E**WPPV	Short root, defective in lateral root formation	Uehara et al. (2008)
MSG2/IAA19	*msg2-1* *msg2-2* *msg2-3* *msg2-4*	GWP**S**V **R**WPPV GWP**L**V GW**L**PV	Few lateral roots	Tatematsu et al. (2004)
Oryza sativa				
OsIAA3	*mOsIAA3*	GWP**L**V	Inhibition of seminal root formation, reduced number of lateral and crown roots	Nakamura et al. (2006)
OsIAA13	*Osiaa13*	**S**WPPC	Reduced number of lateral roots	Kitomi et al. (2012)
OsIAA11	*Osiaa11*	GWP**L**V	Blocks initiation of lateral root primordia	Zhu et al. (2012)
Zea mays				
ZmIAA10	*rum1*	Deletion	No seminal and lateral roots	von Behrens et al. (2011)

2.5.3 The maize *rootless with undetectable meristem 1* (*rum1*) mutant

The maize *rootless with undetectable meristem 1* (*rum1*) encodes an Aux/IAA protein. To date *rum1* is the only maize *Aux/IAA* gene which displayed a developmental defect upon mutation. The mutant *rum1-R* lacks the seminal roots and the lateral roots at the primary root (Figure 2.4 A). Microscopic analyses of the scutellar node of *rum1-R* by transverse sections revealed that no seminal root primordia were initiated (Woll et al., 2005). Similarly, no lateral root primordia were initiated in the primary root of the mutant *rum1-R* (Woll et al., 2005). In contrast, *rum1-R* mutants displayed normal lateral root formation in the shoot borne root system. Similarly, root hair formation was not affected in *rum1-R*. Treatment with exogenous auxin inhibited primary root growth in wild-type and *rum1-R* seedlings while lateral root growth was promoted in the wild-type. However, the pericycle cells did not respond to auxin application in *rum1-R* plants and thus did not develop any lateral roots (Woll et al., 2005). In *Arabidopsis*, lateral root formation is triggered by auxin transport from the shoot towards the roots (Reed et al., 1998). In primary roots of *rum1-R* auxin transport was reduced by 83% compared to the wild-type primary roots, whereas polar auxin transport was enhanced in the coleoptile of the mutant. Moreover, a delayed gravitropic response was detected in primary roots of *rum1-R* (Woll et al., 2005). Latest investigations of the primary root of *rum1-R* displayed a down-regulation of auxin response factors *arf8* and *arf37*. The orthologous *arf* gene in *Arabidopsis* MONOPTEROS/ARF5 (MP/ARF5) is responsible for the differentiation of vascular tissue. Analysis of the primary root displayed disorganization of pith cells around the xylem and of the xylem itself. Besides, enlarged pith cells presented a high lignin deposition (Zhang et al., 2014).

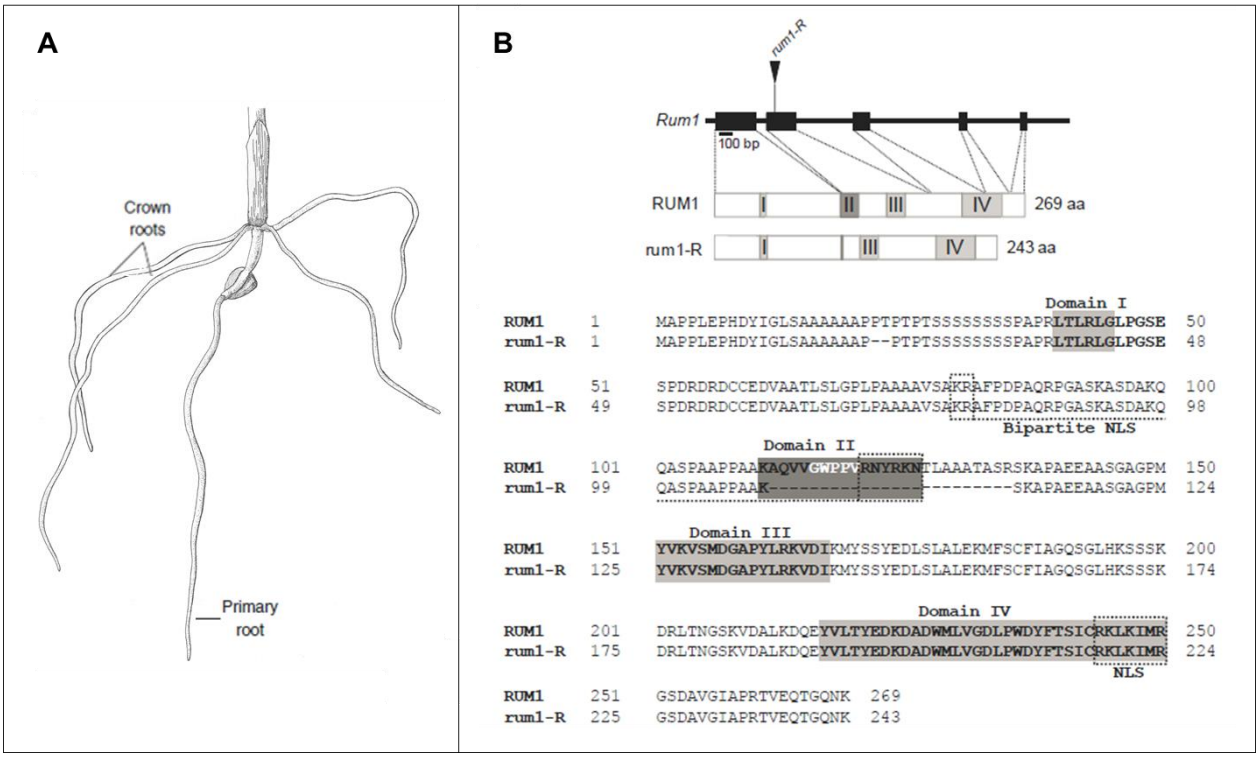

Figure 2.4 Characteristics of the mutant, gene and protein *rootless with undetectable meristem 1* (*rum1*). (A) Root system of 10-day-old *rum1*-R maize seedling which is lacking the seminal and lateral roots (modified after Hochholdinger (2009)). (B) Structure of the *rum1* gene, RUM1 protein and sequence alignment of RUM1 and rum1-R (revised from von Behrens et al. (2011)).

2.5.4 Functional characterization of the maize RUM1 protein and its paralog RUL1

The *rum1* gene which maps to the long arm of chromosome 3 encodes an Aux/IAA protein with a length of 269 amino acids. The mutated form *rum1-R* is lacking 26 amino acids in domain II and a part of the bipartite NLS because of a 1.7 kb mutator insertion in exon 2, which leads to alternative splicing (von Behrens et al., 2011 and Figure 2.4 B).

Investigations revealed that the mutated form *rum1-R* is 5.6 times higher expressed compared to wild-type *rum1* in primary roots. Furthermore, *rum1* displayed auxin inducibility and low expression in different tissues during developmental (von Behrens et al., 2011).

Aux/IAA proteins are localized in the nucleus and are short-lived (Wang et al., 2010). Subcellular localization studies in *Arabidopsis* protoplasts revealed nuclear localization of RUM1 and cytosolic and nuclear localization for rum1-R, which is a consequence of the missing part of the bipartite NLS. An approximately half-life time of 22 min was measured for RUM1 compared to its mutated form which was more stable (von Behrens et al., 2011). Deletion of the domain II influences the protein stability due to the lacking degron-sequence which is responsible for the proteasomal

degradation of the protein (Woodward and Bartel, 2005). Domain I of the Aux/IAA protein confers the transcriptional repression of downstream target genes (Tiwari et al., 2001; Tiwari et al., 2004). RUM1 displayed repressor function in a luciferase assay, where the activity of a downstream reporter gene was decreased by 41% compared to the control (von Behrens et al., 2011). The Aux/IAA domains III and IV can form heterodimers with ARF proteins (Kim et al., 1997; Ulmasov et al., 1997b). In yeast-two-hybrid assays interaction of RUM1 with ZmARF25 and ZmARF34 was demonstrated (von Behrens et al., 2011).

Phylogenetic analyses of the maize *Aux*/*IAA* gene family revealed *ZmIAA29* (GRMZM2G162848) as paralogous gene of *rum1* which was therefore designated *rum1-like* (*rul1*). *Rul1* is located on chromosome 8 and encodes a 273 amino acid protein. RUL1 displays a 92% amino acid sequence identity with RUM1 and is localized in the nucleus (von Behrens et al., 2011). Furthermore a similar half-life time for RUM1 and RUL1 (~23 min) was measured. Like RUM1, RUL1 also interacts with ZmARF25 and ZmARF34 (Zhang, 2013).

2.6 Aims of this work

The overall aim of this thesis was the identification and functional characterization of unique and conserved features of maize Aux/IAA proteins. The following hypotheses were tested:

(1) Additional *Aux/IAA* genes can be identified in version 2 of the maize reference genome which contains around 7,000 genes more compared to version 1.
(2) The evolutionary fate of all members of the maize *Aux/IAA* gene family before and after the last whole genome duplication ca. 5-12 million years ago can be reconstructed by syntenic comparisons with the unduplicated *Sorghum* genome.
(3) *Aux/IAA* genes display root-type and root-tissue specific expression patterns.
(4) *Aux/IAA* genes display different response patterns upon short term auxin treatment.
(5) Aux/IAA proteins are variable in their half-life times and a mutagenized degron motif confers stability to these proteins.
(6) The subcellular localization can be predicted based on the nuclear localization signal of Aux/IAA proteins.
(7) Aux/IAA proteins act as repressors with variable impact on transcriptional activity of downstream genes.
(8) Aux/IAA proteins form homodimers and specifically interact with RUM1 and the paralog RUL1.

3 Materials and Methods

3.1 Material

3.1.1 Plant material

The maize inbred line B73 was used for expression analyses and RNA extraction for cloning the open reading frames of the analyzed *Aux*/*IAA* genes. Etiolated leaf material of the cultivar B73 was utilized for maize protoplast isolation and transformation in subcellular localization studies.

Arabidopsis thaliana (*Col-0*) tissue cultures were used for degradation assays of *Aux*/*IAA* genes, protein-protein interaction studies via bimolecular fluorescence complementation (BiFC) and transient luciferase assays.

3.1.2 Bacterial strain

E. Coli DH5-α

3.1.3 Chemicals/reagents

1-Naphthaleneacetic acid (Sigma-Aldrich, Munich, Germany)
2-Mercaptoethanol (Roth, Karlsruhe, Germany)
2-Propanol (VWR, Darmstadt, Germany)
4',6-diamidino-2-phenylindole (Applichem, Darmstadt, Germany)
Acetic acid (VWR, Darmstadt, Germany)
Agar-Agar (Roth, Karlsruhe, Germany)
Agarose (Applichem, Darmstadt, Germany)
Ammonium persulfate (VWR, Darmstadt, Germany)
Ampicillin (Duchefa, Haarlem, Netherlands)
Bovine serum albumin (Applichem, Darmstadt, Germany)
Bromophenol blue sodium salt (Merck, Darmstadt, Germany)
Calcium chloride (Applichem, Darmstadt, Germany)
Calcium chloride dehyrate (Applichem, Darmstadt, Germany)
Calcium nitrate (VWR, Darmstadt, Germany)
Cycloheximide (Applichem, Darmstadt, Germany)
Dimethyl sulfoxide (Applichem, Darmstadt, Germany)
Ethanol (Zentrale Versorgungsstelle, Universität Bonn, Germany)
Ethylenediaminetetraacetic acid disodium salt (VWR, Darmstadt, Germany)
Glucose-Monohydrate (Roth, Karlsruhe, Germany)

Glycerol (Applichem, Darmstadt, Germany)
Glycine (Roth, Karlsruhe, Germany)
Kanamycin-sulfate (Duchefa, Haarlem, Netherlands)
Magnesium chloride (VWR, Darmstadt, Germany)
Magnesium sulfate (VWR, Darmstadt, Germany)
MES-sodium salt (Roth, Karlsruhe, Germany)
Methanol (VWR, Darmstadt, Germany)
Milk powder (Roth, Karlsruhe, Germany)
NBT/BCIP stock solution (Roche, Mannheim, Germany)
Polyethylene glycol 4000 (Applichem, Darmstadt, Germany)
Potassium acetate (VWR, Darmstadt, Germany)
Potassium chloride (Roth, Karlsruhe, Germany)
Protease inhibitor cocktail (Roche, Mannheim, Germany)
Rotiphorese Gel 30 (Roth, Karlsruhe, Germany)
Saccharose (VWR, Darmstadt, Germany)
SDS-Pellets (Roth, Karlsruhe, Germany)
Sodium acetate (VWR, Darmstadt, Germany)
Sodium chloride (Roth, Karlsruhe, Germany)
Sodium hypochlorite (Roth, Karlsruhe, Germany)
Sybr safe (Invitrogen, Darmstadt, Germany)
TEMED (Roth, Karlsruhe, Germany)
Tris-base (Applichem, Darmstadt, Germany)
Triton-X (Roth, Karlsruhe, Germany)
Tryptone (Roth, Karlsruhe, Germany)
Tween-20 (Roth, Karlsruhe, Germany)
Xylene cyanol (VWR, Darmstadt, Germany)
Yeast extract (Applichem, Darmstadt, Germany)

3.1.4 Enzymes and antibodies

Anti-mouse IgG - Alkaline Phosphatase antibody (Sigma-Aldrich, Munich, Germany)
Cellulase "Onozuka" RS (Serva, Heidelberg, Germany)
Restriction endonucleases (Fermentas, St. Leon-Rot, Germany)
HA-tag (mouse) antibody (Cell Signaling, Frankfurt, Germany)
Macerozyme R-10 (Duchefa, Haarlem, Netherlands)
Myc-tag (mouse) antibody (Cell Signaling, Frankfurt, Germany)

Phusion DNA Polymerase (Fermentas, St. Leon-Rot, Germany)

Self-made Taq-Polymerase (Universität Bonn, AG Hochholdinger, Germany)

T4 DNA Ligase (Fermentas, St. Leon-Rot, Germany)

TaKaRa LA Taq DNA Polymerase (Takara, Saint-Germain-en-Laye, France)

3.1.5 Kits for molecular biology

AccuPrime TM *Pfx* DNA Polymerase (Invitrogen, Darmstadt, Germany)

Dual-Luciferase® Reporter Assay System (Promega, Madison, USA)

E.Z.N.A.® Plasmid Mini Extraction Kit (Omega Bio-tek, Darmstadt, Germany)

GENEART site-directed mutagenesis system (Invitrogen, Darmstadt, Germany)

Mesa Blue qPCR MasterMix Plus for SYBR® Assay (Eurogentec, Cologne, Germany)

MinElute® Gel Extraction Kit (Qiagen, Hilden, Germany)

MinElute® PCR Purification Kit (Qiagen, Hilden, Germany)

NucleoSpin® Plasmid (Macherey-Nagel, Düren, Germany)

pGEM®-T-Easy Vector System I (Promega, Madison, USA)

Plasmid Mini/ Midi/ Maxi Kit (Qiagen, Hilden, Germany)

qScript™ cDNA Super Mix (Quanta BioScience, Darmstadt, Germany)

RevertAid™ H Minus First Strand cDNA Synthesis Kit (Fermentas, St.-Leon-Rot, Germany)

RNeasy Plant Mini kit (Qiagen, Hilden, Germany)

RNase-Free DNase Set (Qiagen, Hilden, Germany)

3.1.6 Oligonucleotides

Table 3.1 Oligonucleotides used in this study.

Oligonucleotide primer	Sequence 5´- 3´
Expression analysis	
ZmIAA1-F	CCTCCTCGTCTGCCATCA
ZmIAA1-R	AACAAAAGAACAAAGCGACCAC
ZmIAA2-F	CAGTGTGCTGCGGTTTTTC
ZmIAA2-R	AATAATAGTCTCATTGATGCCCTTT
ZmIAA3-F	GGTCCGTCCAACTCATGC
ZmIAA3-R	GGGCTGGCCGTAGAACAC
ZmIAA4-F	CTGCTTGTAAAAAGTCCCGAGT
ZmIAA4-R	TATGCCCCAAAACAGAGACC
ZmIAA5-F	CACTGGCGTCTTGAAGGAAA
ZmIAA5-R	TCGGTGCTGTCTGGTCTTATTC

Expression analysis (continued)	
Oligonucleotide primer	Sequence 5´- 3´
ZmIAA6-F	GCTCTTGCTGGACGGGTA
ZmIAA6-R	GGTTCTCGCAATCCTCAGC
ZmIAA7-F	TGGTGTGTCAGTGGAACAAATAA
ZmIAA7-R	CAACGTCTATGCAACCCAAC
ZmIAA8-F	GCGAGGCGAAAGATGAAG
ZmIAA8-R	CAATTACAGAAGCAACGACCAG
ZmIAA9-F	GAAGAGGACCACCAGATTGC
ZmIAA9-R	TGTCGCACAGAACGGGTA
ZmIAA10-F	GGGAGACTATGTTGAAGGCTGA
ZmIAA10-R	CACAAGAACAGCAACCTACGATT
ZmIAA11-F	CGTTGCTGGCTGCCTTAT
ZmIAA11-R	TGGACTAGAGATGCCGACTACA
ZmIAA12-F	TATCGCTGGCATAGTTGTGAG
ZmIAA12-R	TCAACGAGGGCACCACAG
ZmIAA13-F	CCGAAGCAAGATAACCAAGC
ZmIAA13-R	GCTAGCTGGCCGTAGAACAC
ZmIAA14-F	AGATGTTGCCCATTGTATCAGAA
ZmIAA14-R	GGAGACACGGTAGGGGACA
ZmIAA15-F	GGCTTTGGTTCTGTAAGACGAC
ZmIAA15-R	TCAACGACGGTGAAGATAACTGT
ZmIAA16-F	ATCTTTCTTCGTGGTTTCTTCCT
ZmIAA16-R	AACATAGAGCTGGTTCGTCTGA
ZmIAA17-F	ATCAAGGCAATAGTTTGGTGGT
ZmIAA17-R	CACATCGGCAAATCTCCAA
ZmIAA18-F	ACTCCTGGGCGTCATCTG
ZmIAA18-R	CAAAGACGAACCAAATGTGATG
ZmIAA19-F	CAGAGTGTGTGCTGGAAGAGG
ZmIAA19-R	ACCAAAGCCAAGTATGAAAGAAC
ZmIAA20-F	GCGTACCCTGGAGTCTCAAC
ZmIAA20-R	CACCACTCATCTCCTCTAGATTCC
ZmIAA21-F	CCCGCTATTTGATTGTTGCT
ZmIAA21-R	TGTCGAGATGAATGGACCAG
ZmIAA23-F	TCGCTCTGTTTCAGATGTGG
ZmIAA23-R	GGTCTGCTGTCCGATTCCTA
ZmIAA25-F	TAATTTCACCCCCTTTGCAG

Expression analysis (continued)	
Oligonucleotide primer	Sequence 5´- 3´
ZmIAA25-R	CGTCAAGTACGATCCGTGTG
ZmIAA27-F	ACTGGCTTTTAGTGGCTTGG
ZmIAA27-R	AGCCGCCATGTGTATATCAA
ZmIAA28-F	TGGACAAAACACGCTATTCG
ZmIAA28-R	CAGTAAAGCCCGATTCCAAG
ZmIAA29-F	ACCCACGCAAGAAATCTGAG
ZmIAA29-R	GCAAGCATACACAGGAAGCA
ZmIAA30-F	ATCGGCAAGGAATGTATCGT
ZmIAA30-R	GCAAAGCAAAACGAATAGGC
ZmIAA32-F	ATCGTCATGGCCTTATTAATTGTT
ZmIAA32-R	GACACACATGGAGAGTGAACTGA
ZmIAA33-F	CTGGACCTGGAGCCTGAAC
ZmIAA33-R	TACGACACCCCTCATCACC
ZmIAA34-F	AAGCAAGTGTGGTCGCAAG
ZmIAA34-R	ACTTGTTGAGACCAATGTGAGC
myosin -F	AGAAGGCCGTACAGGATCTTACC
myosin -R	CAAGGAGAGACTCTGTGAGCTTCA
actin AY104722 left 210	ATGTGACAATGGCACTGGAA
actin AY104722 right 925	GACCTGACCATCAGGCATCT
Cloning of Aux/IAA genes	
F-ZmIAA2	TAGCCAACCAGCTGCTCATC
R-ZmIAA2	CAACGGGCAGCGTCTTTAAC
F-ZmIAA11	GGCATCAGAGGCCATGAAAC
R-ZmIAA11	TAGCCAGGCCCTAACTAGC
F-ZmIAA15	AGCTTGGGACATGGAAACC
R-ZmIAA15	TTCATTGTCTCGCCGATCCCAG
F2-ZmIAA20	CAGTGTGAGAATCGGAATCG
R2-ZmIAA20	CCGCAAAATGTTCAGAGTTGA
F-ZmIAA33	ATGGCTTGGAATGCCCGCTTCG
R-ZmIAA33	AGGGTGCGTTCAGCACTCAG
Site-directed mutagenesis	
ZmIAA2-P264S-F	GCTGTGGGTTGGTCACCAGTCCGGTCATAC
ZmIAA2-P264S-R	GTATGACCGGACTGGTGACCAACCCACAGC
ZmIAA2-P268L-F	GCTGTGGGTTGGCCACTAGTCCGGTCATAC
ZmIAA2-P268L-R	GTATGACCGGACTAGTGGCCAACCCACAGC

Site-directed mutagenesis (continued)	
Oligonucleotide primer	Sequence 5´- 3´
ZmIAA11-P241S-F	GGTGGGATGGTCACCGGTGGGCGCGTTCCG
ZmIAA11-P241S-R	CGGAACGCGCCCACCGGTGACCATCCCACC
ZmIAA11-P245L-F	GGTGGGATGGCCACTGGTGGGCGCGTTCCG
ZmIAA11-P245L-R	CGGAACGCGCCCACCAGTGGCCATCCCACC
ZmIAA15-P226S-F	GCCCGTGGTCGGATGGTCACCGGTGAGGTC
ZmIAA15-P226S-R	GACCTCACCGGTGACCATCCGACCACGGGC
ZmIAA15-P230L-F	GTGGTCGGATGGCCACTGGTGAGGTCGTAC
ZmIAA15-P230L-R	GTACGACCTCACCAGTGGCCATCCGACCAC
ZmIAA20-P220S-F	GTCGTGGGATGGTCGCCAGTGCGCGCGTTC
ZmIAA20-P220S-R	GAACGCGCGCACTGGCGACCATCCCACGAC
ZmIAA20-P224L-F	GTCGTGGGATGGCCGCTAGTGCGCGCGTTC
ZmIAA20-P224L-R	GAACGCGCGCACTAGCGGCCATCCCACGAC
ZmIAA33-P232S-F	GTCGTGGGATGGTCGCCGGTGCGCGCGTTC
ZmIAA33-P232S-R	GAACGCGCGCACCGGCGACCATCCCACGAC
ZmIAA33-P236L-F	GTCGTGGGATGGCCGCTGGTGCGCGCGTTC
ZmIAA33-P236L-R	GAACGCGCGCACCAGCGGCCATCCCACGAC
Degradation assay/Subcellular localization studies (Restriction sites: small letters)	
ZmIAA2-*Bam*HI-F	GGggatccCGGAGCCGATGGCTGGAG
ZmIAA2-*Xho*I-R2	GGctcgagGCTCCTGTTCTTGCACTT
ZmIAA11-*Bam*HI-F	GGggatccATCAGAGGCCATGAAACTG
ZmIAA11-*Xho*I-R	GGgagctcATTCTTCGTCTTCCTTGG
ZmIAA15-*Bam*HI-F	GGggatccAGCTTGGGACATGGAAACC
ZmIAA15-*Xho*I-R(2)	GGctcgagTTGTCTCGCCGATCCAG
ZmIAA20-*Spe*I-F	GGactagtGAATCGGAGATGGCTTG
ZmIAA20-*Kpn*I-R	GGggtaccAGCTGCAGCTCTCTTC
ZmIAA20-*Xho*I-R	GGctcgagCTAAGCTGCAGCTCTCTTCC
ZmIAA33-*Xba*I-F	GGtctagaGCAGGAAGATGGCTTGGAATG
ZmIAA33-*Bam*HI-R	GGggatccGCACTCAGCTGCGGC
Construct of blank effector plasmid (Restriction sites: small letters)	
TMV-*Xba*I-F	GGtctagaGTATTTTTACAACAATTACC
GAL4DBD-*Sac*I-R	GGgagctcCGATACAGTCAACTGTCTTT
MCS4-*Sac*I-F	GGgagctcATAAGGAAGTTCATTTCA
MCS4-*Sac*I-R	GGgagctcGTTGTGGCGGATCTTGAA
Construct of N-terminal GFP (Restriction sites: small letters)	
GFP-*Xba*I-F	GGtctagaTACGCTATGAGTAAAGGA

Construct of N-terminal GFP **(continued)** (Restriction sites: small letters)	
Oligonucleotide primer	Sequence 5´- 3´
GFP-*Sac*I-R2	GGgagctcTAATTTGTATAGTTC
MCS4-*Sac*I-F	GGgagctcATAAGGAAGTTCATTTCA
MCS4-*Sac*I-R	GGgagctcGTTGTGGCGGATCTTGAA
Dual-Reporter-Assay (Restriction sites: small letters)	
ZmIAA2-*Bam*HI-F2	GGggatccGCGGAGCCGATGGCTGGAG
ZmIAA2-*Kpn*I-R	GGggtaccTCAGCTCCTGTTCTTGCACTT
ZmIAA11-*Bam*HI-F2	GGggatccTCAGAGGCCATGAAACTG
ZmIAA11-*Kpn*I-R	GGggtaccCTAATTCTTCGTCTTCCTTGG
ZmIAA15-*Bam*HI-F2	GGggatccGCTTGGGACATGGAAACC
ZmIAA15-*Sma*I-R	GGcccgggTCATTGTCTCGCCGATCCAG
ZmIAA20-*Spe*I-F	GGactagtGAATCGGAGATGGCTTG
ZmIAA20-*Kpn*I-R2	GGggtaccCTAAGCTGCAGCTCTCTTCC
ZmIAA33-*Bam*HI-F	GGggatccAGCAGGAAGATGGCTTGGAATG
ZmIAA33-*Kpn*I-R	GGggtaccTCAGCACTCAGCTGCGGC

3.1.7 Vectors

Table 3.2: List of vector plasmids used in this study.

Name	***Resistance***	***Tag***	***Experiment***	***Source***
pGEM-t-easy	Amp		cloning of *Aux*/*IAA* genes	Promega
pUC-35S-MCS-HA-GFP	Amp	HA	degradation assay subcellular localization studies	constructed from pUC-SYPCE and CF203 Lab Ac #765
pUC-35S-GFP-MCS-HA	Amp	HA	subcellular localization studies	constructed from pUC-35S-MCS-HA-GFP and pUC-SYPCE Lab Ac #979
pUC-SYPNE-152	Amp	c-Myc	BiFC	Walter et al. (2004) Li et al. (2010) Lab Ac #519
pUC-SYPCE	Amp	HA	BiFC	Walter et al. 2004 Lab Ac #518
blank effector	Amp		transient luciferase assay	constructed from pUC-SYPCE and pre-effector Lab Ac #988
reporter	Amp		transient luciferase assay	modified from pUC-SYPCE Lab Ac #935
control RiLUC (reference)	Amp		transient luciferase assay	modified from pUC-SYPCE Lab Ac #933

3.1.8 Software and internet tools for bioinformatics analyses

Gramene (www.gramene.org)

Maize Genetics and Genomics Database (MaizeGDB, www.maizegdb.org)

National Center for Biotechnology Information (NCBI, www.ncbi.nlm.nih.gov)

Rice Genome Annotation Project (rice.plantbiology.msu.edu)

BioEdit Sequence Alignment Editor Version 7.0.9.0.

ClustalW (www.clustal.org)

Comparative Genomics (CoGe, genomevolution.org/org/CooGe/)

Mega 5.2 (Molecular Evolutionary Genetics Analysis, www.megasoftware.net)

Net Primer (PREMIER Biosoft, www.premierbiosoft.com)

Primer3Plus (www.bioinformatics.nl)

Simple Modular Architecture Research Tool (SMART, smart.embl-heidelberg.de)

Summit V4.3 (Beckman Coulter, Krefeld, Germany)

ZEN2011 (Carl Zeiss, Jena, Germany)

3.2 Methods

3.2.1 Structural analysis of the maize *Aux/IAA* gene family

3.2.1.1 Identification of novel *Aux/IAA* genes

In the initial version of the maize reference genome sequence B73 RefGen_v1 (Schnable et al., 2009) 31 *Aux/IAA* genes were predicted among 32,540 protein-encoding genes (Wang et al., 2010). To obtain a comprehensive overview of the maize *Aux/IAA* gene family the maize filtered gene set based on genome assembly version AGPv2 (http://www.maizegdb.org/) containing 39,656 high confidence gene models was screened for additional sequences homologous to the previously identified *Aux/IAA* genes. Blast searches using the known *Aux/IAA* gene sequences as query sequence was performed.

3.2.1.2 Phylogeny and Synteny of *Aux/IAA* genes

Protein sequences of the maize *Aux/IAA* genes were retrieved from MaizeGDB.org. Moreover, the previously identified rice Aux/IAA protein sequences (Jain et al., 2006) from the rice genome annotation project (http://rice.plantbiology.msu.edu/index.shtml) and the published *Sorghum* sequences (Wang Yi-Jun, 2010) were extracted from Gramene (http://www.gramene.org/) (Table 4.1). The four conserved domains in the maize *Aux/IAA* gene family were determined by multiple alignments with ClustalW. Synteny of the maize sequences was determined with Comparative Genomics software (CoGe, http://genomevolution.org/CoGe/ and Lyons and Freeling (2008)). Association with the maize subgenomes 1 and 2 were based on Schnable et al. (2011).

Phylogenetic analyses comparing maize, rice, *Sorghum* and *Arabidopsis* Aux/IAA protein sequences were conducted using the neighbor-joining algorithm in MEGA version 4 (Tamura et al., 2007) considering 1,000 replications with bootstrap analyses.

3.2.2 Growth conditions

Seeds of the maize inbred line B73 were sterilized with 6% sodium hypochlorite for 10 min and rinsed in distilled water. Subsequently, seeds were rolled up in germination paper (Anchor paper, www.anchorpaper.com) (Hetz et al., 1996) and transferred to 10 l buckets filled with ~3 l distilled water. Germinating seedlings were incubated at 28 °C with a 16 h light and 8 h dark cycle.

For *Aux*/*IAA* gene expression analyses seedling samples were harvested at different developmental stages and were immediately frozen in liquid nitrogen and stored at -80 °C until RNA isolation. Coleoptiles were harvested from seedlings grown for four days at 28 °C in the dark.

To test *Aux*/*IAA* genes for auxin-inducibility five-day-old maize seedlings were treated with 5 mM α-naphthyl acetic acid (α-NAA) working solution for 3 h. The differentiation zone of two to three primary roots per biological replicate was harvested each hour for three hours and immediately frozen in liquid nitrogen and stored at -80 °C.

For cloning of the *Aux/IAA* genes, seedlings were germinated at 28 °C with a 16 h light (2700 lux) and 8 h dark cycle for six days in a plant growth chamber. The primary roots of these seedlings were harvested and immediately frozen in liquid nitrogen and stored at -80 °C until RNA isolation.

For subcellular localization studies, seedlings were germinated in a plant growth chamber (Conviron Adaptis) at 28 °C with a 16 h light and 8 h dark cycle for three to four days until a 1 cm primary root was visible. Afterwards, the seedlings were transferred into an incubator (Binder, Tuttlingen, Germany) at 26 °C in darkness for another eight to ten days. The etiolated leaves were used for protoplast isolation.

3.2.3 RNA isolation and cDNA synthesis

For the qRT-PCR expression analysis, frozen maize shoot and root tissues were ground and approximately 100 mg per biological replicate were used for total RNA extraction via the RNeasy Plant Mini Kit (Qiagen, Hilden, Germany). Subsequently, RNA was treated with RNase-free DNase I (Qiagen, Hilden, Germany). To exclude the possibility of DNA contamination, the RNA samples were tested via PCR with oligonucleotides for maize *actin 1* (AY104722) that bind to exon sequences that flank an intron. For cDNA synthesis 500 ng of total RNA was subjected to the qScript cDNA Synthesis Kit protocol (Quanta BioScience, Darmstadt, Germany).

To clone the open reading frames of representative *Aux*/*IAA* genes, total RNA was extracted with the RNeasy Mini Kit (Qiagen) from 100 mg frozen material of five primary roots per biological replicate, followed by RNase-free DNAse I treatment (Qiagen). For cDNA synthesis 1 µg of total RNA was amplified using the Revert Aid™ H Minus First Strand cDNA Synthesis Kit (Fermentas).

3.2.4 Quantitative real-time PCR (qRT-PCR)

Expression of maize *Aux/IAA* genes was determined by quantitative real-time-PCR in a Bio-Rad CFX 384™ Real-Time System (Bio-Rad, Munich, Germany) using gene-specific oligonucleotides (Table S1). The oligonucleotides were designed by Primer3Plus (http://www.bioinformatics.nl/cgi-bin/primer3plus/primer3plus.cgi) and checked for self-complementarity and hair-pins with NetPrimer (PREMIER Biosoft, http://www.premierbiosoft.com) software. Each reaction contained 4 µl MESA Blue qPCR™ MasterMix Plus for SYBR Assay no ROX (Eurogentec, Cologne,

Germany), 1 µl cDNA sample and 250 nM gene-specific oligonucleotide primers to a final volume of 8 µl. The primer efficiency of each oligonucleotide was calculated using the following dilution series: 1, 1/2, 1/4, 1/8, 1/16, 1/32, 1/64 and 1/128. The relative expression levels of the transcripts were calculated with reference to the housekeeping gene *myosin* (Genbank AC: 486090G09.x1). Differential gene expression was determined by a two sided Student´s t-test.

For each root-type and tissue, five biological replicates were analyzed. For auxin induction experiments three biological replicates were tested. Three technical replicates were measured for each biological replicate.

3.2.5 Cloning

3.2.5.1 Cloning of *Aux*/*IAA* genes and site-directed mutagenesis

To clone the open reading frames of the *Aux/IAA* genes *ZmIAA2* (GRMZM2G159285), *ZmIAA11* (GRMZM2G059544), *ZmIAA15* (GRMZM2G128421), *ZmIAA20* (GRMZM5G864847) and *ZmIAA33* (GRMZM2G359924) oligonucleotide primers were designed by PrimerPlus3 software and checked with NetPrimer Software (PREMIER Biosoft). PCR amplicons of the *Aux/IAA* open reading frames generated by specific oligonucleotide primers (Table 3.1) were introduced into the vector pGEM-t-easy (Promega, Madison, USA). The conserved degron-Sequence VGWPPV in domain II was mutated in all *Aux*/*IAA* genes via the GENEART® site-directed mutagenesis system (Life Technologies, http://www.lifetechnologies.com/). The mutations resulted in a substitution of the first proline residue by serine (VGW**S**PV) or the second proline by leucine (VGWP**L**V). Oligonucleotide primers, which introduce specific mutations, were designed as described by the manufacturer (Table 3.1).

Table 3.3 List of point-mutation in nucleotide sequence of *Aux/IAA* genes		
	P-S substitution	***P-L substitution***
Gene	***nucleotide***	
ZmIAA2	264	268
ZmIAA11	241	245
ZmIAA15	226	230
ZmIAA20	220	224
ZmIAA33	232	236

3.2.5.2 GFP fusion constructs

C-terminal GFP fusion constructs were generated by amplifying either the wild-type or mutated full-length open reading frame of all *Aux/IAA* genes (*ZmIAA2*, *ZmIAA2-P264S*, *ZmIAA2-P268L*, *ZmIAA11*, *ZmIAA11-P241S*, *ZmIAA11-P245L*, *ZmIAA15*, *ZmIAA15-P226S*, *ZmIAA15-P230L*, *ZmIAA20*, *ZmIAA20-P220S*, *ZmIAA20-P224L*, *ZmIAA33*, *ZmIAA33-P232S* and *ZmIAA33-P236L*) without the stop codon using gene-specific oligonucleotides (Table 3.1). The PCR products of the wild-type and mutated *Aux*/*IAA* gene sequences were ligated into the *Bam*HI/*Xho*I (*ZmIAA2*, *ZmIAA11* and *ZmIAA15*), *Spe*I/*Kpn*I (*ZmIAA20*) or *Xba*I/*Bam*HI (*ZmIAA33*) restriction sites of the pUC-35S-MCS-GFP vector (Lab Ac #765).

For *ZmIAA11*, *ZmIAA11-P241S*, *ZmIAA11-P245L*, *ZmIAA20*, *ZmIAA20-P220S* and *ZmIAA20-P224L*, additional N-terminal GFP fusion constructs were generated. To construct the pUC-35S-GFP-MCS the open reading frame of the GFP without stop codon was amplified with the oligonucleotides GFP-*Xba*I-F and GFP-*Sac*I-R2 using the pUC-35S-MCS-GFP vector as template (Lab Ac #765). The GFP PCR-products were inserted in the *Xba*I/*Sac*I site of the backbone vector. The MCS was generated by PCR amplification (oligonucleotide primers: MCS4-*Sac*I-F and MCS4-*Sac*I-R) with the pUC-SYPNE vector (Lab Ac #519) as template. The MCS was inserted at the *Sac*I site of the recipient vector (Lab Ac #949). The vector sequences were confirmed by sequencing.

To construct the N-terminal GFP fusions, the amplified PCR-products were inserted into the *Bam*HI/*Xho*I (oligonucleotide primers: ZmIAA11-*Bam*HI-F2 and ZmIAA11-*Xho*I-R) and *Spe*I/*Xho*I (oligonucleotide primers: ZmIAA20-*Spe*I-F and ZmIAA20-*Xho*I-R) restriction sites of the pUC-35S-GFP-MCS vector (Lab Ac #979).

Table 3.4 List of C-and N-terminal GFP fusion constructs used in subcellular localization studies and degradation assay.

No	*Construct*	*Insertion*	*Lab Ac #*
1	35S::GFP	None	765
2	35S::ZmIAA2-GFP	ZmIAA2 full-length ORF w/o stop codon	880
3	35S::ZmIAA2-P264S-GFP	ZmIAA2 full-length ORF with single point mutation in degron sequence, w/o stop codon	881
4	35S::ZmIAA2-P268L-GFP	ZmIAA2 full-length ORF with single point mutation in degron sequence, w/o stop codon	882
5	35S::ZmIAA11-GFP	ZmIAA11 full-length ORF w/o stop codon	883
6	35S::ZmIAA11-P241S-GFP	ZmIAA11 full-length ORF with single point mutation in degron sequence, w/o stop codon	885
7	35S::ZmIAA11-P245L-GFP	ZmIAA11 full-length ORF with single point mutation in degron sequence, w/o stop codon	886
8	35S::ZmIAA15-GFP	ZmIAA15 full-length ORF w/o stop codon	887
9	35S::ZmIAA15-P226S-GFP	ZmIAA15 full-length ORF with single point mutation in degron sequence, w/o stop codon	1027
10	35S::ZmIAA15-P230L-GFP	ZmIAA15 full-length ORF with single point mutation in degron sequence, w/o stop codon	888
11	35S::ZmIAA20-GFP	ZmIAA20 full-length ORF w/o stop codon	913
12	35S::ZmIAA20-P220S-GFP	ZmIAA20 full-length ORF with single point mutation in degron sequence, w/o stop codon	915
13	35S::ZmIAA20-P224L-GFP	ZmIAA20 full-length ORF with single point mutation in degron sequence, w/o stop codon	914
14	35S::ZmIAA33-GFP	ZmIAA33 full-length ORF w/o stop codon	891
15	35S::ZmIAA33-P232S-GFP	ZmIAA33 full-length ORF with single point mutation in degron sequence, w/o stop codon	889
16	35S::ZmIAA33-P236L-GFP	ZmIAA33 full-length ORF with single point mutation in degron sequence, w/o stop codon	890
17	35S::GFP-MCS	None	979
18	35S::GFP-ZmIAA11	ZmIAA11 full-length ORF w/o stop codon	980
19	35S::GFP-ZmIAA11-P241S	ZmIAA11 full-length ORF with single point mutation in degron sequence, w/o stop codon	982
20	35S::GFP-ZmIAA11-P245L	ZmIAA11 full-length ORF with single point mutation in degron sequence, w/o stop codon	983
21	35S::GFP-ZmIAA20	ZmIAA20 full-length ORF w/o stop codon	984
22	35S::GFP-ZmIAA20-P220S	ZmIAA20 full-length ORF with single point mutation in degron sequence, w/o stop codon	986
23	35S::GFP-ZmIAA20-P224L	ZmIAA20 full-length ORF with single point mutation in degron sequence, w/o stop codon	987

3.2.5.3 Effector constructs

The effector vector (pUC-35S-TMV-GAL4BD-MCS-NosT, Lab Ac #988) was generated by amplifying the TMV-GAL4DBD PCR-fragment (oligonucleotide primers: TMV-*Xba*I-F and GAL4-*Sac*I-R) from the donor vector (pUC-35S-GAL4DBD-cYFP, Lab Ac # 936). The PCR-product was inserted into the restriction site *Xba*I/*Sac*I of the backbone vector (Lab Ac #765), which provided the 35S promoter and the Nos terminator to construct an intermediate vector (pUC-35S-TMV-GAL4-DBD-Nos-T, Lab Ac #954). Moreover a MCS was obtained from the pUC-SYPNE vector (Lab Ac # 519) by PCR with the oligonucleotides MCS4-*Sac*I-F and MCS4-*Sac*I-R. The intermediate vector (Lab Ac #954) was digested with *Sac*I and the MCS-product was inserted. The effector vector sequence was confirmed by sequencing. PCR fragments of the wild-type *Aux/IAA* genes were amplified and ligated into the *Bam*HI/*Kpn*I (*ZmIAA2*, *ZmIAA11* and *ZmIAA33*), *Bam*HI/*Xma*I (*ZmIAA15*) and *Spe*I/*Kpn*I (*ZmIAA20*) restriction sites of pUC-35S-TMV-GAL4-DBD-MCS-NosT (effector plasmid, Lab Ac #988).

3.2.5.4 BiFC constructs

Interaction studies were conducted by bimolecular fluorescence complementation (BiFC) as described by Walter et al. (2004). Fusion plasmids of *ZmIAA2*, *ZmIAA11*, *ZmIAA15*, *ZmIAA20* and *ZmIAA33* were generated with the C or N-terminal fragment of YFP. Donor plasmids encoding the open reading frame without stop codon of the genes of interest (*ZmIAA2*: Lab Ac #880, *ZmIAA11*: Lab Ac #883, *ZmIAA15*: Lab Ac #887, *ZmIAA20*: Lab Ac #913, *ZmIAA33*: Lab Ac #891) were digested with *Bam*HI/*Xba*I (*ZmIAA33*), *Bam*HI/*Xho*I (*ZmIAA2*, *ZmIAA11*, *ZmIAA15*) or *Spe*I/*Kpn*I (*ZmIAA20*) to release the *Aux/IAA* open reading frames. These open reading frames were introduced into the corresponding restriction sites of the recipient vectors pUC-SPYNE-152 (Walter et al., 2004 and Lab Ac #518) and pUC-SPYCE (Li et al., 2010 and Lab Ac #519). Likewise, interactions were studied with RUM1 (*ZmIAA10*: GRMZM2G037368) and RUL1 (*ZmIAA29*: GRMZM2G163848). The split-YFP constructs of RUM1 (Lab Ac #528 and 531) were generated as described in von Behrens et al. (2011). The full-length open reading frame of *rul1* was amplified with the oligonucleotide primer *rul1-BamH*I-fw and *rum1-Kpn*I-rv. The donor vectors pUC-SYPCE and pUC-SYPNE-152 were digested and the PCR product ligated into the restriction site *Bam*HI/*Kpn*I. The sequences of the C- or N-terminal fragment RUL1-YFP constructs (Lab Ac #529 and 530) were validated via sequencing. As a negative control an uncharacterized protein of the *barwin* gene family (*BARW*, GRMZM2G117971) was used. The corresponding C- and N-terminal YFP fusion constructs were co-transformed into *Arabidopsis* protoplasts, according to Berendzen et al. (2012b) and analyzed by flow cytometry. In total, 76 different samples were

measured in three replicates. Per 96 well-plate one biological replicate of each sample was measured.

Table 3.5 List of BiFC constructs

No	*Construct*	*Gene*	*AC maizeGDB*	*Amino acids*	*Vector*	*Comment*
1	ZmIAA2-YFPN-152	*ZmIAA2*	GRMZM2G159285	1-237	pUC-SYPNE-152	Lab Ac #1010
2	ZmIAA2-YFPC	*ZmIAA2*	GRMZM2G159285		pUC-SYPCE	Lab Ac #1011
3	ZmIAA11-YFPN-152	*ZmIAA11*	GRMZM2G059544	1-269	pUC-SYPNE-152	Lab Ac #1022
4	ZmIAA11-YFPC	*ZmIAA11*	GRMZM2G059544		pUC-SYPCE	Lab Ac #1012
5	ZmIAA15-YFPN-152	*ZmIAA15*	GRMZM2G128421	1-251	pUC-SYPNE-152	Lab Ac #1024
6	ZmIAA15-YFPC	*ZmIAA15*	GRMZM2G128421		pUC-SYPCE	Lab Ac #1013
7	ZmIAA20-YFPN-152	*ZmIAA20*	GRMZM5G864847	1-234	pUC-SYPNE-152	Lab Ac #1020
8	ZmIAA20-YFPC	*ZmIAA20*	GRMZM5G864847		pUC-SYPCE	Lab Ac #1014
9	ZmIAA33-YFPN-152	*ZmIAA33*	GRMZM2G359924	1-228	pUC-SYPNE-152	Lab Ac #1023
10	ZmIAA33-YFPC	*ZmIAA33*	GRMZM2G359924		pUC-SYPCE	Lab Ac #1015
11	RUM1-YFPN-152	*Rum1*	GRMZM2G037368	1-269	pUC-SYPNE-152	von Behrens et al. (2011)
12	RUM1-YFPC	*Rum1*	GRMZM2G037368		pUC-SYPCE	
13	RUL1-YFPN-152	*Rul1*	GRMZM2G163848	1-272	pUC-SYPNE-152	Generated by Yanxiang Zhang
14	RUL1-YFPC	*Rul1*	GRMZM2G163848		pUC-SYPCE	
15	Barw-YFPN-152	*Barw*	GRMZM2G117971	1-150	pUC-SYPNE-152	Generated by Changzheng Xu
16	Barw-YFPC	*Barw*	GRMZM2G117971		pUC-SYPCE	

3.2.6 Maize protoplast isolation and transformation

3.2.6.1 Maize mesophyll protoplast isolation

Protoplast isolation of maize leaves was modified according to Sheen (2002) and Nguyen et al. (2010). The middle part (6-8 cm) of etiolated 12 to 14 day-old-maize seedlings were cut in 0.5 - 1 mm strips. Subsequently, leaf digestion was performed with an enzyme solution (1.5% cellulose RS, 0.3% macerozyme R10, 0.4 M sucrose, 10 mM MES, pH 5.7) in a petri dish as described by Sheen (2002). Washing and recovering of the maize protoplast was achieved according to Nguyen et al. (2010) in 14 ml conical falcon tubes. Afterwards, quality and viability of the protoplasts were determined via an Axio Lab.A1 microscope (Zeiss, www.zeiss.de) with a Fuchs-Rosenthal bright-line objective (Labor Optik, Friedrichsdorf, Germany). Protoplasts were resuspended in MMG buffer (0.4 M mannitol, 15 mM $MgCl_2$ and 4 mM MES, pH 5.7) at a density of $7x10^5$ protoplasts/ml and kept on ice.

3.2.6.2 PEG-mediated transformation

For the PEG-mediated transformation, 200 µl of isolated protoplasts, 20 µl plasmid (20-30 µg), 220 µl PEG solution (40% (v/v) PEG4000, in a 0.2 M mannitol, 0.1 M $Ca(NO_3)_2$ buffer) were combined in a 14 ml conical tube and thoroughly mixed. The mixture was incubated at RT for 15 min, and later diluted to 10 ml with wash buffer (5 mM NaCl, 5 mM glucose, 125 mM $CaCl_2 \cdot 2H_2O$, 154 mM KCl). After centrifugation at 200 g for 1 min, the protoplast pellet was dissolved in 200 µl WI solution (0.6 M mannitol, 4 mM MES pH 5.7, and 4 mM KCl) and incubated in the dark at 26 °C ON.

3.2.7 Subcellular localization

The GFP-constructs and the control (35::GFP-MCS or 35S::MCS-GFP) were transformed into maize protoplasts and documented by confocal laser scanning microscopy (Zeiss LSM-780, attached to an Axio Observer Z1, Carl Zeiss Microscopy, Jena, Germany). The transformed maize protoplasts were examined with a 40x objective (C-Apochromat 40x/1.2 W Korr). 4',6-diamidino-2-phenylindole **(**DAPI) was used as nuclear counterstain. GFP was excited with a laser at 488 nm and the emitted fluorescence was detected with a 499-578 nm bandpass filter. The same excitation was used for the auto fluorescence and detected with a 640-728 nm bandpass filter. A laser at 405 nm was used to excite DAPI and sensed with a 410-475 nm bandpass filter. Image processing was performed with ZEN2011 software (Zeiss).

3.2.8 Protein-degradation assay

3.2.8.1 Degradation assay and flow cytometry

The C-terminal GFP fusion constructs established for the subcellular localization experiments were also used for protein stability determination. All constructs of the selected *Aux/IAA* genes and a control (*35S::GFP*; Lab Ac #765) were transformed into *Arabidopsis thaliana* protoplasts as previously described (von Behrens et al., 2011). The transformed protoplasts were treated with α-naphthyl acetic acid (α-NAA, working solution 10 µM) and cycloheximide (working solution 100 µg/ml) after 16 hours after transformation. After α-NAA and cycloheximide treatment, samples were measured in a time course experiment (0, 10, 30, 60 and 120 min) by flow cytometry in a MoFlo cell sorter (Beckman Coulter, www.beckmancoulter.com) as previously described (von Behrens et al., 2011). A 488 nm argon laser (50 mW) was used for the excitation of GFP fluorescence, the signal was recorded in FL1 (504-522 nm) and plotted against auto fluorescence in FL2 (565-605 nm). Each measurement was performed in three biological replicates. The data were documented and analyzed with Summit v4.3 software (Beckman Coulter, Krefeld, Germany).

3.2.8.2 Confirmation of degraded proteins via Western Blot

Protein isolation of the transformed protoplasts and validation of the expressed proteins were performed as described in von Behrens et al. (2011). The primary antibody HA-tag (mouse) (Cell Signaling, Frankfurt, Germany) was used to detect the GFP fusion vectors. As secondary antibody Anti-mouse IgG - Alkaline Phosphatase (AP) (Sigma-Aldrich, Munich, Germany) was employed. Detection was performed with NBT/BCIP stock solution (Roche, Mannheim, Germany) as previously described (Saleem et al., 2010).

3.2.9 Protein-protein interaction experiments

Bimolecular fluorescence complementation (BiFC) studies were performed using flow cell cytometry in combination with split-YPF experiments in maize protoplasts. A small-scale transformation (Berendzen et al., 2012b) was utilized to co-transform the corresponding BiFC vectors (Table 3.5) into *Arabidopsis* Col-0 protoplasts. The YFP signal was examined via the flow cytometry.

3.2.9.1 Quantification of flow cytometry data

A linear model was fitted with an additive effect for treatment, corresponding to the protein interaction partners. In order to normalize the data between different plates, an additive effect for plates was fitted. Inspection of the studentized residuals suggested that a logarithmic transformation stabilized the variance and led to an approximate normal distribution. Thus, all analyses were performed on the logarithmic scale. Note that an additive model on the transformed scale corresponds to a multiplicative model on the original scale. According to this model, responses were expected on the original scale of the different treatments on one plate to be a multiple of the responses on another plate. This expectation also met with the observation.

Each interacting protein pair was compared to the mean of its two controls by specifying the corresponding linear contrast. In this contrast, the protein interacting pair was assigned a coefficient of 2, whereas the two controls were each assigned coefficients of -1. T-tests were performed for all contrasts of interest. The *p*-values were adjusted for multiplicity using the simulation method of Edwards and Berry (1987). The family-wise type I error rate was set at α=5%.

3.2.9.2 Split-YFP experiments

To confirm the protein-protein interaction results obtained from the quantitative BiFC assays, split-YFP experiments were performed in maize protoplasts. Similar settings of the laser confocal microscope were used as described above (paragraph 3.2.7) except for the detection of YFP. It was excited with a laser at 514 nm and the emitted fluorescence was detected with a 526-595 nm bandpass filter. To confirm the expression of the proteins, Western Blot experiments were performed as previously described (von Behrens et al., 2011).

3.2.10 Transient luciferase assay

3.2.10.1 Dual-Luciferase® Reporter Assay

The reference plasmid encoding for *Renilla* LUC (Luciferase) and the reporter plasmid encoding for *firefly* LUC, both driven by a 35S Cauliflower mosaic virus (CaMV) promoter, and the effector plasmid were co-transformed into *Arabidopsis* protoplast (Berendzen et al., 2012b). For the transformation 1 µg plasmid DNA of the reference plasmid, 3 µg of reporter and 5 µg of effector plasmid were used, which were determined by a dose-response assay as described in the Dual-Luciferase® reporter assay system manual (Promega).

To determine the luciferase activities, the Dual-Luciferase® reporter assay system (Promega) was used and quantified in a plate reader (CLARIOstar, Ortenberg, Germany). Three biological

replicates were measured per *Aux/IAA* gene and luciferase activity of each transformant was determined three times independently. The values were normalized with the corresponding values of the internal control *Renilla* LUC, which minimized the experimental variability introduced by the variation of the transfection efficiency and the protoplast viability. Differences of the relative luciferase activities were determined by a one-sided Student´s t-test.

4 Results

4.1 Identification of novel *Aux/IAA* genes in maize

In the initial version of the maize reference genome sequence B73 RefGen_v1 (Schnable et al., 2009) 31 *Aux/IAA* genes were predicted among 32,540 protein-encoding genes (Wang et al., 2010). The latest version of B73 RefGen_v2 presents 39,656 protein-encoding genes which give rise to the assumption of novel *Aux/IAA* genes. To obtain a comprehensive overview of the maize *Aux/IAA* gene family, the maize filtered gene set (ZmB73_5b_FGS; http://www.maizegdb.org/) and the maize accessions in the ProFITS (Protein Families Involved in Transduction of Signalling) database (http://bioinfo.cau.edu.cn/ProFITS/index.php) were screened for novel *Aux/IAA* genes using the sequences of the known 31 *Aux/IAA* genes in maize as query (Wang et al., 2010). All proteins encoded by novel *Aux/IAA* genes were assayed for the presence of the four Aux/IAA domains via a SMART (Simple Modular Architecture Research Tool; http://smart.embl-heidelberg.de/smart/set_mode.cgi) search. As a result 34 maize *Aux/IAA* genes were discovered including the 31 previously identified maize Aux/IA genes (Wang et al., 2010) and three novel genes designated *ZmIAA32* (GRMZM2G366373), *ZmIAA33* (GRMZM2G359924) and *ZmIAA34* (GRMZM2G031615) (Table 4.1). Proteins encoded by 29 *Aux/IAA* genes displayed all four domains. By contrast, in ZmIAA25 domains I and II are lacking and domains III and IV are incomplete. Moreover, domain II is absent in ZmIAA24 and ZmIAA26 whereas domain IV is missing in ZmIAA22 and ZmIAA31. Furthermore, in ZmIAA28 domain IV is split in two parts by the insertion of nine amino acids (Supplemental Figure 1). A summary of the characteristics of the 34 maize *Aux/IAA* genes and the proteins encoded by them is provided in Table 1. The four Aux/IAA domains are highlighted in an alignment of the Aux/IAA protein sequences by ClustalW (Supplemental Figure 1). The five ZmIAA proteins ZmIAA3, ZmIAA9, ZmIAA13, ZMIAA24, and ZmIAA26 displayed a modified LxLxPP instead of the predominant LxLxLP motif in domain I whereas the 13 Aux/IAA protein sequences ZmIAA4, ZmIAA6, ZmIAA9, ZmIAA11, ZmIAA12, ZmIAA16, ZmIAA17, ZmIAA18, ZmIAA20, ZmIAA23, ZmIAA30, ZmIAA33, and ZmIAA34 displayed a variation in the conserved motif of domain III

Table 4.1 Characteristics of the Aux/IAA gene family in maize

Name	*AC maizeGDB*	*Maize chromo-some*	*Genome location*	*Strand*	*Protein length (aa)*	*Sub-genome 1*	*Sub-genome 2*	*Maize chromosome with syntenic region*	*ZmIAA gene in syntenic region*	*Presence in rice and Sorghum*	*Rice chromo-some with syntenic region*	*Sorghum chromosome with syntenic region*
ZmIAA1	GRMZM2G079957_T2	1	170.535.129- 170.536.982	1	227	X		3	*ZmIAA8*	Os, Sb	12	8
ZmIAA2	GRMZM2G159285_T1	1	275.031.309- 275.034.076	-1	237	X		5	*ZmIAA14*	Os, Sb	3	1
ZmIAA3	GRMZM5G809195_T1	1	288.394.822- 288.396.335	-1	202	X		5	*ZmIAA13*	Os, Sb	3	1
ZmIAA4	GRMZM2G104176_T1	3	7.117.449- 7.120.087	-1	229	X				Os, Sb	1	3
ZmIAA5	GRMZM2G004696_T1	3	10.073.330- 10.076.684	1	220	X		8	*ZmIAA27*	Os, Sb	1	3
ZmIAA6	GRMZM2G074742_T1	3	48.981.283- 48.983.063	1	198	X				Os, Sb	1	3
ZmIAA7	GRMZM2G138268_T1	3	117.766.041- 117.770.646	-1	271		X			Os, Sb	12	8
ZmIAA8	GRMZM2G167794_T1	3	118.064.610- 118.066.326	-1	230		X	1	*ZmIAA1*	Os, Sb	12	8
ZmIAA9	GRMZM2G057067_T1	3	199.305.498- 199.307.986	-1	357	X				Os, Sb	1	3
ZmIAA10	GRMZM2G037368_T1	3	209.094.740- 209.098.102	-1	269	X		8	*ZmIAA29*	Os, Sb	1	3
ZmIAA11	GRMZM2G059544_T2	4	39.557.305- 39.558.529	-1	251		X			Os, Sb	8	7
ZmIAA12	GRMZM2G142768_T1	4	171.373.109- 171.375.531	1	293		X			Os, Sb	2	4
ZmIAA13	GRMZM2G152796_T1	5	4.200.507- 4.201.934	-1	181		X	1	*ZmIAA3*	Os, Sb	3	1
ZmIAA14	GRMZM2G077356_T1	5	7.772.505- 7.775.451	1	228		X	1	*ZmIAA2*	Os, Sb	3	1
ZmIAA15	GRMZM2G128421_T1	5	17.343.149- 17.344.582	1	224							
ZmIAA16	GRMZM2G121309_T1	5	151.712.395- 151.716.302	1	289	X				Os, Sb	2	4
ZmIAA17	GRMZM2G030465_T1	5	214.411.995- 214.413.229	1	206	X				Os, Sb	2	4
ZmIAA18	GRMZM2G000158_T4	6	79.914.748- 79.916.495	-1	197		X	9	*ZmIAA30*	Os, Sb	6	10
ZmIAA19	GRMZM2G079200_T1	6	103.139.630- 103.141.327	-1	198		X			Os, Sb	6	10
ZmIAA20	GRMZM5G864847_T1	6	130.004.758- 130.006.167	-1	234							
ZmIAA21	GRMZM2G147243_T2	6	133.196.856- 133.200.588	1	244	X		8	*ZmIAA28*	Os, Sb	5	9
ZmIAA22	GRMZM2G141205_T1	6	146.505.719- 146.506.414	-1	231							
ZmIAA23	GRMZM2G074427_T2	6	160.166.708- 160.170.208	1	346	X				Os, Sb	5	9
ZmIAA24	GRMZM2G149449_T1	7	9.392.913- 9.393.634	1	115							
ZmIAA25	GRMZM2G115357_T2	7	10.970.395- 10.971.721	-1	66	X				Os, Sb	7	2
ZmIAA26	GRMZM2G048131_T1	7	142.773.908- 142.775.365	1	139	X				Os, Sb	9	2
ZmIAA27	GRMZM2G130953_T2	8	18.318.828- 18.320.919	-1	186		X	3	*ZmIAA5*	Os, Sb	1	3
ZmIAA28	GRMZM2G035465_T3	8	110.812.538- 110.816.166	-1	256		X	6	*ZmIAA21*	Os, Sb	1	9
ZmIAA29	GRMZM2G163848_T5	8	150.560.417- 150.563.479	1	272		X	3	*ZmIAA10*	Os, Sb	5	3
ZmIAA30	GRMZM2G001799_T1	9	16.249.556- 16.251.444	1	216	X		6	*ZmIAA18*	Os, Sb	6	10
ZmIAA31	GRMZM2G134517_T1	10	134.255.159- 134.255.926	-1	255							
ZmIAA32	GRMZM2G366373_T2	1	253.302.210- 253.303.545	-1	226							
ZmIAA33	GRMZM2G359924_T1	8	108,568,427- 108,570,670	1	228							
ZmIAA34	GRMZM2G031615_T2	4	16,418,192- 16,426,336	1	355	X				Os, Sb	11	5

4.2 Phylogeny and synteny of the *Aux/IAA* gene family

Phylogenetic reconstructions were based on the full-length sequences of the 34 maize Aux/IAA proteins. Two major groups of Aux/IAA proteins (class A and class B) were observed (Figure 4.1) which coincided with the alteration in the conserved motif in domain III (Supplemental Figure 1).

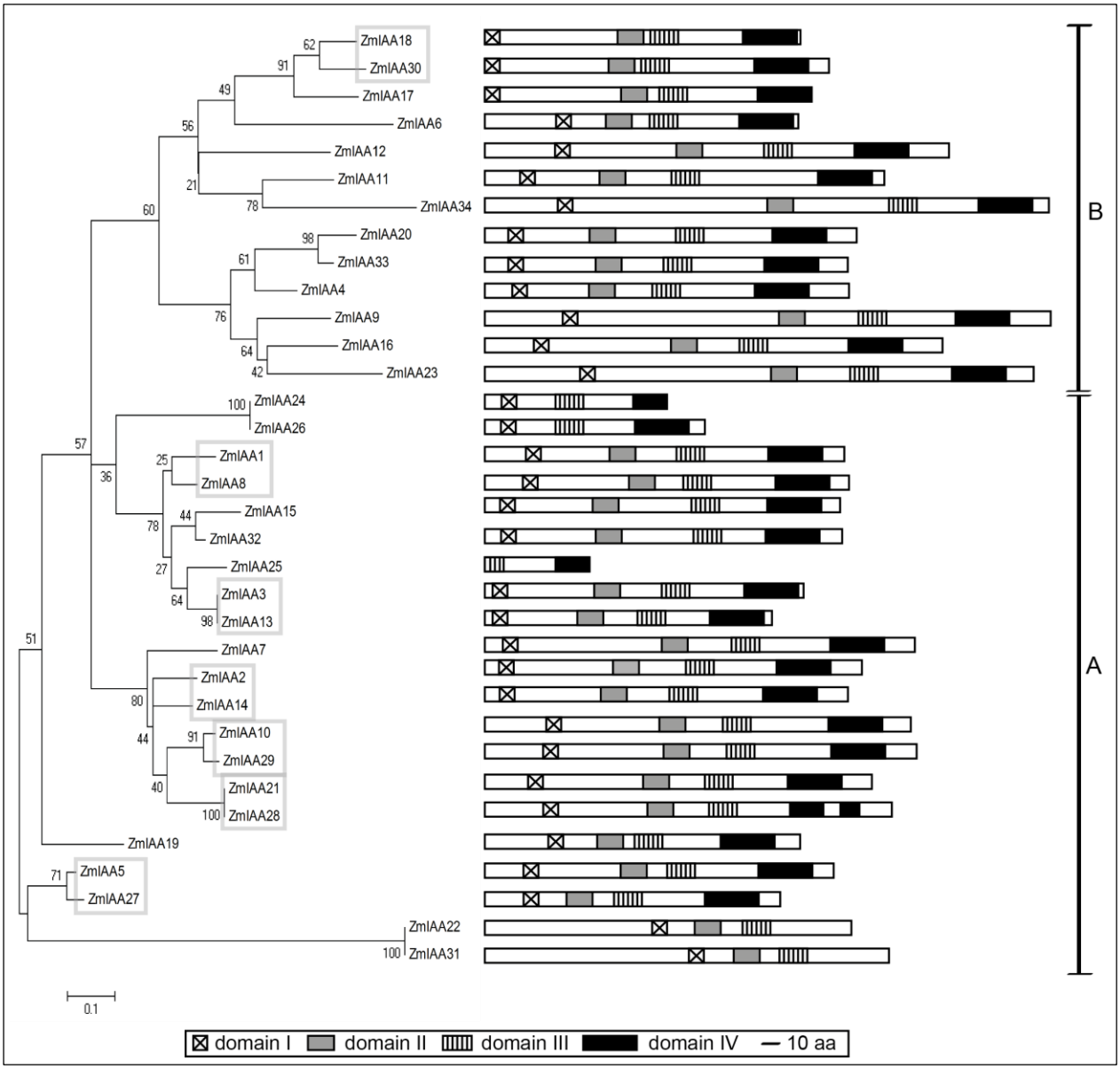

Figure 4.1 Unrooted phylogenetic tree and distribution of conserved domains in maize Aux/IAA proteins. The phylogenetic tree reveals two classes (A and B) of Aux/IAA proteins that differ in the sequence of domain III. The structure of the Aux/IAA proteins and the distribution of their domains are displayed to the right. The scale bar corresponds to 10 amino acids (aa). Paralogous *Aux/IAA* genes are boxed in grey. The values associated to each branch are bootstrap percentages. The size bar indicates sequence divergence: 0.1 = 10%.

Evolution and synteny of the maize *Aux/IAA* gene family was studied via CoGe (http://genomevolution.org/CoGe/ and Table 4.1). Paralogous genes in an organism emerged by a duplication of an ancestral gene (Taylor and Raes, 2004). In maize most paralogous genes emerged from an ancient whole genome duplication. Therefore, the two genes of a paralogous pair can be assigned to subgenomes maize 1 or 2. In total, seven pairs of paralogous maize *Aux/IAA* genes were identified (Table 4.1 and Figure 4.1). Moreover, for seven *Aux/IAA* genes (*ZmIAA15*, *ZmIAA20*, *ZmIAA22*, *ZmIAA24*, *ZmIAA31*, *ZmIAA32* and *ZmIAA33*) no orthologs were found in rice and *Sorghum* suggesting that these genes are the result of gene duplications after the separation of maize from rice and *Sorghum*. These non-syntenc genes could therefore not be allocated to the maize subgenomes.

Functional diversification of monocot maize, rice, and *Sorghum Aux/IAA* genes was studied by a phylogenetic reconstruction of the Aux/IAA proteins of these species (Supplemental Figure 2).

4.3 Expression studies of *Aux/IAA* genes in the maize root system

Aux/IAA gene expression profiles were determined in embryonic primary and seminal roots and in post-embryonic lateral and shoot-borne roots. Moreover, primary roots were surveyed at different developmental stages. Finally, different root tissues of the primary root including the meristematic and elongation zones and cortex and stele tissues of the differentiation zone were analyzed. Expression levels were determined by quantitative RT-PCR for 30 of 34 *Aux/IAA* genes. For the closely related genes *ZmIAA22*/*ZmIAA31* and *ZmIAA24*/*ZmIAA26* (Figure 4.1) no specific oligonucleotides were available that allowed to distinguish between them. Moreover, these four genes encode for Aux/IAA proteins that do not display the canonical four domain structure. Hence, expression profiles were generated for all 29 *Aux/IAA* genes that display the canonical four domain structure, plus for ZmIAA25 which displays only domain III and IV.

Expression patterns largely differed between the maize *Aux/IAA* genes (Figure 4.2 - 4.4). *ZmIAA5*, *ZmIAA8*, *ZmIAA12*, *ZmIAA14*, *ZmIAA15* and *ZmIAA29* displayed the highest expression levels in primary roots (Figure 4.2). *ZmIAA14* contributes to ~40% of all *Aux/IAA* transcripts in 1-2 cm primary roots and to ~35% in later developmental stages of the primary root. While *ZmIAA14* levels in young primary roots (up to the 4-8 cm class) are not significantly different, expression of this gene significantly decreases during the later developmental stages 4-8 cm and 8-16 cm (Supplemental Figures 3 and 4). *ZmIAA5* displays the second highest *Aux/IAA* expression in primary roots and provides 8% of the *Aux/IAA* transcripts in 1-2 cm primary roots and 20% in 8-16 cm primary roots. *ZmIAA5* displays a significant increase in gene expression between 1-2 cm

primary roots and 4-8 cm primary roots (Supplemental Figures 3 and 4). As in *ZmIAA14*, expression of *ZmIAA5* decreases between 4-8 cm and 8-16 cm primary roots.

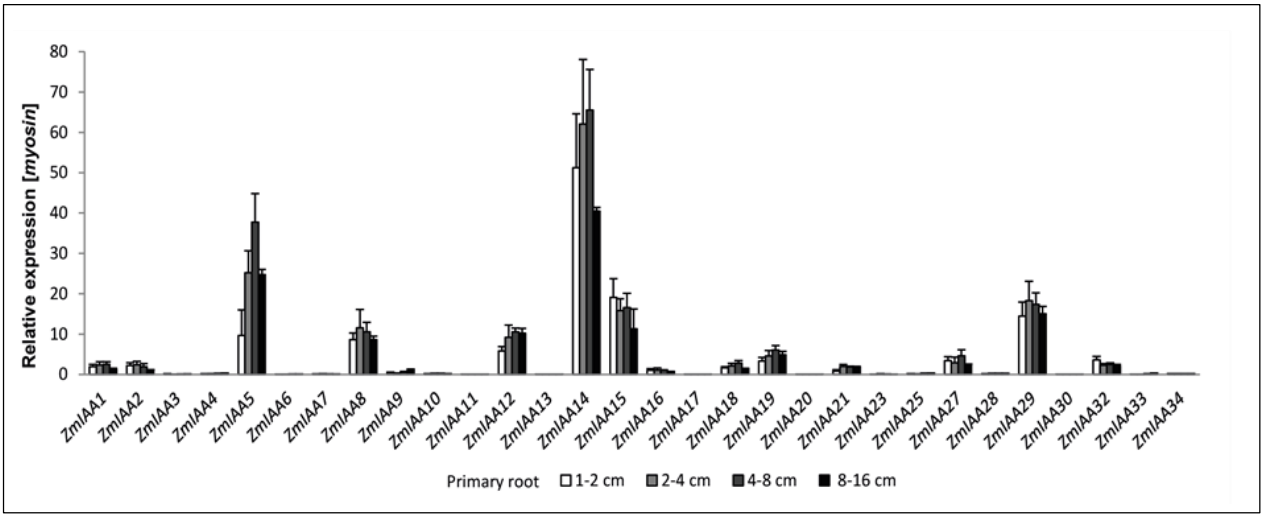

Figure 4.2 Expression of *Aux*/*IAA* genes during primary root development. Relative expression of 30 *Aux*/*IAA* genes was surveyed via qRT-PCR relative to *myosin.*

These six *Aux/IAA* genes also displayed the highest expression in primary root tissues three days after germination (Figure 4.3). Preferential expression in cortex and stele tissues compared to the meristematic and elongation zones was detected for 27 of 30 tested *Aux/IAA* genes (Supplemental Figure 3). Only *ZmIAA11*, *ZmIAA13* displayed the highest expression in the root apical meristem while in *ZmIAA34* expression in the meristematic and elongation zones were slightly higher than in the stele.

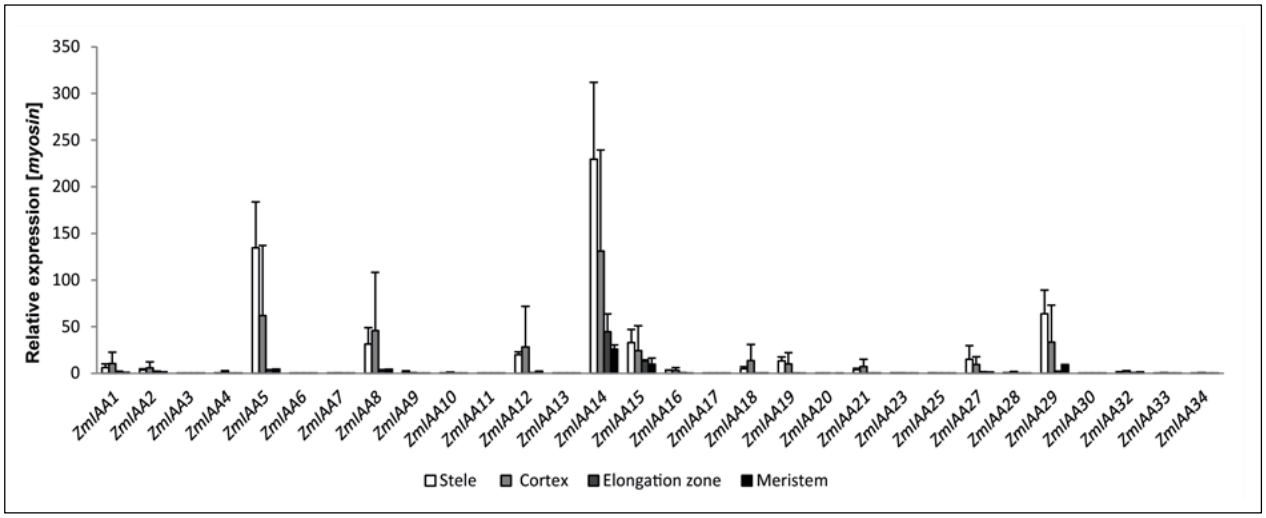

Figure 4.3 Expression of *Aux*/*IAA* genes in different three-day-old primary root tissues. Relative expression of 30 *Aux*/*IAA* genes was surveyed via qRT-PCR relative to *myosin.*

The six genes that displayed the highest expression in primary roots also displayed the highest expression in seminal, crown and lateral roots (Figure 4.4).

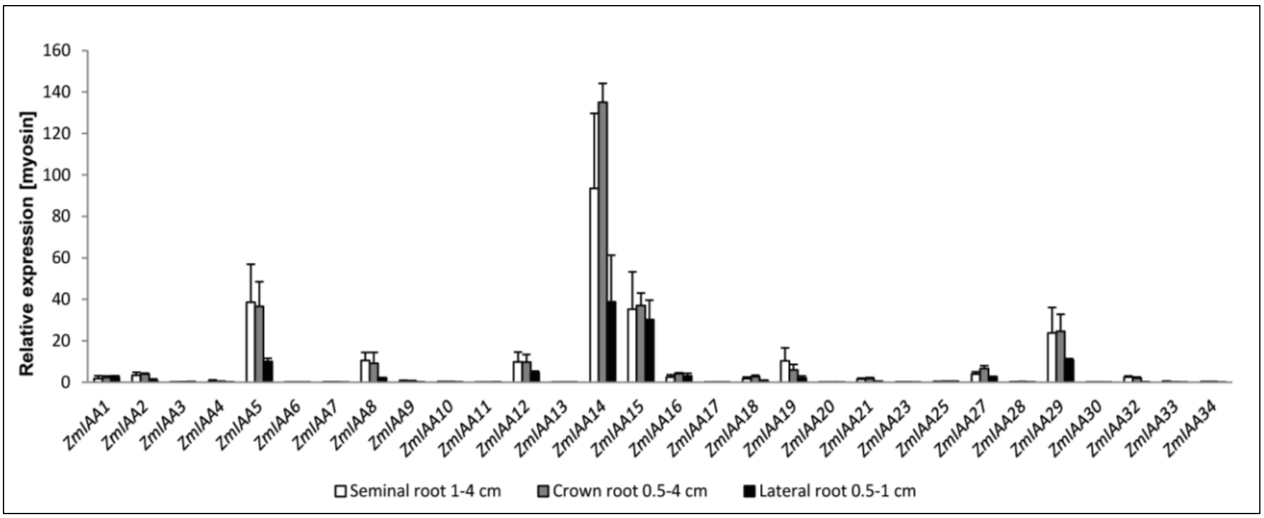

Figure 4.4 Expression of *Aux/IAA* genes in seminal, crown and lateral roots. Relative expression of 30 *Aux/IAA* genes was surveyed via qRT-PCR relative to *myosin.*

When analyzing differential gene expression of maize *Aux/IAA* genes between different root-types a total of 19 genes (*ZmIAA1*, *ZmIAA2*, *ZmIAA4*, *ZmIAA5*, *ZmIAA8*, *ZmIAA13*, *ZmIAA14*, *ZmIAA15*, *ZmIAA16*, *ZmIAA18, ZmIAA20, ZmIAA21, ZmIAA23, ZmIAA25, ZmIAA27, ZmIAA28, ZmIAA30, ZmIAA33, ZmIAA34*) displayed significantly higher expression in crown roots compared to at least one stage of primary root development (Supplemental Figures 3 and 4). In contrast, only *ZmIAA6* was significantly lower expressed in crown roots than at the three stages of primary root development (Supplemental Figure 3 and 4). Moreover, four genes were preferentially expressed in crown versus lateral roots (*ZmIAA2*, *ZmIAA13*, *ZmIAA28* and *ZmIAA30*) and another four genes were preferentially expressed in crown versus seminal roots (*ZmIAA16*, *ZmIAA27*, *ZmIAA28* and *ZmIAA30*). Hence, among 27 genes differentially expressed between crown roots and other root-types 26 displayed a higher expression in crown roots. When comparing differential gene expression between primary, seminal and lateral roots eleven genes were differentially expressed between primary and lateral roots (*ZmIAA5*, *ZmIAA7*, *ZmIAA8*, *ZmIAA9*, *ZmIAA12*, *ZmIAA13*, *ZmIAA18*, *ZmIAA21*, *ZmIAA27*, *ZmIAA32* and *ZmIAA34*). All of these genes except *ZmIAA27* displayed a higher expression in primary versus lateral roots. Moreover, nine genes were differentially expressed between at least one stage of primary root development and seminal roots (*ZmIAA3*, *ZmIAA6*, *ZmIAA9*, *ZmIAA13*, *ZmIAA16*, *ZmIAA21*, *ZmIAA25*, *ZmIAA28* and *ZmIAA30*). Only *ZmIAA6* and *ZmIAA9* were preferentially expressed in primary roots while the remaining seven genes were preferentially expressed in seminal roots. Finally, seven genes were preferentially expressed in seminal versus lateral roots (*ZmIAA7*, *ZmIAA8*, *ZmIAA10*, *ZmIAA13*,

ZmIAA20, *ZmIAA21* and *ZmIAA34*). These differential expression patterns display a strong bias for expression levels between the different root-types which applies to 51 of 55 (93%) of the pairwise differential expression patterns between different root-types observed in the present study. This pattern suggests that differentially expressed *Aux/IAA* genes follow in most instances the following hierarchy of expression: crown roots > seminal roots > primary roots > lateral roots.

To complement the expression profile of the *Aux/IAA* gene family, different shoot tissues of young maize seedling were analyzed (Supplemental Figure 3). The genes *ZmIAA6*, *ZmIAA9*, and *ZmIAA20* displayed a significantly higher expression in shoot tissues than in any root tissue. In all three instances the genes were highly expressed in the mesocotyl. Moreover, for some *Aux/IAA* genes expression in the coleoptile was higher than in some of the root tissues (Supplemental Figure 3). Such a preferential expression was however not observed for leaves and coleoptilar node.

4.4 Correlation of gene expression patterns of paralogous *Aux/IAA* gene pairs

To compare expression patterns between the seven paralogous maize gene pairs in roots coefficients of determination were calculated based on the gene expression data (Figure 4.5). This analysis revealed a strong linear correlation ($p \leq 0.01$) for five of seven gene pairs up to $R^2 = 0.96$ (*ZmIAA21*/*ZmIAA28*). Nevertheless, for all five pairs of paralogs one of the genes displayed on average a significantly higher expression level than the other one. The paralogous pairs *ZmIAA3*/*ZmIAA13* ($R^2 = 0.35$) and *ZmIAA18*/*ZmIAA30* ($R^2 < 0.01$) did not display any significant correlation with respect to their expression patterns in roots.

The paralogous *Aux/IAA* pairs *ZmIAA1*/*ZmIAA8*, *ZmIAA5*/*ZmIAA27*, *ZmIAA21*/*ZmIAA28* and *ZmIAA3*/*ZmIAA13* revealed a higher expression level of the gene located in maize subgenome 1 compared to the paralog in subgenome 2. In the other three pairs *ZmIAA2*/*ZmIAA14*, *ZmIAA10/ZmIAA29* and *ZmIAA18/ZmIAA30* the gene of subgenome 2 was preferentially expressed.

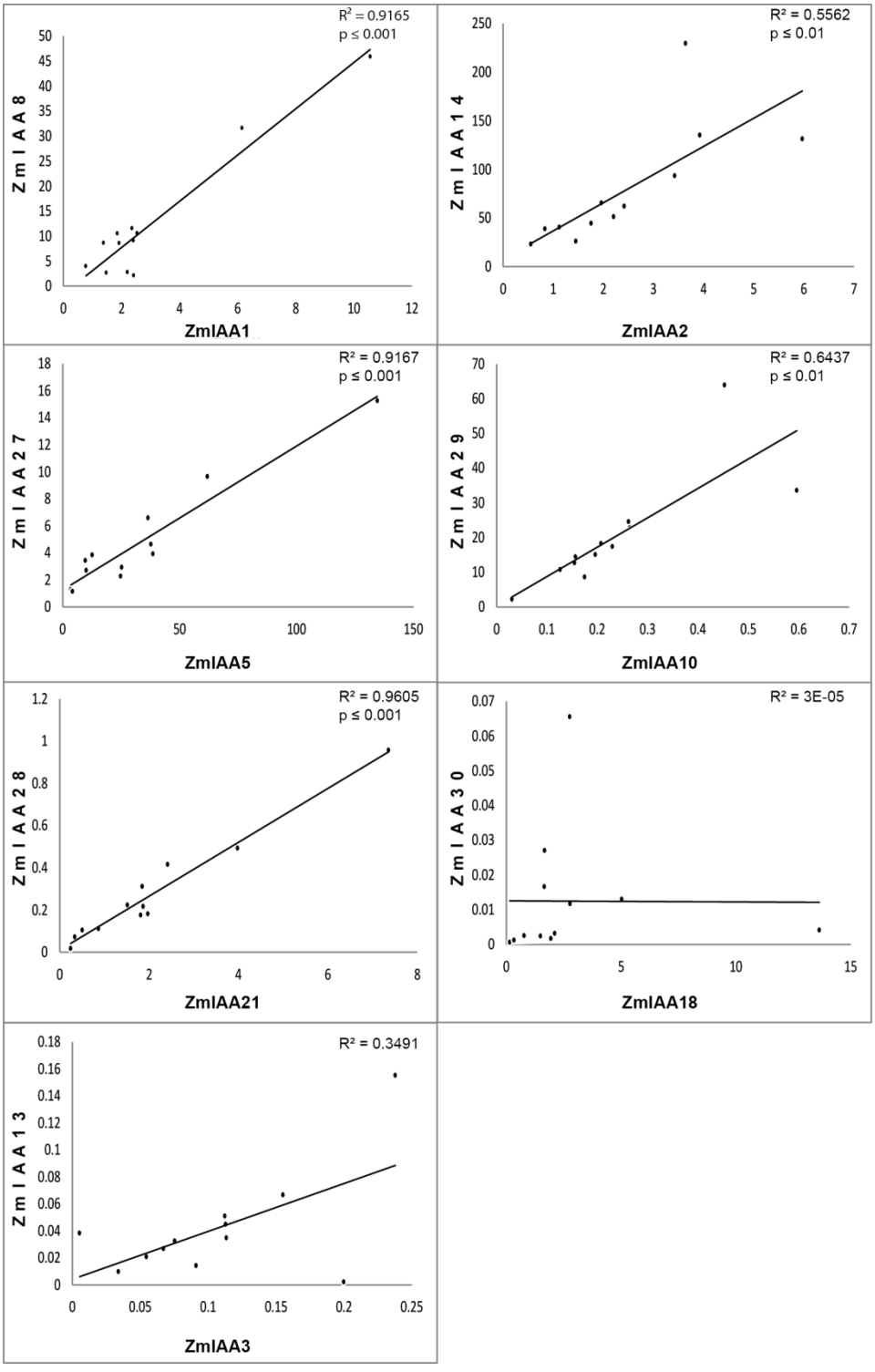

Figure 4.5 Correlation of gene expression of the seven paralogous *Aux/IAA* gene pairs in maize roots. Five of seven paralogous *Aux/IAA* pairs showed a significant correlation in their gene expression patterns in roots (coefficient of determination $R^2 > 0.5$; $p \leq 0.01$). Only *ZmIAA30/ZmIAA18* and *ZmIAA13/ZmIAA3* did not display significant expression correlation in the tested root-types and tissues.

4.5 Auxin inducibility of maize *Aux/IAA* genes

Screening for *cis*–elements in the regulatory region 3 kb upstream of ATG revealed that 28 of 34 analyzed maize *Aux/IAA* promoters contain canonical auxin response elements (AuxRE) 5´ TGTCTC 3´ or its inverted sequence 5´ GAGACA 3´ (Supplemental Table 1). Moreover, all 34 maize *Aux/IAA* promoters contain several multiple tandem copies of the *AuxRE* core sequence 5´ TGTC 3´ or 5´GACA 3´. The presence of AuxRE motifs and its derivative suggests that these genes are regulated by auxin. Therefore, auxin induction of the maize *Aux/IAA* gene family was tested in the differentiation zone of young maize primary roots over a time period of 3 h by quantitative real-time PCR (Supplemental Figure 5). Two distinct expression patterns were observed after auxin treatment (Figure 4.6). In pattern A at least one time point displayed significantly increased expression compared to t_0 and expression at t_3 was still significantly higher than at t_0 (Figure 4.6A and Supplemental Figure 4). Moreover, in pattern B expression at t_1 or t_2 was significantly increased compared to t_0, whereas expression at t_2 or t_3 was significantly decreased compared to t_2 or t_1, respectively (Figure 4.6B and Supplemental Figure 4). The majority (22 of 27) of maize Aux/IAA genes displayed pattern A (Figure 4.6A and Supplemental Figure 4). Pattern B was observed for *ZmIAA8*, *ZmIAA13*, *ZmIAA20*, *ZmIAA25* and *ZmIAA33* (Figure 4.6B and Supplemental Figure 4). Moreover, *ZmIAA30* and *ZmIAA34* were below the detection limit to observe any expression. *ZmIAA23* was the only maize gene that was not induced by auxin (Supplemental Figure 4).

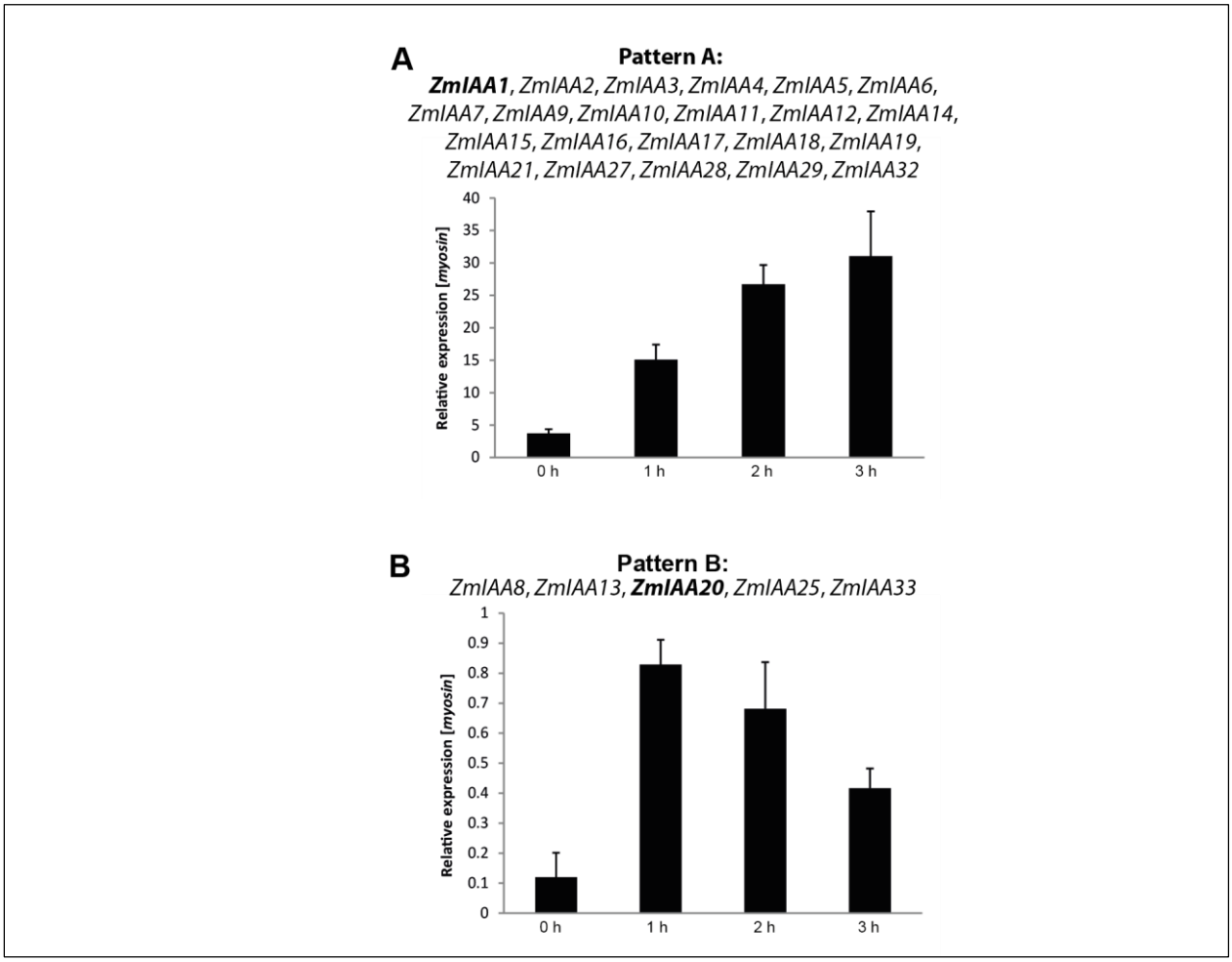

Figure 4.6 Auxin (α-NAA) induction of maize *Aux/IAA* genes. Two patterns of auxin induction were identified by qRT-PCR in the differentiation zone of 5-day-old maize primary roots after 5 µM α- NAA (α-Naphthalene Acetic Acid) treatment over three hours. Genes were either constitutively induced (A) or expression decreased relative to the initial induction (B). Each pattern is illustrated by one example (in bold) while other *Aux/IAA* genes that followed these induction patterns are listed. All tested *Aux/IAA* genes were α-NAA inducible except *ZmIAA23*. A detailed account of the *Aux/IAA* induction results is provided in Supplemental Figure 5.

4.6 Selection of representative maize *Aux/IAA* genes for further analyses

The maize *Aux/IAA* gene family contains 34 members (Ludwig et al., 2013). To investigate functional properties of *Aux/IAA* genes *ZmIAA2* (GRMZM2G159285), *ZmIAA11* (GRMZM2G059544), *ZmIAA15* (GRMZM2G128421), *ZmIAA20* (GRMZM5G864847) and *ZmIAA33* (GRMZM2G359924) were selected for further analyses. Aux/IAA proteins encoded by these five genes display the canonical four domain structure, contain a nuclear localization signal (NLS), and have a size between 224 to 251 amino acids (Supplemental Figure 6). As a reference, the sequences of the previously characterized RUM1 (ZmIAA29) and RUL1 (ZmIAA10) proteins have been added to Supplemental Figure 6. These maize *Aux/IAA* genes were selected because they represent different properties of members of this gene family (Table 4.2). First, these genes have different phylogenetic ancestries and relationships. Based on their relationship to the unduplicated *Sorghum* genome, *ZmIAA2* (subgenome 1) and *ZmIAA11* (subgenome 2) emerged before the last whole genome duplication in maize ca. 5-12 million years ago, while the non-syntenic genes *ZmIAA11*, *ZmIAA20* and *ZmIAA33* emerged more recently by the duplication of individual *ZmIAA* genes. Moreover, these genes encode both classes of maize Aux/IAA proteins that are separated in the maize phylogenetic tree based on their sequence of domain III (class A: ZmIAA2, ZmIAA15; class B: ZmIAA11, ZmIAA20, ZmIAA33). Furthermore, these genes displayed distinct root-type specific gene expression kinetics in response to auxin. While *ZmIAA2*, *ZmIAA11*, *ZmIAA20* and *ZmIAA33* display root-type specific expression patterns, *ZmIAA15* is highly expressed in all root-types. Moreover, *ZmIAA2*, *ZmIAA11* and *ZmIAA15* are significantly increased upon α-NAA treatment within three hours (pattern A), while *ZmIAA20* and *ZmIAA33* are initially induced by auxin followed by a significant decrease of expression (pattern B) (Ludwig et al., 2013).

Table 4.2 Characteristics of maize Aux/IAA proteins selected for functional characterization[a].

Protein	maizegdb.org AC	Subgenome	Phylogenetic class	Auxin inducibility	Expression in maize roots
ZmIAA2	GRMZM2G159285_P1	1	A	A	Crown > Primary
ZmIAA11	GRMZM2G059544_P2	2	B	A	Lateral > All root types
ZmIAA15	GRMZM2G128421_P1	Non-syntenic	A	A	Constitutively high
ZmIAA20	GRMZM5G864847_P1	Non-syntenic	B	B	Seminal > Lateral
ZmIAA33	GRMZM2G359924_P1	Non-syntenic	B	B	Seminal > Primary

[a] according to Ludwig et al. 2013

4.7 Protein stability measurements of Aux/IAA proteins via degradation assays

The rapid degradation of Aux/IAA proteins in response to high auxin levels is crucial for auxin signal transduction and thus controls the activity of downstream gene activity. To compare the stability kinetics of the five selected maize Aux/IAA proteins, C-terminal green fluorescent protein (GFP) fusions were generated. Two different point mutations were introduced into the degron sequence (VGWPPV) of the Aux/IAA proteins. These mutations resulted in a substitution of the first proline (P) by serine (S), or the exchange of the second proline (P) by leucine (L). In *Arabidopsis*, it was demonstrated that these specific substitutions resulted in more stable proteins compared to the wild-type (Worley et al., 2000; Gray et al., 2001). The relative GFP fluorescence intensity was determined over a time period of two hours in *Arabidopsis* protoplasts by flow cytometry, after treatment with the synthetic auxin α-NAA and cycloheximide. As a control, the GFP fluorescence intensity of free GFP was measured. For each of the five Aux/IAA proteins, different average half-life times were determined: ZmIAA2 had an average half-life time of ~11 minutes, ZmIAA20 and ZmIAA33 displayed a half-life time of ~40 minutes and ZmIAA11 and ZmIAA15 displayed the longest average half-life times of ~60 and ~120 minutes, respectively (Figure 4.7). As a consequence of the substitution of the amino acid P to S or L in the degron sequence, all modified Aux/IAA proteins were significantly more stable than their respective wild-type protein during the whole time course of 120 minutes. Most mutated Aux/IAA proteins appeared slightly less stable than the GFP control, as indicated by a minimal decrease of the measured GFP fluorescence intensity over time. However these values were not significantly different from the GFP control. The degradation of the Aux/IAA proteins was independently confirmed by Western Blot experiments (Supplemental Figure 7).

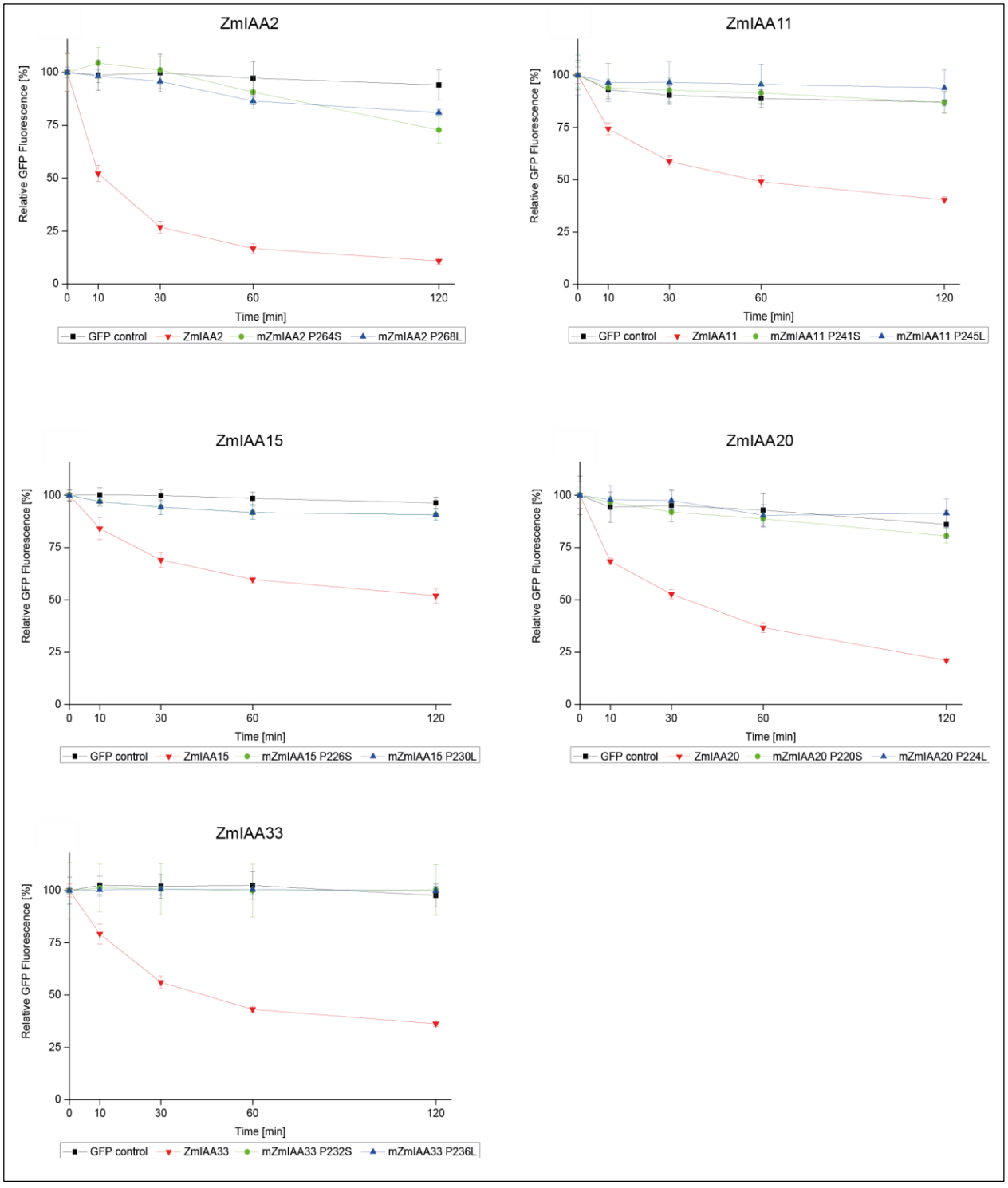

Figure 4.7 Degradation assay of maize Aux/IAA-GFP wild-type fusion proteins and Aux/IAA proteins containing mutations in their degron sequence**.** Detection of relative GFP-fluorescence of the GFP control, wild-type and two mutated forms of Aux/IAA proteins after α-NAA and cycloheximide treatment prior to recording a two hour time course in *Arabidopsis* protoplasts. Red: wild-type, green: substitution of first proline by serine, blue: substitution of second proline by leucine, black: GFP control.

4.8 Subcellular localization of Aux/IAA proteins

Aux/IAA proteins are transcriptional repressors and therefore act in the nucleus. To survey the subcellular localization of the selected Aux/IAA proteins, C-terminal GFP-fusion proteins of wild-type and the two mutated forms (point mutations as describe above paragraph 4.7) were generated for all five *Aux/IAA* genes and transiently expressed in maize mesophyll protoplasts. The wild-type GFP-fusion proteins of ZmIAA2-GFP, ZmIAA11-GFP and ZmIAA15-GFP and their respective mutated forms were exclusively accumulated in the nucleus. In contrast, ZmIAA20-GFP and ZmIAA33-GFP were localized in both the nucleus and the cytosol in maize protoplasts (Figure 4.8 and Supplemental Figure 8). Both, ZmIAA20 and ZmIAA33 have an incomplete NLS lacking the amino acids KR in the first part of the bipartite NLS which might explain their subcellular localization pattern (Supplemental Figure 6). ZmIAA11-GFP and ZmIAA20-GFP displayed a compartmentalized expression in the nucleus (Figure 4.8). To investigate if the compartmentalization in the nucleus is a consequence of the C-terminal GFP fusion, N-terminal GFP-fusion proteins of wild-type and their mutated forms were generated. Identical results, i.e. compartmentalized GFP signals, were observed for GFP-ZmIAA11 and GFP-ZmIAA20 and their mutated forms (Supplemental Figure 8).

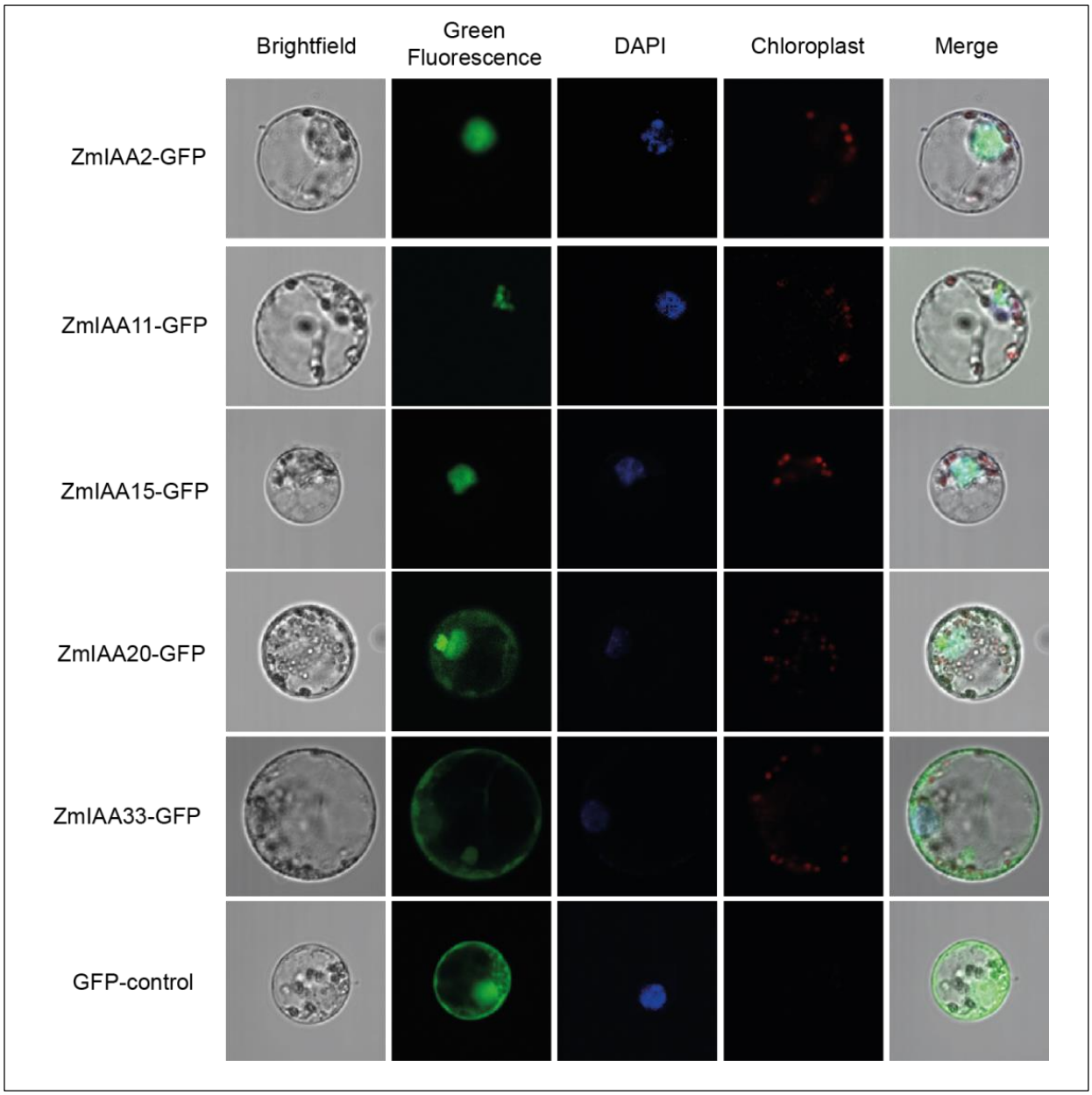

Figure 4.8 Subcellular localization of Aux/IAA-GFP fusion proteins in maize protoplasts by GFP-fluorescence. ZmIAA2, ZmIAA11 and ZmIAA15 were localized in the nucleus. Cytosolic and nuclear localization was identified for ZmIAA20 and ZmIAA33. Green: GFP fluorescence, red: auto fluorescence of chloroplasts, blue: DAPI counterstaining, red: auto fluorescence.

4.9 Transcriptional repression of downstream genes by Aux/IAA proteins

Transcriptional repression of Aux/IAA proteins is mediated by domain I. To investigate the regulation of downstream genes by the five maize Aux/IAA proteins, the Dual-Luciferase® reporter assay was applied in *Arabidopsis* protoplasts. This system allows to test if proteins containing a GAL4-DBD (DNA binding domain), function as repressors or activators of downstream gene expression by their control of *firefly* luciferase activity by binding to a GAL4-UAS (Upstream Activating Sequence) of a reporter gene. *Renilla* luciferase activity is used as internal reference to normalize the determined values.

Fusion proteins containing a N-terminal yeast GAL4 DNA-binding domain and full-length wild-type Aux/IAA proteins at the C-terminus were used as effectors (Figure 4.9). The reporter plasmid encoded *firefly* luciferase (LUC) proteins driven by a minimal TATA box of the CaMV 35S promoter combined with an upstream GAL4-UAS binding site. *Arabidopsis* protoplasts were co-transformed with three plasmids including the reference plasmids encoding for *Renilla* LUC, a reporter plasmids encoding for *firefly* LUC and either the control GAL4-DBD effector plasmid or effector plasmids encoding for one of the five GAL4-DBD-ZmIAA proteins. Relative *firefly* luciferase activity of the Aux/IAA proteins was measured and quantified relative to the control GAL4-DBD protein. All GAL4-DBD-ZmIAA proteins exerted a significant reduction of relative luciferase activity on the downstream reporter gene compared to the GAL4-DBD control (Figure 4.9). GAL4-DBD-ZmIAA2 and GAL4-DBD-ZmIAA15 displayed the strongest reduction, with only ~30% residual relative luciferase activities. Moreover, the relative luciferase activity was ~36% for GAL4-DBD-ZmIAA11 and ~48% for GAL4-DBD-ZmIAA33, whereas GAL4-DBD-ZmIAA20 displayed ~77% activity relative to the GAL4-DBD control (Figure 4.9). These results suggest a significant transcriptional repression of downstream genes by the tested Aux/IAA proteins but also a considerable variability between the repressor function of different Aux/IAA proteins.

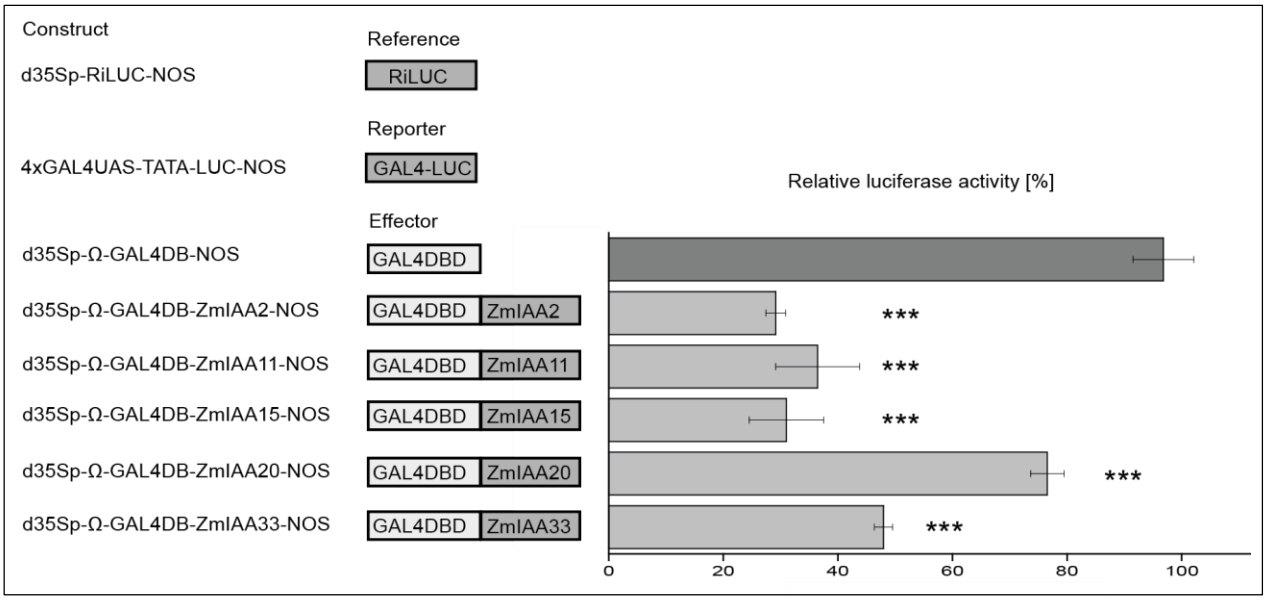

Figure 4.9 Repression of a *firefly* luciferase reporter gene by Aux/IAA proteins fused to a GAL4 DNA binding domain. Aux/IAA proteins fused to GAL4 DNA binding domains were co-transformed with a *firefly* luciferase reporter into *Arabidopsis* protoplasts. All luciferase activities were normalized relative to the empty effector vector (GAL4-DBD) and an internal luciferase control (*Renilla* luciferase). Error bars: SD, n = 3, ***: $p \leq 0.001$.

4.10 Protein – protein interaction of Aux/IAA proteins

Domains III and IV of Aux/IAA proteins allow dimerization with other Aux/IAA proteins or auxin response factors (ARFs) (Kim et al., 1997). To examine homotypic interactions of the five Aux/IAA proteins surveyed in the present study, quantitative bimolecular fluorescence complementation (BiFC) experiments were performed by flow cytometric analysis of transformed protoplasts. Subsequently, the results obtained in flow cytometric analyses were independently confirmed by analyzing BiFC interactions in individual protoplasts under a Zeiss LSM 780 (attached with Axio Observer Z1, Zeiss) confocal laser scanning microscope. Homotypic interaction of the Aux/IAA proteins ZmIAA11, ZmIAA15 and ZmIAA33 was detected in quantitative FACS experiments and confirmed in subsequent confocal laser scanning microscope studies of individual protoplasts. Homotypic interactions of ZmIAA2 and ZmIAA20 were neither detected by flow cytometry nor when analyzing BiFC interactions in individual cells in a confocal laser scanning microscope (Figure 4.10 and Table 4.3). Moreover, interaction of the five maize Aux/IAA proteins studied here was tested with the previously characterized paralogous RUM1 (ZmIAA10) and RUL1 (ZmIAA29) proteins involved in maize lateral and seminal root formation. Interactions were detected for all five tested Aux/IAA proteins with RUM1, whereas only ZmIAA15 and ZmIAA33 interacted with RUL1 (Figure 4.10 and Table 4.3). These interactions were validated quantitatively by flow cytometry and confirmed in individual protoplasts by confocal imaging. None of the negative

controls using the BARW protein, which does not interact with Aux/IAA proteins, revealed an interaction with any of the five Aux/IAA proteins (Supplemental Figure 9). Expression of the proteins in the interaction studies was confirmed by Western Blot analyses (Supplemental Figure 10).

Table 4.3 Statistical evaluation of BiFC data using lineal model for logarithmized data and simulation-based multiple comparisons by Edwards and Berry (1987)

Interacting proteins	Value (log scale)[a]	*p*-value[b]	adj *p*-value[c]	sign[d]
ZmIAA2-YFPN/ZmIAA2-YFPC	0.80	0.41	1	ns
ZmIAA2-YFPN/RUM1-YFPC	2.30	0.02	0.60	ns
RUM1-YFPN/ZmIAA2-YFPC	4.06	< 0.01	< 0.01	*
ZmIAA2-YFPN/RUL1-YFPC	1.43	0.14	1.00	ns
RUL1-YFPN/ZmIAA2-YFPC	2.86	< 0.01	0.17	ns
ZmIAA11-YFPN/ZmIAA11-YFPC	10.06	< 0.01	< 0.01	*
ZmIAA11-YFPN/RUM1-YFPC	0.69	0.47	1	ns
RUM1-YFPN/ZmIAA11-YFPC	5.22	< 0.01	< 0.01	*
ZmIAA11-YFPN/RUL1-YFPC	0.87	0.37	1	ns
RUL1-YFPN/ZmIAA11-YFPC	3.16	< 0.01	0.07	ns
ZmIAA15-YFPN/ZmIAA15-YFPC	11.42	< 0.01	< 0.01	*
ZmIAA15-YFPN/RUM1-YFPC	7.05	< 0.01	< 0.01	*
RUM1-YFPN/ZmIAA15-YFPC	7.93	< 0.01	< 0.01	*
ZmIAA15-YFPN/RUL1-YFPC	5.29	< 0.01	< 0.01	*
RUL1-YFPN/ZmIAA15-YFPC	6.74	< 0.01	< 0.01	*
ZmIAA20-YFPN/ZmIAA20-YFPC	1.65	0.09	0.99	ns
ZmIAA20-YFPN/RUM1-YFPC	3.71	< 0.01	< 0.01	*
RUM1-YFPN/ZmIAA20-YFPC	-0.94	0.33	1	ns
ZmIAA20-YFPN/RUL1-YFPC	2.14	0.03	0.75	ns
RUL1-YFPN/ZmIAA20-YFPC	-0.53	0.58	1	ns
ZmIAA33-YFPN/ZmIAA33-YFPC	9.64	< 0.01	< 0.01	*
ZmIAA33-YFPN/RUM1-YFPC	5.09	< 0.01	< 0.01	*
RUM1-YFPN/ZmIAA33-YFPC	7.57	< 0.01	< 0.01	*
ZmIAA33-YFPN/RUL1-YFPC	2.65	0.01	0.30	ns
RUL1-YFPN/ZmIAA33-YFPC	6.80	< 0.01	< 0.01	*

[a]value after using lineal model for logarithmized data

[b]t-test of value (log scale)

[c]*p*-value adjusted for simulation-based multiple comparisons by Edwards and Berry (1987)

[d]significance: ns - not significant; * significant

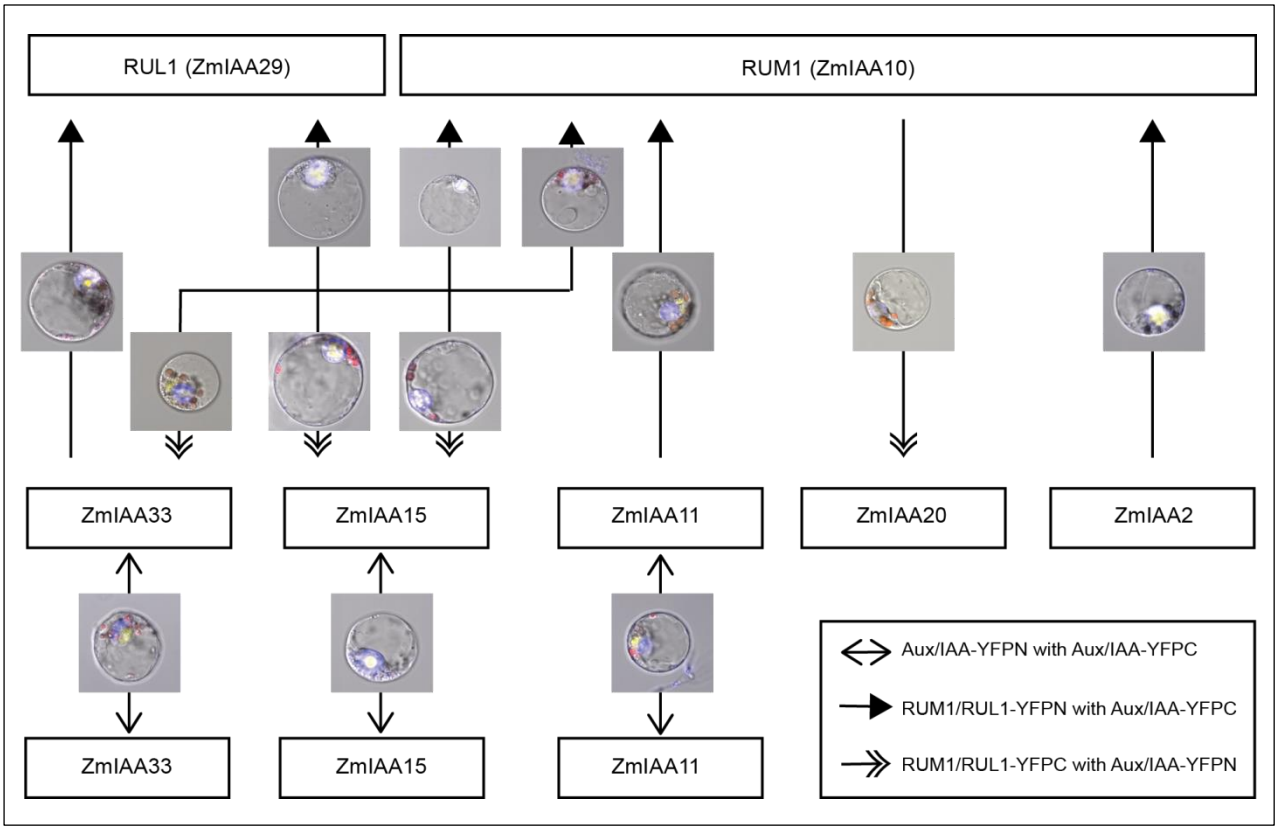

Figure 4.10 Homo and heterointeraction of Aux/IAA proteins. The model summarizes the quantitative BiFC data obtained by flow cytometry and the verification via qualitative BiFC experiments surveyed under a confocal microscope. Homotypic protein interactions of Aux/IAA proteins were identified for ZmIAA11, ZmIAA15 and ZmIAA33 but not for ZmIAA20 and ZmIAA2. Heterotypic interactions of RUM1 were detected with all five tested Aux/IAA proteins. Protein-protein interaction of RUL1 was detected with ZmIAA15 and ZmIAA33. The arrowhead types are indicating the interacting partners. A full arrowhead describes a RUM1/RUL1-YFPN with Aux/IAA-YFPC interaction, while and double arrowhead denotes a RUM1/RUL1-YFPC with Aux/IAA-YFPN interaction. Homotypic interactions of ZmIAA11, ZmIAA15 and ZmIAA33 are highlighted with another arrowhead type because only one combination is possible. Yellow: YFP–fluorescence, red: auto fluorescence of chloroplasts, blue: DAPI counterstaining.

5 Discussion

5.1 Identification of novel Aux/IAA genes and structural analysis of the gene family

Aux/IAA genes are plant-specific transcription factors (Reed, 2001). Initially, 31 maize *Aux/IAA* genes were discovered in the maize genome (Wang et al., 2010). Improved annotation allowed for the identification of three novel *Aux/IAA* genes (*ZmIAA32:* GRMZM2G366373, *ZmIAA33:* GRMZM2G359924, *ZmIAA34*: GRMZM2G031615) in the present study increasing their total number in maize to 34. Similarly, the rice genome contains 31 *Aux/IAA* genes (Jain et al., 2006), while the *Arabidopsis Aux/IAA* gene family consists of 29 members (Liscum and Reed, 2002).

Sequence analysis of the maize Aux/IAA protein family revealed that five maize Aux/IAA proteins do not contain all four domains characteristic for this protein family (Figure 4.1). Similarly, domain II which is required for the degradation of the Aux/IAA proteins is partially or totally missing in OsIAA4, OsIAA8, OsIAA27, OsIAA28 and OsIAA29 in rice (Jain et al., 2006) and in AtIAA20, AtIAA30, AtIAA31, AtIAA32, AtIAA33, and AtIAA34 in *Arabidopsis* (Dreher et al., 2006). Moreover, tomato Sl-IAA32 does not have domain II and Sl-IAA33 is lacking domains I and II (Audran-Delalande et al., 2012).

In several genes modifications of characteristic amino acid sequences were observed. The LxLxLx motif in domain I is known to function as repressor and is characteristic for flowering plants. In contrast, LxLxPP is typically found in mosses or in one of the three *Aux/IAA* genes of the vascular non-seed plant *Selaginella moellendorffii* (Paponov et al., 2009). Nevertheless, the sequence LxLxPP was also observed in five maize Aux/IAA proteins (ZmIAA3, ZmIAA9, ZmIAA13, ZmIAA24 and ZmIAA26), while In *Arabidopsis* and in rice no LxLxPP motives were found. The vascular non-seed plant *S. moellendorffii* and flowering plants do not form monophylentic groups, suggesting that the motif was established independently in each ancestry. In *Arabidopsis* it was reported that specific point-mutations in codons that encode the leucine residue in the domain I motif lead to a weaker repression of ARF-mediated transcription (Tiwari et al., 2004). Although there is no evidence that LxLxPP functions as a repressor domain it was proposed to be functionally important due to its wide distribution outside the flowering plants (Paponov et al., 2009).

5.2 Synteny and correlation of maize *Aux/IAA* genes

The diversity and complexity of the *Aux/IAA* gene family in modern maize can be explained by gene and genome duplications and by gene loss because of partial fractionation. The maize genome was duplicated ~5-12 million years ago which resulted in two maize subgenomes (Woodhouse et al., 2010). As a consequence, pairs of paralogous *Aux/IAA* genes emerged in

maize. Seven pairs of paralogous *Aux/IAA* genes are retained in the maize genome (Figure 4.1). This implies that the maize *Aux/IAA* gene family was already diversified by gene duplications before this whole genome duplication event. Based on their synteny with *Sorghum*, a species which has not been duplicated, maize genes can be allocated to the maize subgenomes 1 or 2. The chromosomal regions with less gene loss were designated subgenome maize 1 (Schnable and Freeling, 2011). A classical model of gene duplication assumes that over time one duplicated gene maintains the original function, while a second copy is lost, silenced, evolves a new function or in rare instances maintains its function (Duarte et al., 2006). Hence some of these gene pairs might have diversified by subfunctionalization or neofunctionalization (Lynch and Force, 2000). Five of the seven paralogous *Aux/IAA* gene pairs displayed a significant correlation of their gene expression patterns in roots (Figure 4.5). Among those, only one pair (*ZmIAA21*/ZmIAA*28*) also showed similar expression patterns in shoot tissues. The correlation in gene expression for five of seven *Aux/IAA* gene pairs might imply functional redundancy of these gene pairs. Nevertheless, even for these gene pairs functional diversification cannot be excluded because the average expression levels of these gene pairs are significantly different. Similarly, functional redundancy has been reported for *Arabidopsis* and rice *Aux/IAA* genes (Overvoorde et al., 2005; Paponov et al., 2009; Song et al., 2009).

In the maize *Aux/IAA* gene family thirteen genes which can be assigned to either subgenome 1 or 2 but for which no paralog was retained are the result of partial fractionation. Finally, seven *Aux/IAA* genes were not assigned to any of the maize subgenomes (Table 4.1). These genes likely emerged after the ancient maize genome duplication. Therefore, the *Aux/IAA* gene family in modern maize is the result of ancient gene duplications, a whole genome duplication, partial fractionation and modern gene duplications.

5.3 Root-type specific expression of *Aux/IAA* genes

In the present study a systematic expression analysis of different maize root-types, primary root tissues and developmental stages of the primary root revealed root and tissue-specific expression patterns. The six maize *Aux/IAA* genes *ZmIAA5*, *ZmIAA8*, *ZmIAA12*, *ZmIAA14*, *ZmIAA15* and *ZmIAA29* displayed an overall high expression in all tested embryonic and postembryonic roots (Figure 4.2 – 4.4). This might suggest that these *Aux/IAA* genes play a constitutive role during maize root development. Similarly, the rice genes *OsIAA5*, *OsIAA6* and *OsIAA23* displayed the highest expression levels in roots (Jain et al., 2006). Among those, *OsIAA5* is the ortholog of the maize paralogs *ZmIAA10/rum1* and *ZmIAA29*. Hence, both of the closely related genes *OsIAA5* and *ZmIAA29* display a very high expression in roots (Jain et al., 2006). Similarly, *OsIAA23* and

ZmIAA5 which both display high expression levels in roots map to the same phylogenetic clade. However, while *ZmIAA14* displays the highest transcript level of all tested maize *Aux/IAA* genes, its rice ortholog *OsIAA13* displays only low expression in roots. Hence, while some rice and maize genes might have conserved their function in root development during evolution other members of the gene family might have not. Interestingly, none of ten cotton *Aux/IAA* genes displayed a major expression peak in roots (Han et al., 2012).

Among the 30 maize *Aux/IAA* genes tested in the present study only three genes displayed significantly higher expression in non-root tissue than in any of the tested root samples Supplemental Figure 3). In contrast, among the 31 rice *Aux/IAA* genes only *OsIAA6* and *OsIAA23* revealed their expression maximum in six day-old roots compared to shoot tissues. The maize ortholog of *OsIAA6* is *ZmIAA9* which displayed its expression maximum in the mesocotyl. In contrast, *ZmIAA19* which is the ortholog of the rice gene *OsIAA23* displays higher expression levels in all root-types than in any of the analyzed shoot tissues. This supports the notion that even among the closely related maize and rice *Aux/IAA* gene families a functional diversification of the gene family members has occurred during evolution (Jain et al., 2006). However, very different tissues and developmental stages were analyzed in these maize and rice studies which makes them difficult to compare.

Thus far mutant analyses of maize *Aux/IAA* genes revealed only for *ZmIAA10* which corresponds to *rootless with undetectable meristem 1* (*rum1*) a defective phenotype during development. The mutant does not initiate seminal roots and lacks lateral roots at the primary root while primary and shoot-borne roots are not affected (von Behrens et al., 2011). In the present study *ZmIAA10* displays the highest expression in stele and cortex tissues of three-day old primary roots (Figure 4.3 and Supplemental Figure 3). This is in line with the observed phenotype because lateral roots are initiated from pericycle cells of the stele and from endodermis cells of the cortex (Fahn, 1990). Moreover, *ZmIAA10*/*rum1* displays significantly lower expression in the elongation zone than in any root-type or tissue (Supplemental Figure 4).

When *Aux/IAA* gene expression was compared pairwise between the four major maize root-types primary, seminal, lateral and crown roots 55 differential gene expression patterns were observed among the 30 maize *Aux/IAA* genes. Remarkably, among these differential expression patterns there was a strong bias with respect to expression levels between the different roots types with the tendency: crown roots > seminal roots > primary roots > lateral roots. Since this is a very general trend it might reflect differential control of auxin signal transduction in the molecular context of different root-types. Root-type-specific expression levels of *Aux/IAA* genes are

controlled by upstream factors that bind to AuxRE in the promoter of *Aux/IAA* genes. Abundance of *Aux/IAA* transcripts and their proteins also affect the activity of downstream genes and thus contribute to the specific forms and functions of the different root-types of maize.

In 27 of 30 maize *Aux/IAA* genes surveyed in the present study preferential expression in cortex and stele tissues of the differentiation zone compared to the meristematic and elongation zones was observed (Figure 4.3). This expression pattern correlates with auxin response in maize roots as visualized by DR5:RFP (Jansen et al., 2012). DR5:RFP reports sites where strong Aux/IAA protein degradation occurs (Jansen et al., 2012). These sites typically correlate with auxin maxima which enhance the transcription of *Aux/IAA* genes. Hence, DR5:RFP is also an indirect sensor for *Aux/IAA* transcriptional activity. In maize roots DR5:RFP maxima were observed in metaxylem elements and phloem poles in the stele (Jansen et al., 2012). Moreover, at early stages of lateral root development auxin response maxima were detected in pericycle and endodermis cells (Jansen et al., 2012). Remarkably, DR5:RFP also displays a strong signal in the meristematic zone of maize roots (Jansen et al., 2012). In this zone only moderate *Aux/IAA* transcription was observed for most members of the gene family. However, while the DR5:RFP peak is mainly in the root cap expression was surveyed in root tips that went beyond the root cap and also included the meristematic zone.

5.4 Patterns of auxin induction in *Aux/IAA* genes

Auxin-responsive (AuxRE) *cis*-elements are characteristic for the promoters of auxin-responsive genes (Hagen and Guilfoyle, 2002). Promoter analyses illustrated that all maize *Aux/IAA* genes contain canonical auxin-response elements or their core sequence (Supplemental Table 1). In contrast, in the promoter region of *Aux/IAA* genes of *Vitis vinifera* no AuxRE motifs were identified (Cakir et al., 2013). Similarly, in *Arabidopsis* only the promoters of *AtIAA26* and *AtIAA29* contain an AuxRE motif (Remington et al., 2004). Consequently, auxin-induced gene expression may be directed by tissue-specific factors different than Aux/IAA proteins in these plants (Remington et al., 2004; Cakir et al., 2013). Other promoter elements like MYB and bZIP related binding sites play a role in the auxin-mediated transcription (Shin et al., 2007; Berendzen et al., 2012a). Similar results were presented for a putative ocs-element in *Arabidopsis* (Chen and Singh, 1999). In line with the presence of AuxRE or their core elements 27 of 28 expressed maize *Aux/IAA* genes were auxin inducible in qRT-PCR experiments. Similarly, in rice 24 of 29 expressed Aux/IAA genes were auxin inducible (Song et al., 2009). The kinetics of *Aux/IAA* gene expression is unique and depends on the variability of the regulation of free auxin, tissue-specific auxin receptors and different regulation of transcriptional and posttranscriptional events (Jain et al., 2006). In maize,

two auxin-dependent expression patterns were observed after αNAA treatment (Figure 4.6). While 22 *Aux/IAA* genes were constantly induced over time, five *Aux/IAA* genes showed a significant decrease after an initial increase in expression. Similarly, in rice 12 of 24 Aux/IAA genes displayed continuously increased expression during the time course while 12 genes displayed decreased expression at later time points (Song et al., 2009). In tomato up-regulation of transcript levels of 17 of 19 *Sl-Aux/IAA* genes was detected in seedlings upon auxin treatment (Audran-Delalande et al., 2012).

5.5 Variability of maize Aux/IAA protein half-life times

Canonical Aux/IAA proteins consist of four conserved domains (I-IV) and a bipartite NLS (Abel and Theologis, 1995). The five *Aux*/*IAA* genes characterized in the present study (ZmIAA2, ZmIAA11, ZmIAA15, ZmIAA20 and ZmIAA33) display all four domains (Supplemental Figure 6). Previously, it has been demonstrated that these five *Aux*/*IAA* genes display specific expression patterns in different root-types and tissues and represent two different patterns of auxin inducibility in primary roots (Ludwig et al., 2013 and Table 4.2).

Domain II of Aux/IAA proteins contains the degron sequence which confers the rapid degradation of Aux/IAA proteins by interacting with the SCF^{TIR1} complex (Dharmasiri et al., 2005a). As a consequence, Aux/IAA proteins are short-lived proteins with a half-life time of ~6 to 8 min in pea (Abel et al., 1994) and ~10 to ~80 min in *Arabidopsis thaliana* (Gray et al., 2001; Ramos et al., 2001). Specific point mutations in the short degron sequence VGWPPV stabilizes these Aux/IAA proteins (Worley et al., 2000; Gray et al., 2001; Ouellet et al., 2001; Dreher et al., 2006). The half-life time of maize RUM1 (ZmIAA10) has been previously determined as ~22 min (von Behrens et al., 2011). In the present study, half-life times of maize Aux/IAA proteins ranged from ~11 min (ZmIAA2), to ~120 min (ZmIAA15). ZmIAA20 and ZmIAA33 displayed a half-life time of ~40 min (Figure 4.7). Both genes are closely related to each other and display 77% identity in their amino acid sequence. Similarly, *Arabidopsis* Aux/IAA proteins, that share a high similarity outside the conserved domain II, displayed similar half-life times (Dreher et al., 2006), suggesting that the degron sequence is required for the degradation of Aux/IAA proteins but the half-life time of these proteins is also determined by sequences outside the degron motif (Dreher et al., 2006). The half-life time of ZmIAA15 (~120 min) exceeded the most stable *Arabidopsis* Aux/IAA proteins AXR3/IAA17 (Ouellet et al., 2001) and IAA28 at ~80 min (Dreher et al., 2006). The difference in stability of different maize Aux/IAA proteins tested here might be a result of tissue-or organ-specific regulation by yet unidentified proteins or unidentified stabilons of degrons outside of domain II (Dreher et al., 2006). In line with the predicted molecular function of the degron motif, point

mutations, substituting the first P by S or the second P by L, in the sequences of the five Aux/IAA proteins analyzed resulted in proteins that displayed almost no degradation (<10%) over a time period of 120 min. Similar results were described for the mutated maize ZmIAA10 protein rum1-R in which the degron sequence was completely deleted (von Behrens et al., 2011). A slight degradation (10-20%) was observed for the two mutated proteins of ZmIAA2 (mZmIAA2-P264S and mZmIAA2-P268L) and mZmIAA20-P220S relative to the control. However, this was not statistically significant different from the degradation observed for free GFP, which was used as a control.

5.6 Nuclear and cytosolic localization of Aux/IAA proteins

Commonly, Aux/IAA proteins hold a bipartite nuclear localization signal (NLS), which directs them into the nucleus. Nuclear localization was observed for the Aux/IAA proteins ZmIAA2, ZmIAA11 and ZmIAA15 and their mutated forms (Figure 4.8 and Supplemental Figure 8). Previously we demonstrated that the RUM1 protein (ZmIAA10) is also localized in the nucleus (von Behrens et al., 2011). Similar results were described for the Aux/IAA proteins AXR2-GUS and AXR3NT-GUS in *Arabidopsis*, which were localized in the nucleus (Gray et al., 2001; Ouellet et al., 2001). In contrast, ZmIAA20 and ZmIAA33 were not exclusively expressed in the nucleus but also in the cytosol (Figure 4.8). This might be a result of the two missing conserved amino acids KR of the first part of the NLS (Supplemental Figure 6). Similarly, in maize the rum1-R protein was localized in the nucleus and cytosol. In *Arabidopsis*, only one Aux/IAA protein, AtIAA8, was thus far localized in the cytosol and nucleus (Arase et al., 2012). A function of Aux/IAA proteins in the cytosol has been described recently by the interaction of LSD1 (LESIONS SIMULATING DISEASE RESISTANCE 1) with AtIAA8 (Coll et al., 2011). LSD1 is a cytosolic protein which negatively controls cell death and disease resistance. Furthermore, it sequesters the transcriptional factor AtbZIP10 (Kaminaka et al., 2006). Hence, ZmIAA20 and ZmIAA33 might not exclusively function in the transcriptional regulation of auxin signaling but may also play a role in cytosolic processes.

5.7 Active repressor function of Aux/IAA proteins

All Aux/IAA proteins analyzed in the present study repressed downstream gene expression as demonstrated by a dual luciferase-assay. Relative luciferase activity was repressed between ~23% (GAL4-DBD-ZmIAA20) and ~70% (GAL4-DBD-ZmIAA2 und GAL4-DBD-ZmIAA15) by the Aux/IAA effectors in comparison to the GAL4-DBD control (Figure 4.9). Previously we demonstrated that maize RUM1 (ZmIAA10) exerted a transcriptional repression of ~59% on downstream target genes (von Behrens et al., 2011). In *Arabidopsis*, the repressor function of domain I of sixteen Aux/IAA proteins was determined by GUS reporter assays. These Aux/IAA

proteins repressed the GUS reporter gene between 51% to 89% relative to the control (Tiwari et al., 2001). In *Arabidopsis*, a correlation was demonstrated between Aux/IAA protein stability in wild-type versus mutant proteins and their repression of early auxin response genes. Stabilizing mutations in domain II, resulted in enhanced repression of downstream targets by these proteins. In contrast, mutations in domain I and III were able to partially reverse repressor function (Tiwari et al., 2001).

5.8 Specific interactions of Aux/IAA proteins with RUM1 and its paralog RUL1

Protein-protein interaction studies revealed homo- and heterotypic interaction of Aux/IAA proteins in maize. Homotypic interaction of ZmIAA11, ZmIAA15 and ZmIAA33 was determined by BiFC experiments which were quantified by flow cytometry and subsequently independently verified by confocal microscopy (Figure 4.10 and Table 4.3). In yeast-two hybrid experiments, homotypic interactions of *Arabidopsis* IAA1 and IAA2 and IAA4 of pea were described (Kim et al., 1997). Aux/IAA proteins have a similar topology as prokaryotic transcriptional repressors which lead to the hypothesis that Aux/IAA dimers may regulates gene activity by binding directly to DNA (Paciorek and Friml, 2006). Protein-protein interaction of five Aux/IAA proteins with RUM1 (ZmIAA10) and RUL1 (ZmIAA29) were quantified in BiFC experiments, and confirmed via confocal microscopy on maize protoplasts (Figure 4.8 and Table 4.3). Hetero-interactions were observed for all Aux/IAA proteins tested with RUM1, while only two of five ZmIAA proteins (ZmIAA15 and ZmIAA33) interacted with RUL1. The *Aux*/*IAA* gene *rul1* is expressed ~84 fold higher than *rum*1. Likewise it is known that *ZmIAA15* is one of the highest expressed genes in the maize *Aux*/*IAA* gene family in contrast to that of *ZmIAA2*, *ZmIAA20* and *ZmIAA33* which display relatively low expression (Ludwig et al., 2013). However, the expression levels of the different *Aux*/*IAA* genes were not correlated with the interaction between them suggesting specificity of Aux/IAA interactions irrespective of their expression levels. In yeast-two hybrid experiments, *Arabidopsis* IAA1 interacted with 15 different Aux/IAA proteins (Kim et al., 1997). It was suggested that several hundred dimer combinations might be responsible for the diversity of physiological and morphological responses of these transcription factors based on the observation of differential spatial and temporal expression patterns of *Aux/IAA* genes in plants (Kim et al., 1997).

5.9 Conclusions

In summary, the analysis of the maize *Aux/IAA* gene family in the present study provides novel insights in the organization and expression of this large gene family that plays a crucial role in auxin signal transduction and thus the regulation of maize development.

Moreover, tissue and root-type-specific expression profiles and auxin induction studies provide starting points for genetic analyses of candidate genes that might be involved in the initiation, emergence or specification of specific root-types in the complex maize root stock.

The functional characterization of selected Aux/IAA proteins revealed a wide variability of different molecular functions of maize Aux/IAA proteins. In combination with specific expression patterns in root and shoot tissues, these results support the notion of a wide range of Aux/IAA protein functions in plant growth and development.

6 References

Abel, S., and Theologis, A. (1995). A polymorphic bipartite motif signals nuclear targeting of early auxin-inducible proteins related to PS-IAA4 from pea (*Pisum sativum*). Plant J **8,** 87-96.

Abel, S., and Theologis, A. (1996). Early genes and auxin action. Plant Physiol **111,** 9-17.

Abel, S., Oeller, P.W., and Theologis, A. (1994). Early auxin-induced genes encode short-lived nuclear proteins. Proc Natl Acad Sci USA **91,** 326-330.

Abel, S., Nguyen, M.D., and Theologis, A. (1995). The *PS-IAA4/5-like* Family of Early Auxin-inducible mRNAs in *Arabidopsis thaliana*. J Mol Biol **251,** 533-549.

Aiken, R.M., and Smucker, A.J.M. (1996). Root system regulation of whole plant growth. Annu Rev Phytopathol **34,** 325-346.

Ainley, W.M., Walker, J.C., Nagao, R.T., and Key, J.L. (1988). Sequence and characterization of two auxin-regulated genes from soybean. J Biol Chem **263,** 10658-10666.

Arase, F., Nishitani, H., Egusa, M., Nishimoto, N., Sakurai, S., Sakamoto, N., and Kaminaka, H. (2012). IAA8 Involved in Lateral Root Formation Interacts with the TIR1 Auxin Receptor and ARF Transcription Factors in *Arabidopsis*. PLoS ONE **7,** e43414.

Audran-Delalande, C., Bassa, C., Mila, I., Regad, F., Zouine, M., and Bouzayen, M. (2012). Genome-Wide Identification, Functional Analysis and Expression Profiling of the *Aux/IAA* Gene Family in Tomato. Plant Cell Physiol **53,** 659-672.

Bais, H.P., Weir, T.L., Perry, L.G., Gilroy, S., and Vivanco, J.M. (2006). The role of root exudates in rhizosphere interactions with plants and other organisms. Annu Rev Plant Biol **57,** 233-266.

Bell, J.K., and McCully, M.E. (1970). A histological study of lateral root initiation and development in *Zea mays*. Protoplasma **70,** 179-205.

Benková, E., Michniewicz, M., Sauer, M., Teichmann, T., Seifertová, D., Jürgens, G., and Friml, J. (2003). Local, Efflux-Dependent Auxin Gradients as a Common Module for Plant Organ Formation. Cell **115,** 591-602.

Berendzen, K., Weiste, C., Wanke, D., Kilian, J., Harter, K., and Droge-Laser, W. (2012a). Bioinformatic *cis*-element analyses performed in Arabidopsis and rice disclose bZIP- and MYB-related binding sites as potential AuxRE-coupling elements in auxin-mediated transcription. BMC Plant Biol **12,** 125.

Berendzen, K., Bohmer, M., Wallmeroth, N., Peter, S., Vesic, M., Zhou, Y., Tiesler, F., Schleifenbaum, F., and Harter, K. (2012b). Screening for in planta protein-protein interactions combining bimolecular fluorescence complementation with flow cytometry. Plant Meth **8,** 25.

Cakir, B., Kilickaya, O., and Olcay, A.C. (2013). Genome-wide analysis of *Aux/IAA* genes in *Vitis vinifera*: cloning and expression profiling of a grape *Aux/IAA* gene in response to phytohormone and abiotic stresses. Acta Physiol Plant **35,** 365-377.

Chapman, E.J., and Estelle, M. (2009). Mechanism of Auxin-Regulated Gene Expression in Plants. Annu Rev Genet **43,** 265-285.

Chen, W., and Singh, K.B. (1999). The auxin, hydrogen peroxide and salicylic acid induced expression of the Arabidopsis GST6 promoter is mediated in part by an *ocs* element. Plant J **19,** 667-677.

Coll, N.S., Epple, P., and Dangl, J.L. (2011). Programmed cell death in the plant immune system. Cell Death Differ **18,** 1247-1256.

del Pozo, J.C., and Estelle, M. (1999). The Arabidopsis cullin AtCUL1 is modified by the ubiquitin-related protein RUB1. Proc Natl Acad Sci USA **96,** 15342-15347.

Dharmasiri, N., Dharmasiri, S., and Estelle, M. (2005a). The F-box protein TIR1 is an auxin receptor. Nature **435,** 441-445.

Dharmasiri, N., Dharmasiri, S., Weijers, D., Lechner, E., Yamada, M., Hobbie, L., Ehrismann, J.S., Jürgens, G., and Estelle, M. (2005b). Plant Development Is Regulated by a Family of Auxin Receptor F Box Proteins. Dev Cell **9,** 109-119.

Dharmasiri, S., Dharmasiri, N., Hellmann, H., and Estelle, M. (2003). The RUB/Nedd8 conjugation pathway is required for early development in *Arabidopsis*. EMBO J **22,** 1762-1770.

Dreher, K.A., Brown, J., Saw, R.E., and Callis, J. (2006). The Arabidopsis Aux/IAA Protein Family has Diversified in Degradation and Auxin Responsiveness. Plant Cell **18,** 699-714.

Drew, M.C., and Saker, L.R. (1975). Nutrient Supply and the Growth of the Seminal Root System in Barley: II. Localized, compensatory increases in lateral root growth and rates up nitrate uptake when nitrate supply is restricted to only parts of the root system. J Exp Bot **26,** 79-90.

Duarte, J.M., Cui, L., Wall, P.K., Zhang, Q., Zhang, X., Leebens-Mack, J., Ma, H., Altman, N., and dePamphilis, C.W. (2006). Expression Pattern Shifts Following Duplication Indicative of Subfunctionalization and Neofunctionalization in Regulatory Genes of *Arabidopsis*. Mol Biol Evol **23,** 469-478.

Edwards, D., and Berry, J.J. (1987). The Efficiency of Simulation-Based Multiple Comparisons. Biometrics **43,** 913–928.

Erdelska, O., and Vidovencova, Z. (1993). Development of adventitious seminal root primordia during embryogenesis. Biologia **48,** 85-88.

Esau, K. (1965). *Plant Anatomy*. 2nd edn. John Wiley and Sons**,** New York.

Estelle, M. (1992). The Plant Hormone Auxin - Insight in Sight. BioEssays **14,** 439-444.

Fahn, A. (1990). Plant Anatomy. (Pergamon Press, Oxford).

Feldman, L. (1994). The Maize Root. In The Maize Handbook, M. Freeling and V. Walbot, eds (Springer New York), pp. 29-37.

Fukaki, H., Taniguchi, N., and Tasaka, M. (2006). PICKLE is required for SOLITARY-ROOT/IAA14-mediated repression of ARF7 and ARF19 activity during Arabidopsis lateral root initiation. Plant J **48,** 380-389.

Fukaki, H., Tameda, S., Masuda, H., and Tasaka, M. (2002). Lateral root formation is blocked by a gain-of-function mutation in the *SOLITARY-ROOT/IAA14* gene of *Arabidopsis*. Plant J **29,** 153-168.

Gray, W.M., Hellmann, H., Dharmasiri, S., and Estelle, M. (2002). Role of the Arabidopsis RING-H2 Protein RBX1 in RUB Modification and SCF Function. Plant Cell **14,** 2137-2144.

Gray, W.M., Kepinski, S., Rouse, D., Leyser, O., and Estelle, M. (2001). Auxin regulates SCFTIR1-dependent degradation of AUX/IAA proteins. Nature **414,** 271-276.

Gray, W.M., del Pozo, J.C., Walker, L., Hobbie, L., Risseeuw, E., Banks, T., Crosby, W.L., Yang, M., Ma, H., and Estelle, M. (1999). Identification of an SCF ubiquitin–ligase complex required for auxin response in *Arabidopsis thaliana*. Genes Dev **13,** 1678-1691.

Guilfoyle, T.J., and Hagen, G. (2012). Getting a grasp on domain III/IV responsible for Auxin Response Factor–IAA protein interactions. Plant Sci **190,** 82-88.

Hagen, G., and Guilfoyle, T. (2002). Auxin-responsive gene expression: genes, promoters and regulatory factors. Plant Mol Biol **49,** 373-385.

Hamann, T., Mayer, U., and Jurgens, G. (1999). The auxin-insensitive *bodenlos* mutation affects primary root formation and apical-basal patterning in the Arabidopsis embryo. Development **126,** 1387-1395.

Han, X., Xu, X., Fang, D.D., Zhang, T., and Guo, W. (2012). Cloning and expression analysis of novel Aux/IAA family genes in *Gossypium hirsutum*. Gene **503,** 83-91.

Hetz, W., Hochholdinger, F., Schwall, M., and Feix, G. (1996). Isolation and characterization of rtcs, a maize mutant deficient in the formation of nodal roots. Plant J **10,** 845-857.

Hochholdinger, F., Woll, K., Sauer, M., Feix, and G. (2005). Functional genomic tools in support of the genetic analysis of root development in maize (*Zea mays* L.). Maydica **50,** 437-442.

Hochholdinger, F. (2009). The Maize Root System: Morphology, Anatomy, and Genetics. In Handbook of Maize: Its Biology, J.L. Bennetzen and S.C. Hake, eds (Springer New York), pp. 145-160.

Hochholdinger, F., Park, W.J., Sauer, M., and Woll, K. (2004a). From weeds to crops: genetic analysis of root development in cereals. Trends Plant Sci **9,** 42-48.

Hochholdinger, F., Woll, K., Sauer, M., and Dembinsky, D. (2004b). Genetic Dissection of Root Formation in Maize (*Zea mays*) Reveals Root-type Specific Developmental Programmes. Ann Bot-London **93,** 359-368.

Hoppe, D.C., McCully, M.E., and Wenzel, C.L. (1986). The nodal roots of Zea: their development in relation to structural features of the stem. Can J Bot **64,** 2524-2537.

Ikeda, M., and Ohme-Takagi, M. (2009). A Novel Group of Transcriptional Repressors in *Arabidopsis*. Plant Cell Physiol **50,** 970-975.

Jain, M., Kaur, N., Garg, R., Thakur, J., Tyagi, A., and Khurana, J. (2006). Structure and expression analysis of early auxin-responsive *Aux*/*IAA* gene family in rice (*Oryza sativa*). Funct Integr Genomics **6,** 47-59.

Jansen, L., Roberts, I., De Rycke, R., and Beeckman, T. (2012). Phloem-associated auxin response maxima determine radial positioning of lateral roots in maize. Phil Trans R Soc B Biol Sci **367,** 1525-1533.

Kaminaka, H., Näke, C., Epple, P., Dittgen, J., Schütze, K., Chaban, C., Holt, B.F., Merkle, T., Schäfer, E., Harter, K., and Dangl, J.L. (2006). bZIP10-LSD1 antagonism modulates basal defense and cell death in *Arabidopsis* following infection. EMBO J **25,** 4400-4411.

Kim, J., Harter, K., and Theologis, A. (1997). Protein–protein interactions among the Aux/IAA proteins. Proc Natl Acad Sci USA **94,** 11786-11791.

Kitomi, Y., Inahashi, H., Takehisa, H., Sato, Y., and Inukai, Y. (2012). OsIAA13-mediated auxin signaling is involved in lateral root initiation in rice. Plant Sci **190,** 116-122.

Korasick, D.A., Westfall, C.S., Lee, S.G., Nanao, M.H., Dumas, R., Hagen, G., Guilfoyle, T.J., Jez, J.M., and Strader, L.C. (2014). Molecular basis for AUXIN RESPONSE FACTOR protein interaction and the control of auxin response repression. Proc Natl Acad Sci USA**,** Early edition.

Li, H., Cheng, Y., Murphy, A., Hagen, G., and Guilfoyle, T.J. (2009). Constitutive Repression and Activation of Auxin Signaling in *Arabidopsis*. Plant Physiol **149,** 1277-1288.

Li, M., Doll, J., Weckermann, K., Oecking, C., Berendzen, K.W., and Schöffl, F. (2010). Detection of in vivo interactions between Arabidopsis class A-HSFs, using a novel BiFC fragment, and identification of novel class B-HSF interacting proteins. Eur J Cell Biol **89,** 126-132.

Liscum, E., and Reed, J.W. (2002). Genetics of Aux/IAA and ARF action in plant growth and development. Plant Mol Biol **49,** 387-400.

Ludwig, Y., Zhang, Y., and Hochholdinger, F. (2013). The Maize (*Zea mays* L.) *AUXIN/INDOLE-3-ACETIC ACID* Gene Family: Phylogeny, Synteny, and Unique Root-Type and Tissue-Specific Expression Patterns during Development. PLoS ONE **8,** e78859.

Lynch, J. (1995). Root Architecture and Plant Productivity. Plant Physiol **109,** 7-13.

Lynch, M., and Force, A. (2000). The probability of duplicate gene preservation by subfunctionalization. Genetics **154,** 459-473.

Lyons, E., and Freeling, M. (2008). How to usefully compare homologous plant genes and chromosomes as DNA sequences. Plant J **53,** 661-673.

Martin, E.M., and Harris, W.M. (1976). Adventitious root development from the coleoptilar node in *Zea mays* L. Am J Bot **63,** 890-897.

McClintock, B. (1950). The origin and behavior of mutable loci in maize. Proc Natl Acad Sci USA **36,** 344-355.

McCully, M.E. (1999). ROOTS IN SOIL: Unearthing the Complexities of Roots and Their Rhizospheres. Annu Rev Plant Physiol Plant Mol Biol **50,** 695-718.

McCully, M.E., and Canny, M.J. (1988). Pathways and processes of water and nutrient movement in roots. Plant Soil **111,** 159-170.

Mockaitis, K., and Estelle, M. (2008). Auxin receptors and plant development: a new signaling paradigm. Annu Rev Cell Dev Biol **24,** 55-80.

Morgan, K.E., Zarembinski, T.I., Theologis, A., and Abel, S. (1999). Biochemical characterization of recombinant polypeptides corresponding to the predicted βαα fold in Aux/IAA proteins. FEBS Lett **454,** 283-287.

Nagpal, P., Walker, L.M., Young, J.C., Sonawala, A., Timpte, C., Estelle, M., and Reed, J.W. (2000). *AXR2* Encodes a Member of the Aux/IAA Protein Family. Plant Physiol **123,** 563-574.

Nakamura, A., Umemura, I., Gomi, K., Hasegawa, Y., Kitano, H., Sazuka, T., and Matsuoka, M. (2006). Production and characterization of auxin-insensitive rice by overexpression of a mutagenized rice IAA protein. Plant J **46,** 297-306.

Neuffer, M., Coe, E., and Wessler, S. (1997). Mutants of maize. (Cold Spring Harbor Laboratory Press, Cold Spring Harbor).

Nguyen, H.P., Chakravarthy, S., Velasquez, A.C., McLane, H.L., Zeng, L.R., Nakayashiki, H., Park, D.H., Collmer, A., and Martin, G.B. (2010). Methods to Study PAMP-Triggered Immunity Using Tomato and *Nicotiana benthamiana*. Mol Plant-Microbe Interact **23,** 991-999.

Ogas, J., Kaufmann, S., Henderson, J., and Somerville, C. (1999). PICKLE is a CHD3 chromatin-remodeling factor that regulates the transition from embryonic to vegetative development in Arabidopsis. Proc Natl Acad Sci USA **96,** 13839-13844.

Ouellet, F., Overvoorde, P.J., and Theologis, A. (2001). IAA17/AXR3: Biochemical Insight into an Auxin Mutant Phenotype. Plant Cell **13,** 829-841.

Overvoorde, P.J., Okushima, Y., Alonso, J.M., Chan, A., Chang, C., Ecker, J.R., Hughes, B., Liu, A., Onodera, C., Quach, H., Smith, A., Yu, G., and Theologis, A. (2005). Functional Genomic Analysis of the *AUXIN/INDOLE-3-ACETIC ACID* Gene Family Members in *Arabidopsis thaliana*. Plant Cell **17,** 3282-3300.

Paciorek, T., and Friml, J. (2006). Auxin signaling. J Cell Sci **119,** 1199-1202.

Paponov, I.A., Teale, W., Lang, D., Paponov, M., Reski, R., Rensing, S.A., and Palme, K. (2009). The evolution of nuclear auxin signalling. BMC Evol Biol **9,** 126.

Park, J.-Y., Kim, H.-J., and Kim, J. (2002). Mutation in domain II of IAA1 confers diverse auxin-related phenotypes and represses auxin-activated expression of Aux/IAA genes in steroid regulator-inducible system. Plant J **32,** 669-683.

Péret, B., De Rybel, B., Casimiro, I., Benková, E., Swarup, R., Laplaze, L., Beeckman, T., and Bennett, M.J. (2009). *Arabidopsis* lateral root development: an emerging story. Trends Plant Sci **14,** 399-408.

Petroski, M.D., and Deshaies, R.J. (2005). Function and regulation of cullin–RING ubiquitin ligases. Nat Rev Mol Cell Biol **6,** 9-20.

Pfluger, J., and Zambryski, P. (2004). The role of SEUSS in auxin response and floral organ patterning. Development **131,** 4697-4707.

Ramos, J.A., Zenser, N., Leyser, O., and Callis, J. (2001). Rapid degradation of auxin/indoleacetic acid proteins requires conserved amino acids of domain II and is proteasome dependent. Plant Cell **13,** 2349-2360.

Reed, J.W. (2001). Roles and activities of Aux/IAA proteins in *Arabidopsis*. Trends Plant Sci **6,** 420-425.

Reed, R.C., Brady, S.R., and Muday, G.K. (1998). Inhibition of Auxin Movement from the Shoot into the Root Inhibits Lateral Root Development in *Arabidopsis*. Plant Physiol **118,** 1369-1378.

Remington, D.L., Vision, T.J., Guilfoyle, T.J., and Reed, J.W. (2004). Contrasting Modes of Diversification in the *Aux/IAA* and *ARF* Gene Families. Plant Physiol **135,** 1738-1752.

Rinaldi, M., Liu, J., Enders, T., Bartel, B., and Strader, L. (2012). A gain-of-function mutation in IAA16 confers reduced responses to auxin and abscisic acid and impedes plant growth and fertility. Plant Mol Biol **79,** 359-373.

Rogg, L.E., Lasswell, J., and Bartel, B. (2001). A Gain-of-Function Mutation in *IAA28* Suppresses Lateral Root Development. Plant Cell **13,** 465-480.

Rouse, D., Mackay, P., Stirnberg, P., Estelle, M., and Leyser, O. (1998). Changes in Auxin Response from Mutations in an *AUX/IAA* Gene. Science **279,** 1371-1373.

Saleem, M., Lamkemeyer, T., Schützenmeister, A., Madlung, J., Sakai, H., Piepho, H.-P., Nordheim, A., and Hochholdinger, F. (2010). Specification of Cortical Parenchyma and Stele of Maize Primary Roots by Asymmetric Levels of Auxin, Cytokinin, and Cytokinin-Regulated Proteins. Plant Physiol **152,** 4-18.

Santner, A., A. Calderon-Villalobos, L.I., and Estelle, M. (2009). Plant hormones are versatile chemical regulators of plant growth. Nat Chem Biol **5,** 301-307.

Schiefelbein, J.W., Masucci, J.D., and Wang, H. (1997). Building a root: the control of patterning and morphogenesis during root development. Plant Cell **9,** 1089-1098.

Schnable, J.C., and Freeling, M. (2011). Genes Identified by Visible Mutant Phenotypes Show Increased Bias toward One of Two Subgenomes of Maize. PLoS ONE **6,** e17855-e17855.

Schnable, J.C., Springer, N.M., and Freeling, M. (2011). Differentiation of the maize subgenomes by genome dominance and both ancient and ongoing gene loss. Proc Natl Acad Sci USA **108,** 4069-4074.

Schnable, P.S., Ware, D., Fulton, R.S., Stein, J.C., Wei, F., Pasternak, S., Liang, C., Zhang, J., Fulton, L., Graves, T.A., Minx, P., Reily, A.D., Courtney, L., Kruchowski, S.S., Tomlinson, C., Strong, C., Delehaunty, K., Fronick, C., Courtney, B., Rock, S.M., Belter, E., Du, F., Kim, K., Abbott, R.M., Cotton, M., Levy, A., Marchetto, P., Ochoa, K., Jackson, S.M., Gillam, B., Chen, W., Yan, L., Higginbotham, J., Cardenas, M., Waligorski, J., Applebaum, E., Phelps, L., Falcone, J., Kanchi, K., Thane, T., Scimone, A., Thane, N., Henke, J., Wang, T., Ruppert, J., Shah, N., Rotter, K., Hodges, J., Ingenthron, E., Cordes, M., Kohlberg, S., Sgro, J., Delgado, B., Mead, K., Chinwalla, A., Leonard, S., Crouse, K., Collura, K., Kudrna, D., Currie, J., He, R., Angelova, A., Rajasekar, S., Mueller, T., Lomeli, R., Scara, G., Ko, A., Delaney, K., Wissotski, M., Lopez, G., Campos, D., Braidotti, M., Ashley, E., Golser, W., Kim, H., Lee, S., Lin, J., Dujmic, Z., Kim, W., Talag, J., Zuccolo, A., Fan, C., Sebastian, A., Kramer, M., Spiegel, L., Nascimento, L., Zutavern, T., Miller, B., Ambroise, C., Muller, S., Spooner, W., Narechania, A., Ren, L., Wei, S., Kumari, S., Faga, B., Levy, M.J., McMahan, L., Van Buren, P., Vaughn, M.W., Ying, K., Yeh, C.-T., Emrich, S.J., Jia, Y., Kalyanaraman, A., Hsia, A.-P., Barbazuk, W.B., Baucom, R.S., Brutnell, T.P., Carpita, N.C., Chaparro, C., Chia, J.-M., Deragon, J.-M., Estill, J.C., Fu, Y., Jeddeloh, J.A., Han, Y., Lee, H., Li, P., Lisch, D.R., Liu, S., Liu, Z., Nagel, D.H., McCann, M.C., SanMiguel, P., Myers, A.M., Nettleton, D., Nguyen, J., Penning, B.W., Ponnala, L., Schneider, K.L., Schwartz, D.C., Sharma, A., Soderlund, C., Springer, N.M., Sun, Q., Wang, H., Waterman, M., Westerman, R., Wolfgruber, T.K., Yang, L., Yu, Y., Zhang, L., Zhou, S., Zhu, Q., Bennetzen, J.L., Dawe, R.K., Jiang, J., Jiang, N., Presting, G.G., Wessler, S.R., Aluru, S., Martienssen, R.A., Clifton, S.W., McCombie, W.R., Wing, R.A., and Wilson, R.K. (2009). The B73 Maize Genome: Complexity, Diversity, and Dynamics. Science **326,** 1112-1115.

Sheen, J. (2002). A transient expression assay using maize mesophyll protoplasts. http ://genetics.mgh.harvard.edu/sheenweb/.

Shin, R., Burch, A.Y., Huppert, K.A., Tiwari, S.B., Murphy, A.S., Guilfoyle, T.J., and Schachtman, D.P. (2007). The Arabidopsis Transcription Factor MYB77 Modulates Auxin Signal Transduction. Plant Cell **19,** 2440-2453.

Slotkin, R.K., Freeling, M., and Lisch, D. (2003). *Mu killer* Causes the Heritable Inactivation of the Mutator Family of Transposable Elements in *Zea mays*. Genetics **165,** 781-797.

Song, Y., Wang, L., and Xiong, L. (2009). Comprehensive expression profiling analysis of *OsIAA* gene family in developmental processes and in response to phytohormone and stress treatments. Planta **229,** 577-591.

Sorefan, K., Girin, T., Liljegren, S.J., Ljung, K., Robles, P., Galván-Ampudia, C.S., Offringa, R., Friml, J., Yanofsky, M.F., and Østergaard, L. (2009). A regulated auxin minimum is required for seed dispersal in *Arabidopsis*. Nature **459,** 583-586.

Sridhar, V.V., Surendrarao, A., and Liu, Z. (2006). APETALA1 and SEPALLATA3 interact with SEUSS to mediate transcription repression during flower development. Development **133,** 3159-3166.

Sridhar, V.V., Surendrarao, A., Gonzalez, D., Conlan, R.S., and Liu, Z. (2004). Transcriptional repression of target genes by LEUNIG and SEUSS, two interacting regulatory proteins for Arabidopsis flower development. Proc Natl Acad Sci U S A **101,** 11494-11499.

Strable, J., and Scanlon, M.J. (2009). Maize (*Zea mays*): A Model Organism for Basic and Applied Research in Plant Biology. Cold Spring Harbor Protocols **2009,** pdb.emo132.

Szemenyei, H., Hannon, M., and Long, J.A. (2008). TOPLESS Mediates Auxin-Dependent Transcriptional Repression During Arabidopsis Embryogenesis. Science **319,** 1384-1386.

Tamura, K., Dudley, J., Nei, M., and Kumar, S. (2007). MEGA4: Molecular Evolutionary Genetics Analysis (MEGA) Software Version 4.0. Mol Biol Evol **24,** 1596-1599.

Tanaka, H., Dhonukshe, P., Brewer, P.B., and Friml, J. (2006). Spatiotemporal asymmetric auxin distribution: a means to coordinate plant development. Cell Mol Life Sci **63,** 2738-2754.

Tao, Y., Ferrer, J.-L., Ljung, K., Pojer, F., Hong, F., Long, J.A., Li, L., Moreno, J.E., Bowman, M.E., Ivans, L.J., Cheng, Y., Lim, J., Zhao, Y., Ballaré, C.L., Sandberg, G., Noel, J.P., and Chory, J. (2008). Rapid Synthesis of Auxin via a New Tryptophan-Dependent Pathway Is Required for Shade Avoidance in Plants. Cell **133,** 164-176.

Tatematsu, K., Kumagai, S., Muto, H., Sato, A., Watahiki, M.K., Harper, R.M., Liscum, E., and Yamamoto, K.T. (2004). *MASSUGU2* Encodes Aux/IAA19, an Auxin-Regulated Protein That Functions Together with the Transcriptional Activator NPH4/ARF7 to Regulate Differential Growth Responses of Hypocotyl and Formation of Lateral Roots in *Arabidopsis thaliana*. Plant Cell **16,** 379-393.

Taylor, J.S., and Raes, J. (2004). Duplication and Divergence: The Evolution of New Genes and Old Ideas. Annu Rev Genet **38,** 615-643.

Tian, Q., and Reed, J.W. (1999). Control of auxin-regulated root development by the Arabidopsis thaliana *SHY2/IAA3* gene. Development **126,** 711-721.

Till, B., Reynolds, S., Weil, C., Springer, N., Burtner, C., Young, K., Bowers, E., Codomo, C., Enns, L., Odden, A., Greene, E., Comai, L., and Henikoff, S. (2004). Discovery of induced point mutations in maize genes by TILLING. BMC Plant Biol **4,** 12.

Tiwari, S.B., Hagen, G., and Guilfoyle, T. (2003). The Roles of Auxin Response Factor Domains in Auxin-Responsive Transcription. Plant Cell **15,** 533-543.

Tiwari, S.B., Hagen, G., and Guilfoyle, T.J. (2004). Aux/IAA Proteins Contain a Potent Transcriptional Repression Domain. Plant Cell **16,** 533-543.

Tiwari, S.B., Wang, X.-J., Hagen, G., and Guilfoyle, T.J. (2001). AUX/IAA Proteins Are Active Repressors, and Their Stability and Activity Are Modulated by Auxin. Plant Cell **13,** 2809-2822.

Uehara, T., Okushima, Y., Mimura, T., Tasaka, M., and Fukaki, H. (2008). Domain II Mutations in CRANE/IAA18 Suppress Lateral Root Formation and Affect Shoot Development in *Arabidopsis thaliana*. Plant Cell Physiol **49,** 1025-1038.

Ulmasov, T., Hagen, G., and Guilfoyle, T.J. (1997a). ARF1, a Transcription Factor That Binds to Auxin Response Elements. Science **276,** 1865-1868.

Ulmasov, T., Hagen, G., and Guilfoyle, T.J. (1999). Activation and repression of transcription by auxin-response factors. Proc Natl Acad Sci USA **96,** 5844-5849.

Ulmasov, T., Liu, Z.B., Hagen, G., and Guilfoyle, T.J. (1995). Composite structure of auxin response elements. Plant Cell **7,** 1611-1623.

Ulmasov, T., Murfett, J., Hagen, G., and Guilfoyle, T.J. (1997b). Aux/IAA proteins repress expression of reporter genes containing natural and highly active synthetic auxin response elements. Plant Cell **9,** 1963-1971.

Vanneste, S., and Friml, J. (2009). Auxin: A Trigger for Change in Plant Development. Cell **136,** 1005-1016.

Varney, G.T., and Canny, M.J. (1993). Rates of water uptake into the mature root system of maize plants. New Phytol **123,** 775-786.

Vert, G., Walcher, C.L., Chory, J., and Nemhauser, J.L. (2008). Integration of auxin and brassinosteroid pathways by Auxin Response Factor 2. Proc Natl Acad Sci USA **105,** 9829-9834.

von Behrens, I., Komatsu, M., Zhang, Y., Berendzen, K.W., Niu, X., Sakai, H., Taramino, G., and Hochholdinger, F. (2011). *Rootless with undetectable meristem 1* encodes a monocot-specific AUX/IAA protein that controls embryonic seminal and post-embryonic lateral root initiation in maize. Plant J **66,** 341-353.

Walter, M., Chaban, C., Schütze, K., Batistic, O., Weckermann, K., Näke, C., Blazevic, D., Grefen, C., Schumacher, K., Oecking, C., Harter, K., and Kudla, J. (2004). Visualization of protein interactions in living plant cells using bimolecular fluorescence complementation. Plant J **40,** 428-438.

Wang, X.L., McCully, M.E., and Canny, M.J. (1994). The branch roots of *Zea*. IV. The maturation and openness of xylem conduits in first-order branches of soil-grown roots. New Phytol **126,** 21-29.

Wang, Y., Deng, D., Bian, Y., Lv, Y., and Xie, Q. (2010). Genome-wide analysis of primary auxin-responsive *Aux*/*IAA* gene family in maize (*Zea mays* L.). Mol Biol Rep **37,** 3991-4001.

Wang Yi-Jun, L.Y.-P., Xie Qin,Deng De-Xiang,Bian Yun-Long. (2010). Whole-Genome Sequence Characterization of Primary Auxin-Responsive *Aux*/*IAA* Gene Family in Sorghum (*Sorghum bicolor* L.). Acta Agron Sin **36,** 688-694.

Watt, M., Silk, W.K., and Passioura, J.B. (2006). Rates of Root and Organism Growth, Soil Conditions, and Temporal and Spatial Development of the Rhizosphere. Ann Bot-London **97,** 839-855.

Weijers, D., Benkova, E., Jager, K.E., Schlereth, A., Hamann, T., Kientz, M., Wilmoth, J.C., Reed, J.W., and Jurgens, G. (2005). Developmental specificity of auxin response by pairs of ARF and Aux/IAA transcriptional regulators. EMBO J **24,** 1874-1885.

Woll, K., Borsuk, L.A., Stransky, H., Nettleton, D., Schnable, P.S., and Hochholdinger, F. (2005). Isolation, Characterization, and Pericycle-Specific Transcriptome Analyses of the Novel Maize Lateral and Seminal Root Initiation Mutant *rum*1. Plant Physiol **139,** 1255-1267.

Woodhouse, M.R., Schnable, J.C., Pedersen, B.S., Lyons, E., Lisch, D., Subramaniam, S., and Freeling, M. (2010). Following tetraploidy in maize, a short deletion mechanism removed genes preferentially from one of the two homologs. PLoS Biol **8,** e1000409.

Woodward, A.W., and Bartel, B. (2005). Auxin: Regulation, Action, and Interaction. Ann Bot-London **95,** 707-735.

Worley, C.K., Zenser, N., Ramos, J., Rouse, D., Leyser, O., Theologis, A., and Callis, J. (2000). Degradation of Aux/IAA proteins is essential for normal auxin signalling. Plant J **21,** 553-562.

Zhang, Y. (2013). Conserved and Unique Features of Maize (*Zea mays* L.) *Rum1* (*Rootless with Undetectable Meristem 1*) and *Rum1*-like Which Encode Aux/IAA Proteins Involved in Lateral and Seminal Root Initiation (Inaugural Dissertation: University of Tübingen).

Zhang, Y., Paschold, A., Marcon, C., Liu, S., Tai, H., Nestler, J., Yeh, C.-T., Opitz, N., Lanz, C., Schnable, P.S., and Hochholdinger, F. (2014). The *Aux/IAA* gene *rum1* involved in seminal and lateral root formation controls vascular patterning in maize (*Zea mays* L.) primary roots. J Exp Bot.

Zheng, N., Schulman, B.A., Song, L., Miller, J.J., Jeffrey, P.D., Wang, P., Chu, C., Koepp, D.M., Elledge, S.J., Pagano, M., Conaway, R.C., Conaway, J.W., Harper, J.W., and Pavletich, N.P. (2002). Structure of the Cul1–Rbx1–Skp1–F boxSkp2 SCF ubiquitin ligase complex. Nature **416,** 703-709.

Zhu, Z.-X., Liu, Y., Liu, S.-J., Mao, C.-Z., Wu, Y.-R., and Wu, P. (2012). A Gain-of-Function Mutation in *OsIAA11* Affects Lateral Root Development in Rice. Mol Plant **5,** 154-161.

7 Supplemental data

7.1 Supplemental Figures

Supplemental Figure 1

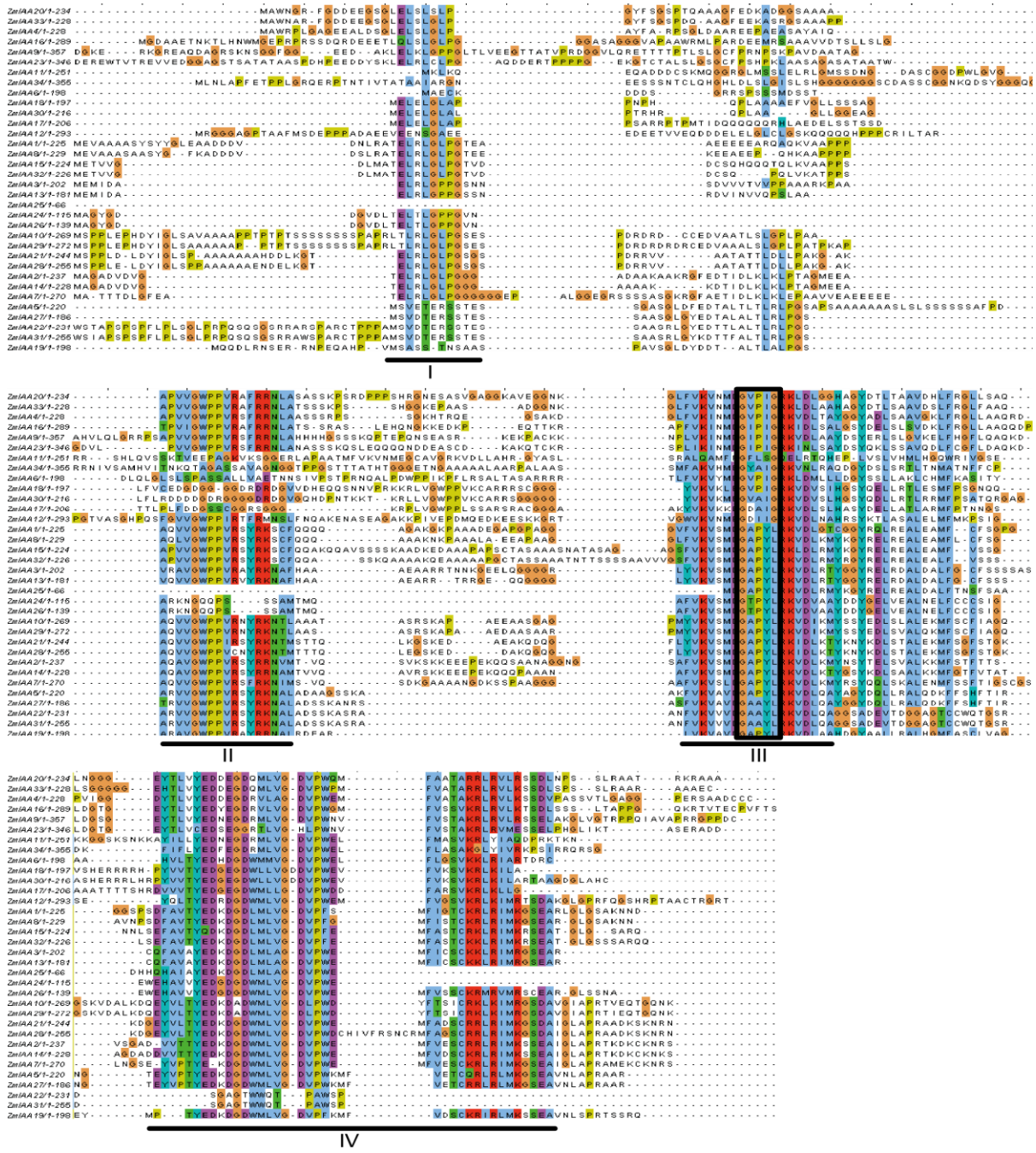

Supplemental Figure 1 Alignment of the maize Aux/IAA protein sequences. Aux/IAA protein sequences were compared by multiple alignments of the four conserved domains with ClustalW. Differences in the amino acid sequences of the domain III, which distinguish class A and class B Aux/IAA proteins (Figure 4.1) are boxed. The four domains are highlighted.

Supplemental Figure 2

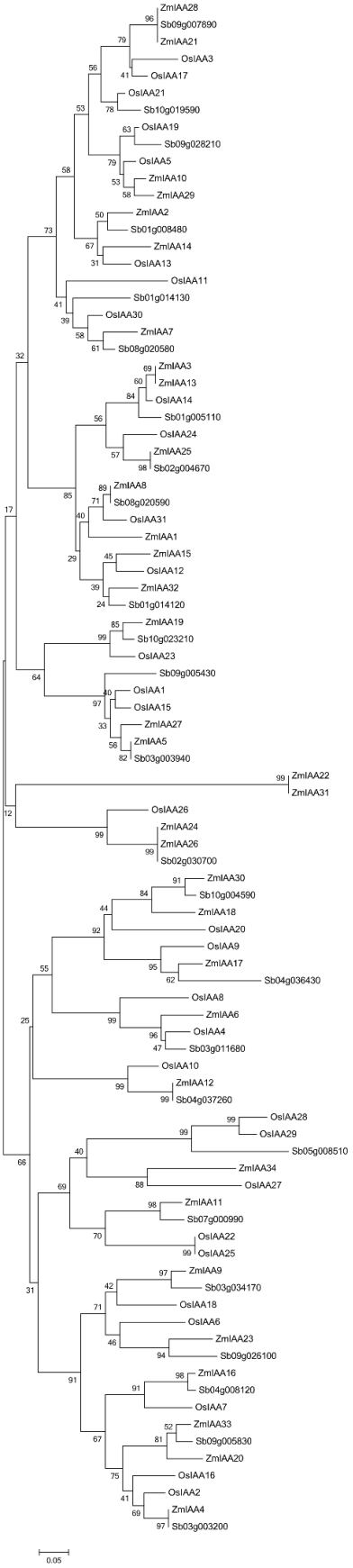

Supplemental Figure 2 Phylogenetic reconstruction of the Aux/IAA protein families in different monocotyledonous species. Phylogenetic reconstruction of maize (*Zea mays*, Zm), *Sorghum* (*Sorghum bicolor*, Sb), and rice (*Oryza sativa*, Os) Aux/IAA protein families in an unrooted tree with the neighbor-joining algorithm of MEGA5. The values associated to each branch are bootstrap percentages. The size bar indicates sequence divergence: 0.05 = 5%.

Supplemental Figure 3

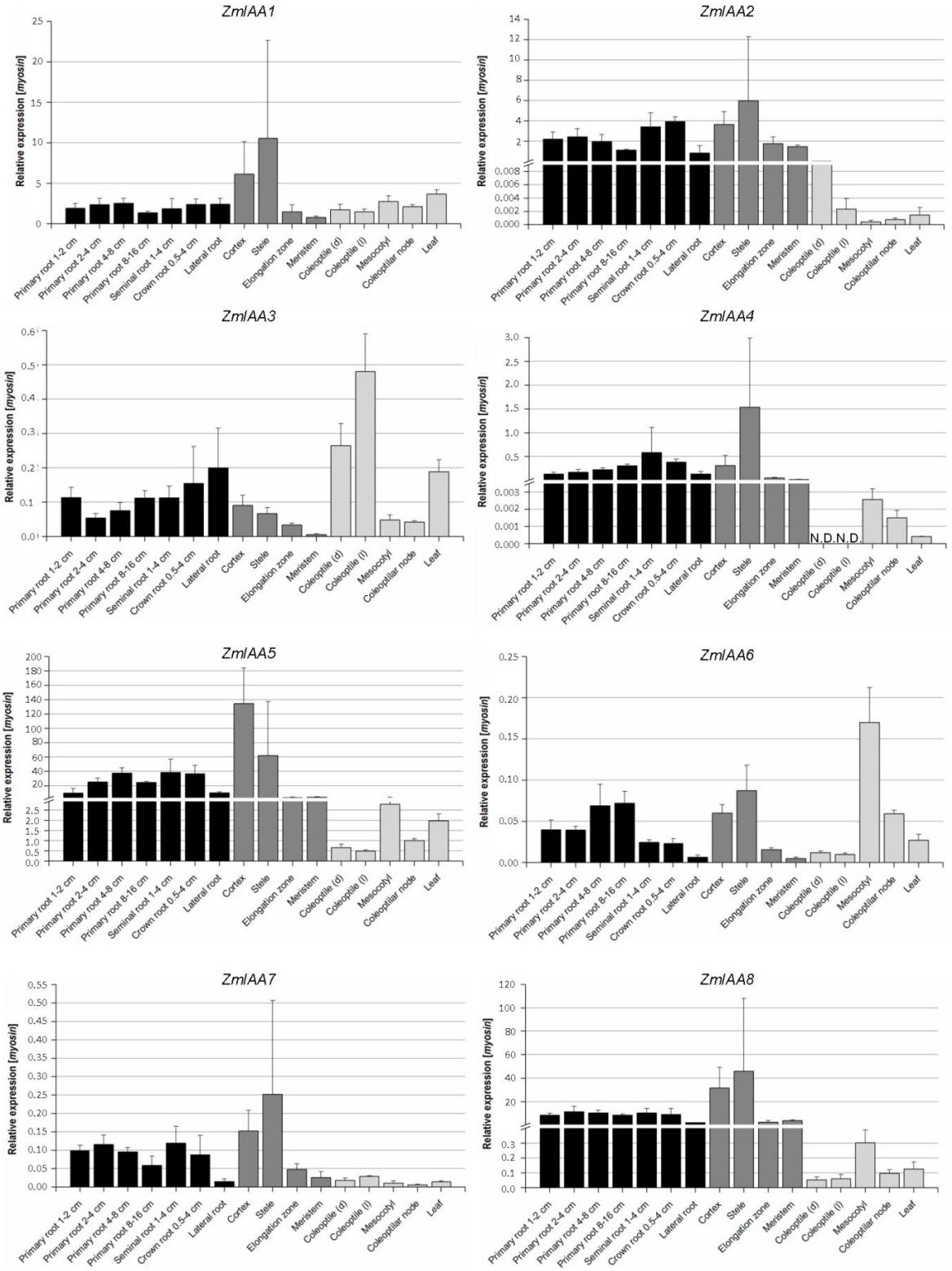

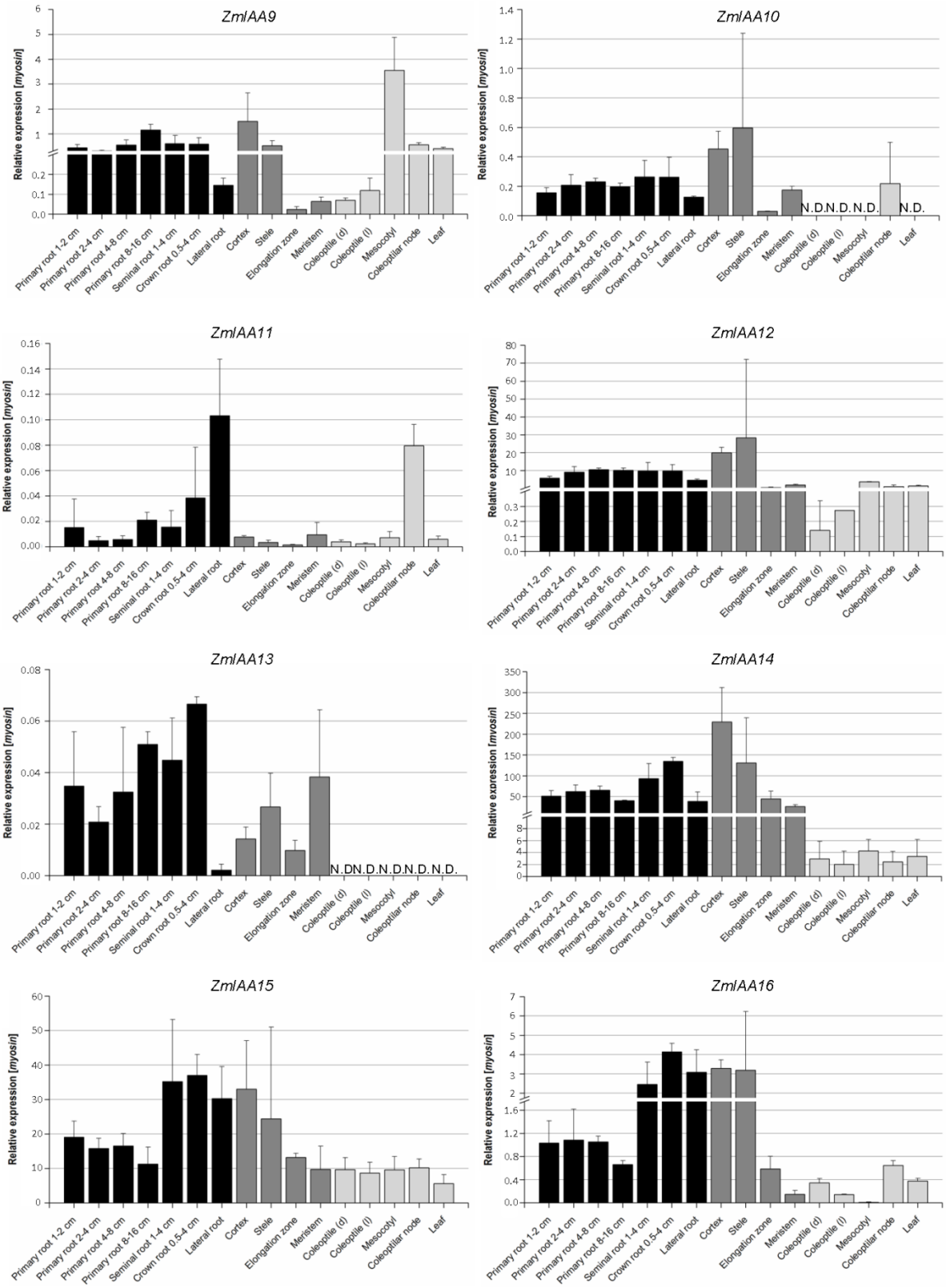
ZmIAA9
ZmIAA10
ZmIAA11
ZmIAA12
ZmIAA13
ZmIAA14
ZmIAA15
ZmIAA16
Relative expression [myosin]
N.D.
Primary root 1-2 cm
Primary root 2-4 cm
Primary root 4-8 cm
Primary root 8-16 cm
Seminal root 1-4 cm
Crown root 0.5-4 cm
Lateral root
Cortex
Stele
Elongation zone
Meristem
Coleoptile (d)
Coleoptile (l)
Mesocotyl
Coleoptilar node
Leaf

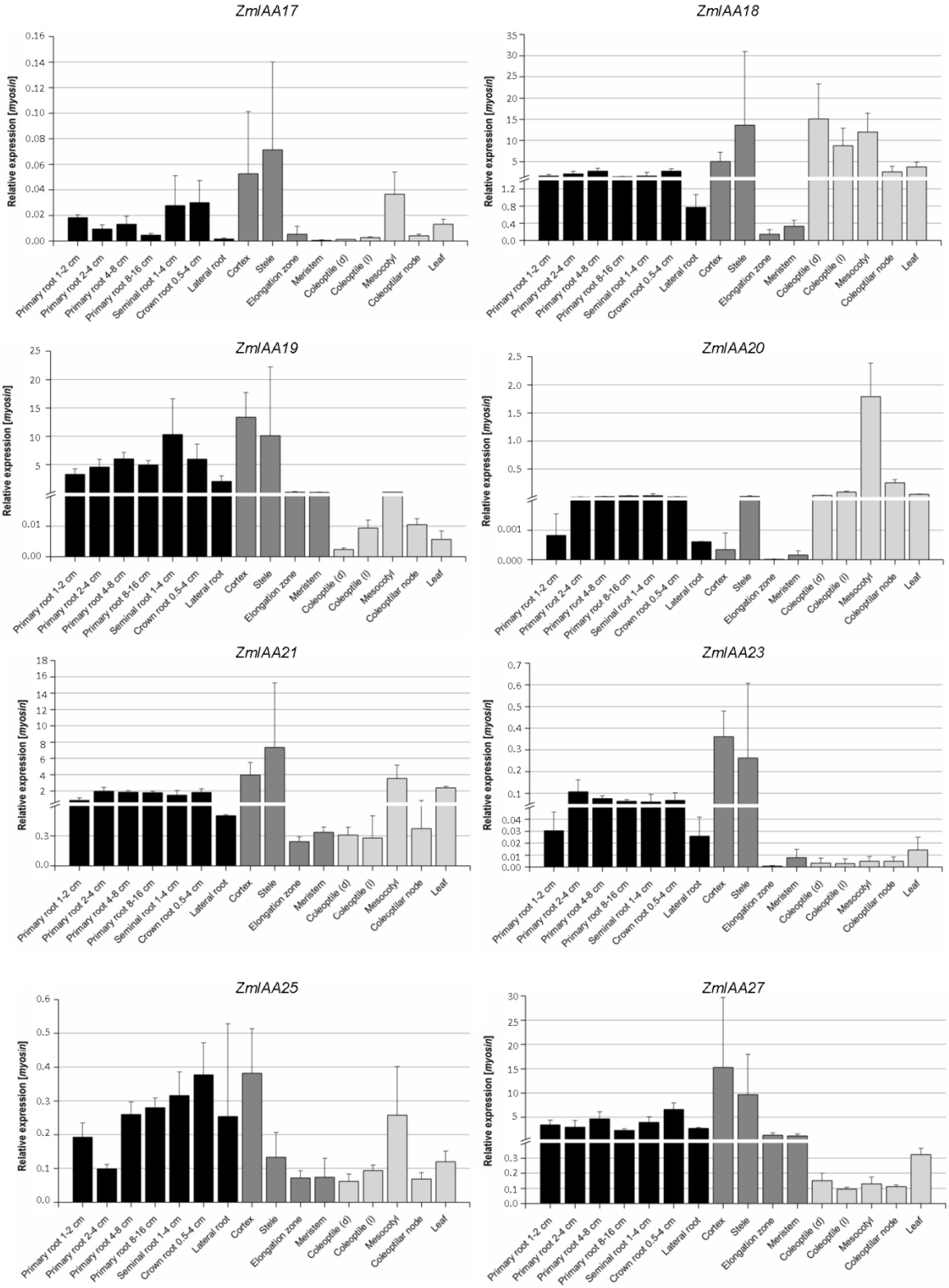
ZmIAA17
ZmIAA18
ZmIAA19
ZmIAA20
ZmIAA21
ZmIAA23
ZmIAA25
ZmIAA27
Relative expression [myosin]
Primary root 1-2 cm
Primary root 2-4 cm
Primary root 4-8 cm
Primary root 8-16 cm
Seminal root 1-4 cm
Crown root 0.5-4 cm
Lateral root
Cortex
Stele
Elongation zone
Meristem
Coleoptile (d)
Coleoptile (l)
Mesocotyl
Coleoptilar node
Leaf

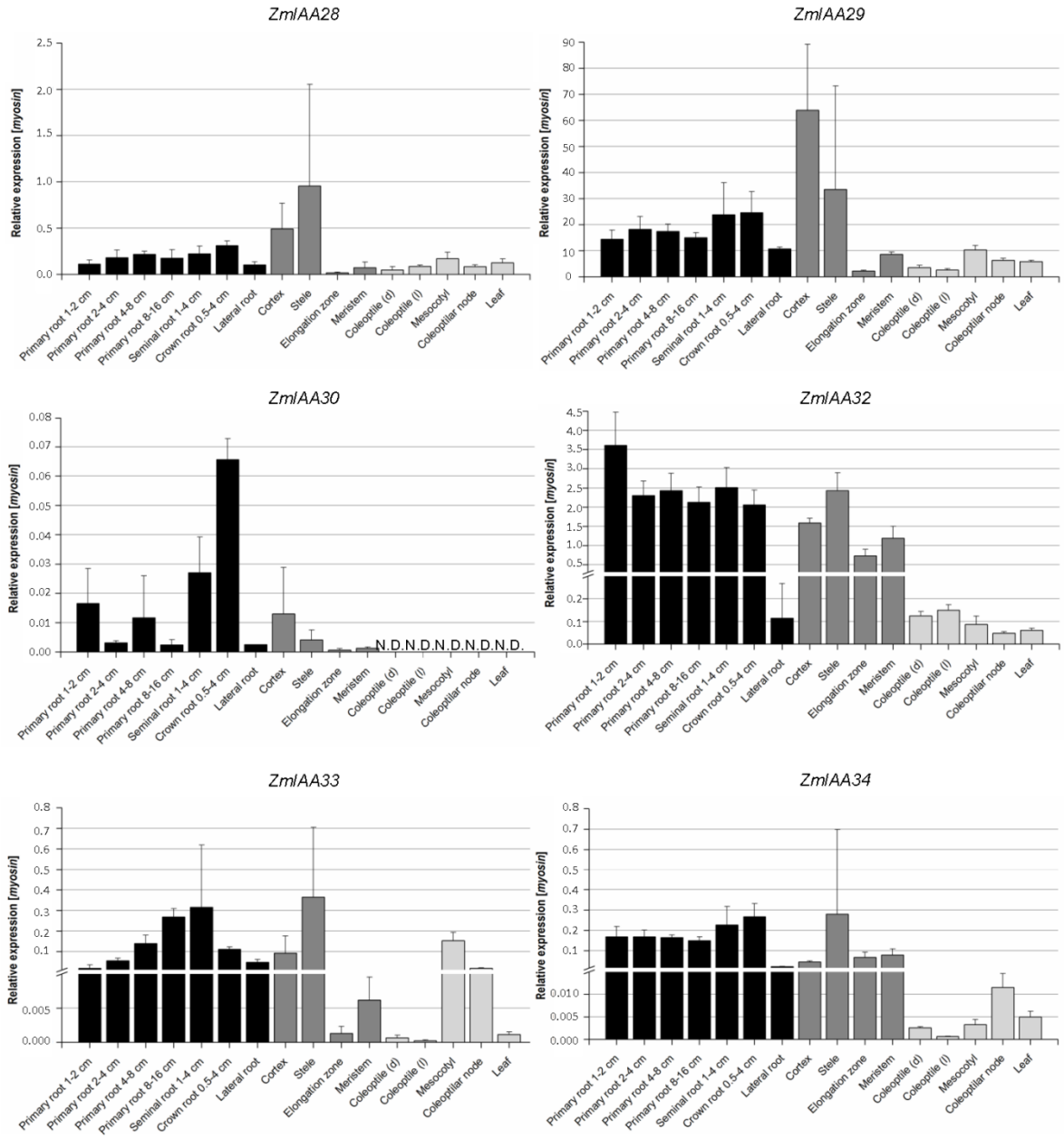

Supplemental Figure 3 Summary of *Aux/IAA* gene expression patterns in maize. Gene expression patterns obtained by qRT-PCR experiments in root and shoot tissues. Expression values in whole roots are highlighted in black, expression in primary root tissues in dark grey, and expression in shoot organs in light grey. *ZmIAA10*, *ZmIAA13*, and *ZmIAA30* did not display any expression in shoot tissues. l: light, d: dark, N.D.: no expression detected.

Supplemental Figure 4

ZmIAA1

Primary root 1-2 cm	Primary root 2-4 cm	Primary root 4-8 cm	Primary root 8-16 cm	Seminal root 1-4 cm	Crown root 0.5-4 cm	Stele	Cortex	Elongation zone	Meristem	Lateral root	Coleoptile (d)	Coleoptile (l)	Mesocotyl	Coleoptilar node	Leaf	
x	0.404	0.35	0.195	0.911	0.211	0.258	0.138	0.264	0.049	0.361	0.312	0.131	0.208	0.518	0.013	**Primary root 1-2 cm**
	x	0.638	0.103	0.537	0.936	0.275	0.113	0.254	0.03	0.894	0.263	0.164	0.592	0.625	0.122	**Primary root 2-4 cm**
		x	0.033	0.45	0.826	0.274	0.13	0.222	0.008	0.655	0.246	0.099	0.709	0.343	0.129	**Primary root 4-8 cm**
			x	0.479	0.034	0.229	0.094	0.864	0.008	0.323	0.349	0.521	0.042	0.002	0.005	**Primary root 8-16 cm**
				x	0.179	0.282	0.118	0.681	0.227	0.501	0.786	0.529	0.418	0.648	0.092	**Seminal root 1-4 cm**
					x	0.289	0.158	0.213	0.028	0.685	0.044	0.022	0.633	0.269	0.066	**Crown root 0.5-4 cm**
						x	0.576	0.223	0.199	0.392	0.257	0.236	0.265	0.263	0.33	**Stele**
							x	0.139	0.075	0.477	0.117	0.109	0.227	0.137	0.353	**Cortex**
								x	0.208	0.085	0.613	0.974	0.046	0.27	0.004	**Elongation zone**
									x	0.168	0.098	0.054	0.006	0.006	0.002	**Meristem**
										x	0.411	0.259	0.301	0.593	0.044	**Lateral root**
											x	0.335	0.202	0.242	0.02	**Coleoptile (d)**
												x	0.062	0.005	0.003	**Coleoptile (l)**
													x	0.25	0.033	**Mesocotyl**
														x	0.014	**Coleopilar node**
															x	**Leaf**

	$p \leq 0.05$
	$p \leq 0.01$
	$p \leq 0.001$
N.D.	not detectable

ZmIAA2

Primary root 1-2 cm	Primary root 2-4 cm	Primary root 4-8 cm	Primary root 8-16 cm	Seminal root 1-4 cm	Crown root 0.5-4 cm	Stele	Cortex	Elongation zone	Meristem	Lateral root	Coleoptile (d)	Coleoptile (l)	Mesocotyl	Coleoptilar node	Leaf	
x	0.776	0.674	0.058	0.146	0.053	0.338	0.19	0.097	0.117	0.47	0.008	0.008	0.008	0.008	0.008	**Primary root 1-2 cm**
	x	0.563	0.041	0.375	0.025	0.356	0.046	0.394	0.085	0.086	0.01	0.01	0.01	0.01	0.01	**Primary root 2-4 cm**
		x	0.116	0.124	0.016	0.267	0.159	0.676	0.294	0.486	0.011	0.011	0.011	0.011	0.011	**Primary root 4-8 cm**
			x	0.044	1E-03	0.226	0.024	0.165	0.294	0.606	1E-04	1E-04	1E-04	1E-04	1E-04	**Primary root 8-16 cm**
				x	0.525	0.531	0.831	0.115	0.078	0.141	0.015	0.015	0.015	0.015	0.015	**Seminal root 1-4 cm**
					x	0.566	0.615	0.029	0.003	0.042	4E-04	4E-04	4E-04	4E-04	4E-04	**Crown root 0.5-4 cm**
						x	0.561	0.271	0.247	0.385	0.156	0.156	0.156	0.156	0.156	**Stele**
							x	0.13	0.041	0.205	0.01	0.01	0.01	0.01	0.01	**Cortex**
								x	0.385	0.65	0.013	0.012	0.012	0.012	0.012	**Elongation zone**
									x	0.421	5E-04	4E-04	4E-04	4E-04	4E-04	**Meristem**
										x	0.354	0.349	0.349	0.349	0.349	**Lateral root**
											x	0.091	0.035	0.038	0.036	**Coleoptile (d)**
												x	0.11	0.167	0.52	**Coleoptile (l)**
													x	0.004	0.114	**Mesocotyl**
														x	0.214	**Coleopilar node**
															x	**Leaf**

ZmIAA3

Primary root 1-2 cm	Primary root 2-4 cm	Primary root 4-8 cm	Primary root 8-16 cm	Seminal root 1-4 cm	Crown root 0.5-4 cm	Stele	Cortex	Elongation zone	Meristem	Lateral root	Coleoptile (d)	Coleoptile (l)	Mesocotyl	Coleoptilar node	Leaf	
x	0.034	0.153	0.964	0.986	0.464	0.042	0.25	0.01	0.006	0.481	0.039	0.008	0.009	0.021	0.08	**Primary root 1-2 cm**
	x	0.297	0.018	0.082	0.126	0.42	0.051	0.016	0.006	0.301	0.011	0.004	0.583	0.204	0.008	**Primary root 2-4 cm**
		x	0.164	0.075	0.293	0.302	0.587	0.054	0.007	0.476	0.006	0.008	0.205	0.05	0.014	**Primary root 4-8 cm**
			x	0.978	0.494	0.08	0.222	0.006	0.007	0.371	0.015	0.004	0.01	0.007	0.006	**Primary root 8-16 cm**
				x	0.589	0.065	0.51	0.027	0.007	0.568	0.002	0.008	0.049	0.019	0.008	**Seminal root 1-4 cm**
					x	0.23	0.233	0.099	0.071	0.298	0.283	0.015	0.134	0.134	0.645	**Crown root 0.5-4 cm**
						x	0.331	0.042	0.004	0.417	0.008	0.007	0.187	0.049	0.011	**Stele**
							x	0.02	0.013	0.292	0.028	0.003	0.029	0.056	0.027	**Cortex**
								x	0.004	0.286	0.007	0.004	0.125	0.153	0.004	**Elongation zone**
									x	0.262	0.004	0.003	0.015	8E-05	0.002	**Meristem**
										x	0.361	0.088	0.294	0.31	0.983	**Lateral root**
											x	0.044	0.009	0.005	0.036	**Coleoptile (d)**
												x	0.003	0.004	0.008	**Coleoptile (l)**
													x	0.495	0.005	**Mesocotyl**
														x	0.003	**Coleopilar node**
															x	**Leaf**

ZmIAA4

Primary root 1-2 cm	Primary root 2-4 cm	Primary root 4-8 cm	Primary root 8-16 cm	Seminal root 1-4 cm	Crown root 0.5-4 cm	Stele	Cortex	Elongation zone	Meristem	Lateral root	Coleoptile (d)	Coleoptile (l)	Mesocotyl	Coleoptilar node	Leaf	
x	0.443	0.032	0.016	0.162	0.013	0.152	0.222	0.025	0.013	0.318	N.D.	0.5	0.007	0.007	0.126	**Primary root 1-2 cm**
	x	0.237	0.002	0.228	0.003	0.157	0.202	0.021	0.009	0.57	N.D.	0.5	0.008	0.008	0.155	**Primary root 2-4 cm**
		x	0.078	0.253	0.045	0.175	0.431	8E-04	0.002	0.469	N.D.	0.5	0.001	0.001	0.075	**Primary root 4-8 cm**
			x	0.364	0.021	0.187	0.942	0.001	0.002	0.205	N.D.	0.5	5E-04	5E-04	0.053	**Primary root 8-16 cm**
				x	0.498	0.373	0.405	0.132	0.12	0.339	N.D.	0.5	0.112	0.112	0.09	**Seminal root 1-4 cm**
					x	0.204	0.54	0.003	0.001	0.129	N.D.	0.5	0.002	0.001	0.035	**Crown root 0.5-4 cm**
						x	0.22	0.135	0.126	0.283	N.D.	0.5	0.125	0.125	0.277	**Stele**
							x	0.082	0.068	0.637	N.D.	0.5	0.061	0.06	0.43	**Cortex**
								x	0.026	0.294	N.D.	0.5	0.004	0.004	0.13	**Elongation zone**
									x	0.185	N.D.	0.5	0.028	0.021	0.088	**Meristem**
										x	N.D.	0.5	0.173	0.173	0.172	**Lateral root**
											x	N.D.	N.D.	N.D.	N.D.	**Coleoptile (d)**
												x	0.5	0.5	0.5	**Coleoptile (l)**
													x	0.078	0.09	**Mesocotyl**
														x	0.083	**Coleopilar node**
															x	**Leaf**

	$p \leq 0.05$
	$p \leq 0.01$
	$p \leq 0.001$
N.D.	not detectable

ZmIAA5

Primary root 1-2 cm	Primary root 2-4 cm	Primary root 4-8 cm	Primary root 8-16 cm	Seminal root 1-4 cm	Crown root 0.5-4 cm	Stele	Cortex	Elongation zone	Meristem	Lateral root	Coleoptile (d)	Coleoptile (l)	Mesocotyl	Coleoptilar node	Leaf	
x	0.018	0.019	0.024	0.091	0.009	0.249	0.016	0.142	0.152	0.316	0.07	0.062	0.109	0.072	0.092	**Primary root 1-2 cm**
	x	0.039	0.893	0.232	0.071	0.422	0.017	0.004	0.004	0.272	0.003	0.003	0.005	0.003	0.004	**Primary root 2-4 cm**
		x	0.041	0.894	0.879	0.591	0.024	0.002	0.003	0.118	0.002	0.002	0.003	0.002	0.002	**Primary root 4-8 cm**
			x	0.234	0.17	0.391	0.022	1E-04	0.003	0.015	3E-05	4E-05	4E-05	4E-05	3E-05	**Primary root 8-16 cm**
				x	0.879	0.635	0.023	0.031	0.035	0.276	0.026	0.026	0.034	0.027	0.029	**Seminal root 1-4 cm**
					x	0.575	0.019	0.012	0.011	0.247	0.01	0.009	0.011	0.01	0.011	**Crown root 0.5-4 cm**
						x	0.323	0.217	0.221	0.468	0.202	0.2	0.21	0.203	0.207	**Stele**
							x	0.013	0.013	0.306	0.012	0.012	0.013	0.012	0.013	**Cortex**
								x	0.129	0.096	0.003	0.001	0.434	0.003	0.019	**Elongation zone**
									x	0.149	0.003	0.001	0.107	0.002	0.007	**Meristem**
										x	0.067	0.066	0.037	0.064	0.053	**Lateral root**
											x	0.193	0.034	0.039	0.007	**Coleoptile (d)**
												x	0.026	8E-04	0.002	**Coleoptile (l)**
													x	0.043	0.161	**Mesocotyl**
														x	0.004	**Coleopilar node**
															x	**Leaf**

ZmIAA6

Primary root 1-2 cm	Primary root 2-4 cm	Primary root 4-8 cm	Primary root 8-16 cm	Seminal root 1-4 cm	Crown root 0.5-4 cm	Stele	Cortex	Elongation zone	Meristem	Lateral root	Coleoptile (d)	Coleoptile (l)	Mesocotyl	Coleoptilar node	Leaf	
x	0.938	0.204	0.003	0.101	0.141	0.086	0.274	0.026	0.008	0.197	0.016	0.017	0.01	0.082	0.178	**Primary root 1-2 cm**
	x	0.126	0.024	0.017	0.012	0.042	0.069	0.001	3E-04	0.054	4E-04	0.002	0.011	0.004	0.064	**Primary root 2-4 cm**
		x	0.886	0.032	0.026	0.442	0.937	0.025	0.018	0.275	0.025	0.017	0.011	0.459	0.058	**Primary root 4-8 cm**
			x	0.008	0.014	0.52	0.442	0.004	0.018	0.081	0.004	0.004	0.021	0.234	0.021	**Primary root 8-16 cm**
				x	0.664	0.03	0.012	0.005	0.003	0.179	0.015	0.002	0.006	2E-04	0.624	**Seminal root 1-4 cm**
					x	0.02	0.006	0.065	0.01	0.286	0.037	0.02	0.007	4E-05	0.491	**Crown root 0.5-4 cm**
						x	0.186	0.02	0.012	0.07	0.014	0.015	0.091	0.153	0.02	**Stele**
							x	0.011	0.013	0.138	0.017	0.012	0.009	0.858	0.075	**Cortex**
								x	0.004	0.241	0.104	0.04	0.006	1E-04	0.09	**Elongation zone**
									x	0.64	4E-04	0.051	0.005	2E-04	0.008	**Meristem**
										x	0.101	0.39	0.01	0.081	0.029	**Lateral root**
											x	0.301	0.006	3E-04	0.017	**Coleoptile (d)**
												x	0.004	2E-04	0.015	**Coleoptile (l)**
													x	0.015	0.007	**Mesocotyl**
														x	0.006	**Coleopilar node**
															x	**Leaf**

ZmIAA7

Primary root 1-2 cm	Primary root 2-4 cm	Primary root 4-8 cm	Primary root 8-16 cm	Seminal root 1-4 cm	Crown root 0.5-4 cm	Stele	Cortex	Elongation zone	Meristem	Lateral root	Coleoptile (d)	Coleoptile (l)	Mesocotyl	Coleoptilar node	Leaf	
x	0.417	0.127	0.034	0.333	0.708	0.325	0.129	0.019	0.007	0.058	0.003	0.004	0.003	0.001	0.002	**Primary root 1-2 cm**
	x	0.326	0.043	0.921	0.304	0.359	0.252	0.005	0.008	0.108	0.003	0.006	0.002	0.003	0.004	**Primary root 2-4 cm**
		x	0.044	0.294	0.78	0.317	0.116	0.019	0.006	0.062	0.002	0.002	0.002	6E-04	0.001	**Primary root 4-8 cm**
			x	0.114	0.389	0.218	0.039	0.28	0.006	0.047	0.036	0.104	0.032	0.021	0.033	**Primary root 8-16 cm**
				x	0.463	0.412	0.434	0.089	0.039	0.029	0.029	0.031	0.023	0.016	0.02	**Seminal root 1-4 cm**
					x	0.349	0.007	0.215	0.145	0.473	0.076	0.116	0.063	0.055	0.072	**Crown root 0.5-4 cm**
						x	0.551	0.199	0.158	0.363	0.159	0.176	0.151	0.147	0.156	**Stele**
							x	0.029	0.029	0.29	0.017	0.023	0.016	0.014	0.017	**Cortex**
								x	0.046	0.116	0.008	0.087	0.009	0.01	0.016	**Elongation zone**
									x	0.222	0.289	0.741	0.118	0.064	0.17	**Meristem**
										x	0.352	0.158	0.892	0.277	0.836	**Lateral root**
											x	0.031	0.016	0.022	0.211	**Coleoptile (d)**
												x	0.003	3E-04	0.001	**Coleoptile (l)**
													x	0.131	0.251	**Mesocotyl**
														x	5E-04	**Coleopilar node**
															x	**Leaf**

	$p \leq 0.05$
	$p \leq 0.01$
	$p \leq 0.001$
N.D.	not detectable

ZmIAA8

Primary root 1-2 cm	Primary root 2-4 cm	Primary root 4-8 cm	Primary root 8-16 cm	Seminal root 1-4 cm	Crown root 0.5-4 cm	Stele	Cortex	Elongation zone	Meristem	Lateral root	Coleoptile (d)	Coleoptile (l)	Mesocotyl	Coleoptilar node	Leaf	
x	0.354	0.319	0.988	0.439	0.874	0.309	0.079	0.022	0.007	0.146	0.002	0.002	0.002	0.002	0.002	**Primary root 1-2 cm**
	x	0.786	0.228	0.812	0.014	0.357	0.061	0.029	0.052	0.203	0.015	0.015	0.016	0.015	0.015	**Primary root 2-4 cm**
		x	0.238	0.973	0.708	0.348	0.116	0.005	0.013	0.022	0.003	0.003	0.003	0.003	0.003	**Primary root 4-8 cm**
			x	0.436	0.839	0.32	0.074	0.003	0.013	0.075	3E-04	3E-04	4E-04	3E-04	3E-04	**Primary root 8-16 cm**
				x	0.758	0.354	0.117	0.016	0.049	0.002	0.012	0.012	0.013	0.012	0.012	**Seminal root 1-4 cm**
					x	0.328	0.045	0.093	0.159	0.251	0.041	0.042	0.044	0.042	0.042	**Crown root 0.5-4 cm**
						x	0.701	0.267	0.268	0.429	0.238	0.238	0.24	0.238	0.238	**Stele**
							x	0.043	0.053	0.222	0.036	0.036	0.037	0.036	0.036	**Cortex**
								x	0.253	0.94	0.026	0.028	0.035	0.029	0.031	**Elongation zone**
									x	0.213	1E-03	9E-04	0.001	8E-04	8E-04	**Meristem**
										x	0.01	0.018	0.021	0.022	0.029	**Lateral root**
											x	0.6	0.017	0.11	0.086	**Coleoptile (d)**
												x	0.022	0.086	0.038	**Coleoptile (l)**
													x	0.018	0.042	**Mesocotyl**
														x	0.103	**Coleopilar node**
															x	**Leaf**

ZmIAA9

Primary root 1-2 cm	Primary root 2-4 cm	Primary root 4-8 cm	Primary root 8-16 cm	Seminal root 1-4 cm	Crown root 0.5-4 cm	Stele	Cortex	Elongation zone	Meristem	Lateral root	Coleoptile (d)	Coleoptile (l)	Mesocotyl	Coleoptilar node	Leaf	
x	0.137	0.472	0.02	0.437	0.447	0.204	0.141	0.006	0.007	0.17	0.01	0.005	0.015	0.298	0.711	**Primary root 1-2 cm**
	x	0.128	0.005	0.181	0.139	0.131	0.128	1E-04	5E-04	0.018	6E-04	0.005	0.016	0.013	0.081	**Primary root 2-4 cm**
		x	0.041	0.746	0.796	0.859	0.23	0.014	0.017	0.33	0.016	0.033	0.028	0.895	0.264	**Primary root 4-8 cm**
			x	0.024	0.077	0.035	0.574	0.002	0.017	0.132	0.003	0.005	0.041	0.018	0.004	**Primary root 8-16 cm**
				x	0.929	0.647	0.189	0.038	0.044	0.082	0.047	0.078	0.031	0.809	0.293	**Seminal root 1-4 cm**
					x	0.781	0.279	0.024	0.031	0.201	0.027	0.037	0.025	0.842	0.251	**Crown root 0.5-4 cm**
						x	0.145	0.013	0.015	0.237	0.02	0.02	0.017	0.781	0.422	**Stele**
							x	0.08	0.084	0.472	0.088	0.092	0.043	0.222	0.158	**Cortex**
								x	0.004	0.146	0.006	0.034	0.013	0.001	0.002	**Elongation zone**
									x	0.22	0.602	0.123	0.013	0.002	0.004	**Meristem**
										x	0.296	0.738	0.087	0.079	0.042	**Lateral root**
											x	0.182	0.013	9E-04	0.002	**Coleoptile (d)**
												x	0.012	0.004	0.016	**Coleoptile (l)**
													x	0.022	0.019	**Mesocotyl**
														x	0.018	**Coleopilar node**
															x	**Leaf**

ZmIAA10

Primary root 1-2 cm	Primary root 2-4 cm	Primary root 4-8 cm	Primary root 8-16 cm	Seminal root 1-4 cm	Crown root 0.5-4 cm	Stele	Cortex	Elongation zone	Meristem	Lateral root	Coleoptile (d)	Coleoptile (l)	Mesocotyl	Coleoptilar node	Leaf	
x	0.357	0.001	0.231	0.074	0.272	0.277	0.01	0.005	0.056	0.752	N.D.	N.D.	N.D.	0.718	N.D.	**Primary root 1-2 cm**
	x	0.645	0.67	0.536	0.203	0.329	0.03	0.015	0.564	0.337	N.D.	N.D.	N.D.	0.979	N.D.	**Primary root 2-4 cm**
		x	0.235	0.513	0.703	0.344	0.027	5E-04	0.002	0.076	N.D.	N.D.	N.D.	0.97	N.D.	**Primary root 4-8 cm**
			x	0.376	0.32	0.305	0.024	8E-04	0.002	0.132	N.D.	N.D.	N.D.	0.91	N.D.	**Primary root 8-16 cm**
				x	0.991	0.423	0.023	0.026	0.381	0.008	N.D.	N.D.	N.D.	0.949	N.D.	**Seminal root 1-4 cm**
					x	0.401	0.11	0.041	0.347	0.336	N.D.	N.D.	N.D.	0.461	N.D.	**Crown root 0.5-4 cm**
						x	0.732	0.006	0.339	0.42	N.D.	N.D.	N.D.	0.459	N.D.	**Stele**
							x	0.006	0.071	0.244	N.D.	N.D.	N.D.	0.257	N.D.	**Cortex**
								x	0.011	0.034	N.D.	N.D.	N.D.	0.365	N.D.	**Elongation zone**
									x	0.115	N.D.	N.D.	N.D.	0.818	N.D.	**Meristem**
										x	N.D.	N.D.	N.D.	0.684	N.D.	**Lateral root**
											x	N.D.	N.D.	N.D.	N.D.	**Coleoptile (d)**
												x	N.D.	N.D.	N.D.	**Coleoptile (l)**
													x	N.D.	N.D.	**Mesocotyl**
														x	N.D.	**Coleopilar node**
															x	**Leaf**

	$p \leq 0.05$
	$p \leq 0.01$
	$p \leq 0.001$
N.D.	not detectable

ZmIAA11

Primary root 1-2 cm	Primary root 2-4 cm	Primary root 4-8 cm	Primary root 8-16 cm	Seminal root 1-4 cm	Crown root 0.5-4 cm	Stele	Cortex	Elongation zone	Meristem	Lateral root	Coleoptile (d)	Coleoptile (l)	Mesocotyl	Coleoptilar node	Leaf	
x	0.439	0.457	0.636	0.986	0.096	0.352	0.523	0.326	0.695	0.189	0.377	0.322	0.503	0.001	0.429	**Primary root 1-2 cm**
	x	0.949	0.008	0.406	0.241	0.662	0.534	0.249	0.493	0.215	0.623	0.329	0.882	0.03	0.595	**Primary root 2-4 cm**
		x	0.04	0.265	0.196	0.331	0.043	0.071	0.572	0.198	0.094	0.07	0.314	0.003	0.996	**Primary root 4-8 cm**
			x	0.484	0.43	0.007	0.038	0.002	0.572	0.241	0.018	0.009	0.079	0.009	0.008	**Primary root 8-16 cm**
				x	0.418	0.313	0.538	0.266	0.097	0.136	0.198	0.148	0.364	0.013	0.22	**Seminal root 1-4 cm**
					x	0.216	0.373	0.208	0.288	0.31	0.175	0.161	0.202	0.064	0.187	**Crown root 0.5-4 cm**
						x	0.24	0.134	0.352	0.186	0.854	0.44	0.387	0.02	0.008	**Stele**
							x	0.103	0.618	0.207	0.024	0.035	0.033	0.058	0.648	**Cortex**
								x	0.274	0.189	0.107	0.178	0.212	0.022	0.032	**Elongation zone**
									x	0.156	0.388	0.256	0.753	0.008	0.463	**Meristem**
										x	0.197	0.195	0.197	0.412	0.189	**Lateral root**
											x	0.052	0.164	0.002	0.35	**Coleoptile (d)**
												x	0.121	0.003	0.073	**Coleoptile (l)**
													x	0.002	0.689	**Mesocotyl**
														x	0.003	**Coleopilar node**
															x	**Leaf**

ZmIAA12

Primary root 1-2 cm	Primary root 2-4 cm	Primary root 4-8 cm	Primary root 8-16 cm	Seminal root 1-4 cm	Crown root 0.5-4 cm	Stele	Cortex	Elongation zone	Meristem	Lateral root	Coleoptile (d)	Coleoptile (l)	Mesocotyl	Coleoptilar node	Leaf	
x	0.062	0.003	0.004	0.093	0.072	0.251	4E-04	0.007	0.031	0.205	0.014	N.D.	0.14	0.157	0.123	**Primary root 1-2 cm**
	x	0.687	0.181	0.836	0.716	0.335	0.003	0.01	0.018	0.374	0.187	N.D.	0.299	0.068	0.239	**Primary root 2-4 cm**
		x	0.256	0.564	0.895	0.327	0.004	2E-04	3E-04	0.023	0.052	N.D.	0.061	0.002	0.032	**Primary root 4-8 cm**
			x	0.365	0.256	0.357	0.004	4E-04	3E-04	0.116	0.04	N.D.	0.074	0.006	0.068	**Primary root 8-16 cm**
				x	0.772	0.333	0.002	0.04	0.065	0.901	0.089	N.D.	0.537	0.191	0.203	**Seminal root 1-4 cm**
					x	0.34	0.007	0.015	0.022	0.335	0.181	N.D.	0.274	0.052	0.226	**Crown root 0.5-4 cm**
						x	0.649	0.21	0.215	0.49	0.465	N.D.	0.487	0.296	0.471	**Stele**
							x	5E-04	9E-04	0.112	0.072	N.D.	0.093	0.012	0.088	**Cortex**
								x	0.038	0.082	0.103	N.D.	0.032	0.272	0.182	**Elongation zone**
									x	0.01	0.225	N.D.	0.1	0.389	0.646	**Meristem**
										x	0.083	N.D.	0.249	0.009	0.046	**Lateral root**
											x	N.D.	0.038	0.231	0.166	**Coleoptile (d)**
												x	N.D.	N.D.	N.D.	**Coleoptile (l)**
													x	0.1	0.043	**Mesocotyl**
														x	0.737	**Coleopilar node**
															x	**Leaf**

ZmIAA13

Primary root 1-2 cm	Primary root 2-4 cm	Primary root 4-8 cm	Primary root 8-16 cm	Seminal root 1-4 cm	Crown root 0.5-4 cm	Stele	Cortex	Elongation zone	Meristem	Lateral root	Coleoptile (d)	Coleoptile (l)	Mesocotyl	Coleoptilar node	Leaf	
x	0.301	0.914	0.148	0.527	0.18	0.552	0.281	0.255	0.899	0.252	N.D.	N.D.	N.D.	N.D.	N.D.	**Primary root 1-2 cm**
	x	0.41	0.005	0.021	8E-04	0.249	0.06	0.017	0.426	0.069	N.D.	N.D.	N.D.	N.D.	N.D.	**Primary root 2-4 cm**
		x	0.249	0.467	0.179	0.624	0.348	0.256	0.698	0.483	N.D.	N.D.	N.D.	N.D.	N.D.	**Primary root 4-8 cm**
			x	0.556	0.063	0.035	0.003	0.008	0.698	0.027	N.D.	N.D.	N.D.	N.D.	N.D.	**Primary root 8-16 cm**
				x	0.05	0.048	0.015	0.009	0.448	0.013	N.D.	N.D.	N.D.	N.D.	N.D.	**Seminal root 1-4 cm**
					x	0.015	0.003	5E-04	0.171	0.042	N.D.	N.D.	N.D.	N.D.	N.D.	**Crown root 0.5-4 cm**
						x	0.022	0.018	0.706	0.201	N.D.	N.D.	N.D.	N.D.	N.D.	**Stele**
							x	0.136	0.257	0.263	N.D.	N.D.	N.D.	N.D.	N.D.	**Cortex**
								x	0.172	0.409	N.D.	N.D.	N.D.	N.D.	N.D.	**Elongation zone**
									x	0.29	N.D.	N.D.	N.D.	N.D.	N.D.	**Meristem**
										x	N.D.	N.D.	N.D.	N.D.	N.D.	**Lateral root**
											x	N.D.	N.D.	N.D.	N.D.	**Coleoptile (d)**
												x	N.D.	N.D.	N.D.	**Coleoptile (l)**
													x	N.D.	N.D.	**Mesocotyl**
														x	N.D.	**Coleopilar node**
															x	**Leaf**

	$p \leq 0.05$
	$p \leq 0.01$
	$p \leq 0.001$
N.D.	not detectable

ZmIAA14

Primary root 1-2 cm	Primary root 2-4 cm	Primary root 4-8 cm	Primary root 8-16 cm	Seminal root 1-4 cm	Crown root 0.5-4 cm	Stele	Cortex	Elongation zone	Meristem	Lateral root	Coleoptile (d)	Coleoptile (l)	Mesocotyl	Coleoptilar node	Leaf	
x	0.43	0.306	0.194	0.055	0.003	0.257	0.029	0.215	0.034	0.786	0.009	0.007	0.007	0.006	0.008	**Primary root 1-2 cm**
	x	0.706	0.081	0.242	6E-04	0.298	0.021	0.34	0.012	0.508	0.004	0.004	0.006	0.005	0.005	**Primary root 2-4 cm**
		x	0.017	0.279	0.001	0.304	0.023	0.24	0.008	0.354	7E-04	6E-04	0.001	0.001	0.001	**Primary root 4-8 cm**
			x	0.058	3E-04	0.194	0.019	0.688	0.008	0.965	3E-04	6E-05	1E-04	9E-05	3E-04	**Primary root 8-16 cm**
				x	0.148	0.631	0.052	0.051	0.037	0.521	0.019	0.015	0.018	0.017	0.019	**Seminal root 1-4 cm**
					x	0.947	0.102	0.006	5E-05	0.124	4E-05	9E-05	8E-05	6E-05	5E-05	**Crown root 0.5-4 cm**
						x	0.32	0.219	0.145	0.24	0.094	0.098	0.097	0.094	0.094	**Stele**
							x	0.033	0.016	0.305	0.012	0.011	0.013	0.012	0.012	**Cortex**
								x	0.154	0.512	0.029	0.027	0.024	0.022	0.026	**Elongation zone**
									x	0.654	0.001	0.003	0.002	9E-04	0.002	**Meristem**
										x	0.286	0.285	0.254	0.259	0.261	**Lateral root**
											x	0.636	0.343	0.62	0.606	**Coleoptile (d)**
												x	0.303	0.82	0.565	**Coleoptile (l)**
													x	0.034	0.277	**Mesocotyl**
														x	0.24	**Coleopilar node**
															x	**Leaf**

ZmIAA15

Primary root 1-2 cm	Primary root 2-4 cm	Primary root 4-8 cm	Primary root 8-16 cm	Seminal root 1-4 cm	Crown root 0.5-4 cm	Stele	Cortex	Elongation zone	Meristem	Lateral root	Coleoptile (d)	Coleoptile (l)	Mesocotyl	Coleoptilar node	Leaf	
x	0.366	0.486	0.042	0.169	0.027	0.738	0.199	0.075	0.119	0.216	0.007	0.019	0.063	0.069	0.023	**Primary root 1-2 cm**
	x	0.831	0.326	0.148	0.006	0.568	0.068	0.139	0.187	0.367	0.128	0.092	0.008	0.008	0.015	**Primary root 2-4 cm**
		x	0.08	0.096	0.009	0.594	0.124	0.242	0.204	0.231	0.053	0.016	0.151	0.108	0.014	**Primary root 4-8 cm**
			x	0.065	0.014	0.394	0.102	0.512	0.204	0.059	0.253	0.095	0.704	0.778	0.121	**Primary root 8-16 cm**
				x	0.836	0.627	0.852	0.104	0.122	0.78	0.065	0.059	0.099	0.09	0.057	**Seminal root 1-4 cm**
					x	0.475	0.446	0.006	0.021	0.707	0.009	0.007	0.006	0.004	0.004	**Crown root 0.5-4 cm**
						x	0.657	0.455	0.254	0.623	0.35	0.303	0.33	0.343	0.215	**Stele**
							x	0.072	0.088	0.818	0.074	0.065	0.042	0.043	0.038	**Cortex**
								x	0.328	0.217	0.126	0.07	0.096	0.062	0.008	**Elongation zone**
									x	0.011	0.983	0.742	0.96	0.883	0.166	**Meristem**
										x	0.096	0.086	0.226	0.227	0.119	**Lateral root**
											x	0.337	0.982	0.856	0.15	**Coleoptile (d)**
												x	0.774	0.57	0.145	**Coleoptile (l)**
													x	0.558	0.129	**Mesocotyl**
														x	0.032	**Coleopilar node**
															x	**Leaf**

ZmIAA16

Primary root 1-2 cm	Primary root 2-4 cm	Primary root 4-8 cm	Primary root 8-16 cm	Seminal root 1-4 cm	Crown root 0.5-4 cm	Stele	Cortex	Elongation zone	Meristem	Lateral root	Coleoptile (d)	Coleoptile (l)	Mesocotyl	Coleoptilar node	Leaf	
x	0.846	0.905	0.147	0.045	1E-04	0.284	0.007	0.041	0.018	0.208	0.045	0.02	0.014	0.102	0.031	**Primary root 1-2 cm**
	x	0.916	0.242	0.071	4E-04	0.318	0.004	0.111	0.033	0.369	0.072	0.038	0.027	0.209	0.072	**Primary root 2-4 cm**
		x	0.001	0.086	7E-04	0.254	0.003	0.021	8E-04	0.211	0.002	5E-04	3E-04	6E-04	4E-04	**Primary root 4-8 cm**
			x	0.051	6E-04	0.192	0.001	0.598	8E-04	0.188	0.005	8E-04	4E-04	0.611	0.005	**Primary root 8-16 cm**
				x	0.022	0.743	0.25	0.041	0.029	0.391	0.033	0.028	0.024	0.045	0.034	**Seminal root 1-4 cm**
					x	0.621	0.06	3E-04	4E-04	0.604	4E-04	4E-04	3E-04	4E-04	3E-04	**Crown root 0.5-4 cm**
						x	0.954	0.199	0.14	0.471	0.159	0.139	0.127	0.195	0.164	**Stele**
							x	0.003	9E-04	0.927	6E-04	7E-04	6E-04	0.001	0.001	**Cortex**
								x	0.012	0.205	0.181	0.029	0.014	0.634	0.103	**Elongation zone**
									x	0.177	0.072	0.982	0.034	0.005	0.007	**Meristem**
										x	0.186	0.173	0.165	0.189	0.182	**Lateral root**
											x	0.013	0.003	0.009	0.568	**Coleoptile (d)**
												x	6E-06	0.002	0.003	**Coleoptile (l)**
													x	7E-04	8E-04	**Mesocotyl**
														x	0.003	**Coleopilar node**
															x	**Leaf**

	$p \leq 0.05$
	$p \leq 0.01$
	$p \leq 0.001$
N.D.	not detectable

ZmIAA17

Primary root 1-2 cm	Primary root 2-4 cm	Primary root 4-8 cm	Primary root 8-16 cm	Seminal root 1-4 cm	Crown root 0.5-4 cm	Stele	Cortex	Elongation zone	Meristem	Lateral root	Coleoptile (d)	Coleoptile (l)	Mesocotyl	Coleoptilar node	Leaf	
x	0.031	0.282	0.001	0.488	0.306	0.218	0.265	0.038	6E-04	0.066	6E-04	9E-04	0.093	0.002	0.074	**Primary root 1-2 cm**
	x	0.239	0.114	0.241	0.071	0.158	0.16	0.35	0.008	0.121	0.014	0.014	0.062	0.037	0.071	**Primary root 2-4 cm**
		x	0.081	0.337	0.063	0.185	0.16	0.213	0.025	0.332	0.03	0.043	0.115	0.077	0.982	**Primary root 4-8 cm**
			x	0.136	0.067	0.151	0.146	0.863	0.025	0.121	0.009	0.106	0.033	0.608	0.037	**Primary root 8-16 cm**
				x	0.901	0.404	0.47	0.088	0.103	0.203	0.106	0.123	0.647	0.132	0.349	**Seminal root 1-4 cm**
					x	0.294	0.248	0.084	0.041	0.311	0.045	0.05	0.7	0.06	0.148	**Crown root 0.5-4 cm**
						x	0.64	0.166	0.13	0.067	0.134	0.137	0.372	0.144	0.172	**Stele**
							x	0.159	0.121	0.423	0.124	0.131	0.637	0.142	0.203	**Cortex**
								x	0.225	0.308	0.27	0.451	0.061	0.687	0.156	**Elongation zone**
									x	0.432	0.038	0.002	0.025	0.008	0.005	**Meristem**
										x	0.647	0.143	0.265	0.021	0.053	**Lateral root**
											x	0.028	0.026	0.02	0.008	**Coleoptile (d)**
												x	0.029	0.046	0.007	**Coleoptile (l)**
													x	0.034	0.064	**Mesocotyl**
														x	0.012	**Coleopilar node**
															x	**Leaf**

ZmIAA18

Primary root 1-2 cm	Primary root 2-4 cm	Primary root 4-8 cm	Primary root 8-16 cm	Seminal root 1-4 cm	Crown root 0.5-4 cm	Stele	Cortex	Elongation zone	Meristem	Lateral root	Coleoptile (d)	Coleoptile (l)	Mesocotyl	Coleoptilar node	Leaf	
x	0.248	0.075	0.362	0.977	0.049	0.266	0.045	0.002	0.007	0.042	0.1	0.082	0.022	0.321	0.059	**Primary root 1-2 cm**
	x	0.083	0.12	0.55	0.034	0.283	0.04	0.005	0.009	0.2	0.103	0.084	0.023	0.593	0.087	**Primary root 2-4 cm**
		x	0.024	0.224	0.967	0.296	0.126	0.003	0.004	0.011	0.129	0.133	0.021	0.775	0.138	**Primary root 4-8 cm**
			x	0.714	0.018	0.256	0.045	1E-05	0.004	0.136	0.104	0.089	0.017	0.195	0.027	**Primary root 8-16 cm**
				x	0.153	0.263	0.071	0.043	0.049	0.497	0.106	0.098	0.021	0.388	0.07	**Seminal root 1-4 cm**
					x	0.303	0.085	0.002	0.002	0.1	0.117	0.109	0.024	0.845	0.16	**Crown root 0.5-4 cm**
						x	0.437	0.219	0.222	0.425	0.937	0.632	0.828	0.264	0.317	**Stele**
							x	0.019	0.022	0.345	0.098	0.06	0.098	0.235	0.428	**Cortex**
								x	0.132	0.119	0.088	0.065	0.013	0.037	0.008	**Elongation zone**
									x	0.261	0.091	0.069	0.012	0.042	0.007	**Meristem**
										x	0.337	0.295	0.119	0.29	0.096	**Lateral root**
											x	0.125	0.837	0.16	0.171	**Coleoptile (d)**
												x	0.418	0.198	0.236	**Coleoptile (l)**
													x	0.011	0.016	**Mesocotyl**
														x	0.092	**Coleopilar node**
															x	**Leaf**

ZmIAA19

Primary root 1-2 cm	Primary root 2-4 cm	Primary root 4-8 cm	Primary root 8-16 cm	Seminal root 1-4 cm	Crown root 0.5-4 cm	Stele	Cortex	Elongation zone	Meristem	Lateral root	Coleoptile (d)	Coleoptile (l)	Mesocotyl	Coleoptilar node	Leaf	
x	0.309	0.006	0.061	0.083	0.185	0.36	0.012	0.008	0.007	0.613	0.006	0.006	0.006	0.006	0.006	**Primary root 1-2 cm**
	x	0.256	0.68	0.21	0.119	0.447	0.028	0.007	0.007	0.34	0.007	0.007	0.008	0.007	0.007	**Primary root 2-4 cm**
		x	0.275	0.206	0.975	0.57	0.031	0.002	0.002	0.187	0.002	0.002	0.002	0.002	0.002	**Primary root 4-8 cm**
			x	0.197	0.511	0.451	0.031	0.001	0.002	0.095	0.001	0.001	0.001	0.001	0.001	**Primary root 8-16 cm**
				x	0.348	0.981	0.296	0.049	0.049	0.228	0.047	0.047	0.048	0.047	0.047	**Seminal root 1-4 cm**
					x	0.591	0.041	0.019	0.02	0.388	0.02	0.02	0.021	0.02	0.02	**Crown root 0.5-4 cm**
						x	0.716	0.201	0.199	0.484	0.195	0.195	0.199	0.195	0.195	**Stele**
							x	0.009	0.009	0.295	0.009	0.009	0.009	0.009	0.009	**Cortex**
								x	0.284	0.246	0.044	0.05	0.884	0.05	0.049	**Elongation zone**
									x	0.233	0.026	0.031	0.627	0.03	0.031	**Meristem**
										x	0.204	0.205	0.213	0.204	0.203	**Lateral root**
											x	0.008	0.001	0.003	0.107	**Coleoptile (d)**
												x	0.001	0.502	0.17	**Coleoptile (l)**
													x	0.002	0.001	**Mesocotyl**
														x	0.102	**Coleopilar node**
															x	**Leaf**

	$p \leq 0.05$
	$p \leq 0.01$
	$p \leq 0.001$
N.D.	not detectable

ZmIAA20

Primary root 1-2 cm	Primary root 2-4 cm	Primary root 4-8 cm	Primary root 8-16 cm	Seminal root 1-4 cm	Crown root 0.5-4 cm	Stele	Cortex	Elongation zone	Meristem	Lateral root	Coleoptile (d)	Coleoptile (l)	Mesocotyl	Coleoptilar node	Leaf	
x	0.067	0.007	0.009	0.215	0.039	0.083	0.038	0.112	0.201	0.412	6E-04	0.002	0.009	0.003	5E-04	**Primary root 1-2 cm**
	x	0.07	0.004	0.292	0.023	0.215	0.05	0.032	0.036	0.259	0.003	0.002	0.009	0.003	0.001	**Primary root 2-4 cm**
		x	0.133	0.456	0.356	0.746	0.007	0.009	0.01	0.081	5E-04	0.004	0.009	0.003	0.002	**Primary root 4-8 cm**
			x	0.829	0.002	0.414	0.008	0.007	0.01	0.137	0.125	0.003	0.009	0.003	0.015	**Primary root 8-16 cm**
				x	0.385	0.55	0.21	0.204	0.207	0.032	0.692	0.017	0.008	0.002	0.263	**Seminal root 1-4 cm**
					x	0.476	0.034	0.027	0.029	0.266	0.008	0.002	0.009	0.003	0.003	**Crown root 0.5-4 cm**
						x	0.074	0.07	0.07	0.457	0.063	0.007	0.01	0.006	1E-03	**Stele**
							x	0.335	0.597	0.028	6E-04	0.002	0.009	0.003	4E-04	**Cortex**
								x	0.125	0.007	8E-04	0.002	0.009	0.003	5E-04	**Elongation zone**
									x	0.195	8E-04	0.002	0.009	0.003	4E-04	**Meristem**
										x	0.02	0.047	0.093	0.149	0.086	**Lateral root**
											x	0.008	0.01	0.004	0.026	**Coleoptile (d)**
												x	0.01	0.006	0.033	**Coleoptile (l)**
													x	0.011	0.01	**Mesocotyl**
														x	0.008	**Coleopilar node**
															x	**Leaf**

ZmIAA21

Primary root 1-2 cm	Primary root 2-4 cm	Primary root 4-8 cm	Primary root 8-16 cm	Seminal root 1-4 cm	Crown root 0.5-4 cm	Stele	Cortex	Elongation zone	Meristem	Lateral root	Coleoptile (d)	Coleoptile (l)	Mesocotyl	Coleoptilar node	Leaf	
x	0.02	0.005	0.025	0.046	0.014	0.209	0.028	0.024	0.059	0.507	0.027	0.001	0.11	0.412	0.108	**Primary root 1-2 cm**
	x	0.748	0.65	0.359	0.6	0.277	0.056	0.005	0.007	0.193	0.035	0.033	0.215	0.079	0.741	**Primary root 2-4 cm**
		x	0.64	0.193	0.936	0.26	0.082	3E-04	5E-04	0.045	0.005	0.011	0.219	0.043	0.034	**Primary root 4-8 cm**
			x	0.389	0.914	0.249	0.075	5E-04	5E-04	0.081	0.009	0.018	0.212	0.014	0.052	**Primary root 8-16 cm**
				x	0.322	0.252	0.06	0.02	0.029	0.014	0.077	0.058	0.221	0.211	0.063	**Seminal root 1-4 cm**
					x	0.277	0.036	0.006	0.008	0.253	0.03	0.015	0.276	0.125	0.472	**Crown root 0.5-4 cm**
						x	0.504	0.169	0.172	0.384	0.254	0.258	0.379	0.228	0.436	**Stele**
							x	0.017	0.018	0.268	0.048	0.04	0.675	0.101	0.503	**Cortex**
								x	0.057	0.018	0.27	0.735	0.068	0.734	0.039	**Elongation zone**
									x	0.124	0.661	0.715	0.071	0.936	0.031	**Meristem**
										x	0.232	0.368	0.067	0.901	0.042	**Lateral root**
											x	0.765	0.078	0.644	0.062	**Coleoptile (d)**
												x	0.087	0.632	0.092	**Coleoptile (l)**
													x	0.012	0.089	**Mesocotyl**
														x	0.075	**Coleopilar node**
															x	**Leaf**

ZmIAA23

Primary root 1-2 cm	Primary root 2-4 cm	Primary root 4-8 cm	Primary root 8-16 cm	Seminal root 1-4 cm	Crown root 0.5-4 cm	Stele	Cortex	Elongation zone	Meristem	Lateral root	Coleoptile (d)	Coleoptile (l)	Mesocotyl	Coleoptilar node	Leaf	
x	0.075	0.013	0.052	0.224	0.052	0.28	0.008	0.031	0.111	0.826	0.047	0.036	0.054	0.066	0.249	**Primary root 1-2 cm**
	x	0.399	0.221	0.338	0.203	0.46	0.031	0.029	0.034	0.216	0.025	0.025	0.026	0.033	0.032	**Primary root 2-4 cm**
		x	0.159	0.322	0.698	0.356	0.016	9E-04	0.003	0.277	0.003	0.002	0.003	0.001	0.01	**Primary root 4-8 cm**
			x	0.879	0.87	0.323	0.016	4E-04	0.003	0.285	0.001	0.001	0.001	8E-05	0.002	**Primary root 8-16 cm**
				x	0.838	0.332	0.02	0.038	0.069	0.728	0.054	0.052	0.053	0.048	0.119	**Seminal root 1-4 cm**
					x	0.368	0.007	0.033	0.057	0.293	0.033	0.03	0.035	0.047	0.073	**Crown root 0.5-4 cm**
						x	0.656	0.226	0.23	0.5	0.231	0.231	0.234	0.228	0.239	**Stele**
							x	0.009	0.01	0.029	0.009	0.009	0.009	0.009	0.011	**Cortex**
								x	0.138	0.276	0.352	0.351	0.168	0.105	0.09	**Elongation zone**
									x	0.572	0.309	0.308	0.515	0.224	0.104	**Meristem**
										x	0.236	0.222	0.223	0.419	0.886	**Lateral root**
											x	0.679	0.172	0.644	0.088	**Coleoptile (d)**
												x	0.165	0.583	0.104	**Coleoptile (l)**
													x	0.981	0.157	**Mesocotyl**
														x	0.121	**Coleopilar node**
															x	**Leaf**

	$p \leq 0.05$
	$p \leq 0.01$
	$p \leq 0.001$
N.D.	not detectable

ZmIAA25

Primary root 1-2 cm	Primary root 2-4 cm	Primary root 4-8 cm	Primary root 8-16 cm	Seminal root 1-4 cm	Crown root 0.5-4 cm	Stele	Cortex	Elongation zone	Meristem	Lateral root	Coleoptile (d)	Coleoptile (l)	Mesocotyl	Coleoptilar node	Leaf	
x	0.013	0.116	0.022	0.092	0.029	0.371	0.086	0.03	0.039	0.685	0.009	0.01	0.493	0.022	0.121	**Primary root 1-2 cm**
	x	0.007	9E-04	0.008	0.034	0.438	0.025	0.145	0.492	0.559	0.009	0.615	0.131	0.154	0.383	**Primary root 2-4 cm**
		x	0.543	0.314	0.154	0.064	0.183	0.004	9E-04	0.986	0.006	0.004	0.977	5E-04	0.005	**Primary root 4-8 cm**
			x	0.448	0.163	0.043	0.169	0.002	9E-04	0.874	4E-04	2E-04	0.782	0.002	0.004	**Primary root 8-16 cm**
				x	0.69	0.002	0.457	0.002	0.022	0.814	0.004	0.012	0.558	0.007	0.014	**Seminal root 1-4 cm**
					x	0.153	0.636	0.048	0.025	0.517	0.03	0.024	0.405	0.036	0.057	**Crown root 0.5-4 cm**
						x	0.035	0.1	0.357	0.812	0.142	0.419	0.194	0.166	0.718	**Stele**
							x	0.017	0.034	0.308	0.016	0.019	0.094	0.017	0.017	**Cortex**
								x	0.963	0.571	0.505	0.294	0.079	0.818	0.049	**Elongation zone**
									x	0.473	0.777	0.559	0.081	0.852	0.25	**Meristem**
										x	0.509	0.529	0.603	0.528	0.663	**Lateral root**
											x	0.076	0.087	0.741	0.074	**Coleoptile (d)**
												x	0.102	0.173	0.215	**Coleoptile (l)**
													x	0.061	0.094	**Mesocotyl**
														x	0.018	**Coleopilar node**
															x	**Leaf**

ZmIAA27

Primary root 1-2 cm	Primary root 2-4 cm	Primary root 4-8 cm	Primary root 8-16 cm	Seminal root 1-4 cm	Crown root 0.5-4 cm	Stele	Cortex	Elongation zone	Meristem	Lateral root	Coleoptile (d)	Coleoptile (l)	Mesocotyl	Coleoptilar node	Leaf	
x	0.681	0.276	0.129	0.463	0.01	0.264	0.206	0.018	0.021	0.852	0.005	0.005	0.006	0.006	0.008	**Primary root 1-2 cm**
	x	0.099	0.374	0.365	0.042	0.183	0.169	0.116	0.082	0.276	0.028	0.026	0.026	0.026	0.03	**Primary root 2-4 cm**
		x	0.057	0.482	0.033	0.334	0.2	0.012	0.013	0.412	0.009	0.008	0.009	0.009	0.01	**Primary root 4-8 cm**
			x	0.051	0.012	0.175	0.171	0.075	0.013	0.028	8E-04	8E-04	6E-04	8E-04	8E-04	**Primary root 8-16 cm**
				x	0.043	0.307	0.217	0.034	0.031	0.614	0.007	0.007	0.007	0.007	0.009	**Seminal root 1-4 cm**
					x	0.554	0.293	0.002	0.003	0.252	0.002	0.002	0.003	0.002	0.003	**Crown root 0.5-4 cm**
						x	0.55	0.138	0.13	0.247	0.108	0.105	0.105	0.106	0.11	**Stele**
							x	0.142	0.141	0.427	0.127	0.126	0.127	0.127	0.13	**Cortex**
								x	0.251	0.205	0.017	0.013	0.019	0.015	0.029	**Elongation zone**
									x	0.132	0.014	0.01	0.014	0.011	0.021	**Meristem**
										x	0.03	0.028	0.015	0.026	0.019	**Lateral root**
											x	0.078	0.584	0.143	0.024	**Coleoptile (d)**
												x	0.28	0.034	0.004	**Coleoptile (l)**
													x	0.481	8E-04	**Mesocotyl**
														x	0.003	**Coleopilar node**
															x	**Leaf**

ZmIAA28

Primary root 1-2 cm	Primary root 2-4 cm	Primary root 4-8 cm	Primary root 8-16 cm	Seminal root 1-4 cm	Crown root 0.5-4 cm	Stele	Cortex	Elongation zone	Meristem	Lateral root	Coleoptile (d)	Coleoptile (l)	Mesocotyl	Coleoptilar node	Leaf	
x	0.287	0.076	0.16	0.047	5E-04	0.225	0.066	0.03	0.445	0.809	0.175	0.463	0.328	0.146	0.691	**Primary root 1-2 cm**
	x	0.488	0.933	0.643	0.109	0.251	0.067	0.031	0.108	0.165	0.036	0.09	0.83	0.132	0.369	**Primary root 2-4 cm**
		x	0.527	0.905	0.103	0.266	0.163	0.001	0.014	0.236	0.002	0.002	0.191	0.014	0.023	**Primary root 4-8 cm**
			x	0.483	0.06	0.235	0.114	0.049	0.014	0.314	0.069	0.167	0.947	0.092	0.308	**Primary root 8-16 cm**
				x	0.05	0.29	0.194	0.014	0.1	0.317	0.054	0.062	0.518	0.032	0.142	**Seminal root 1-4 cm**
					x	0.337	0.272	0.001	0.02	0.02	0.008	0.005	0.095	0.001	0.02	**Crown root 0.5-4 cm**
						x	0.497	0.187	0.187	0.369	0.187	0.21	0.227	0.209	0.215	**Stele**
							x	0.043	0.07	0.311	0.051	0.062	0.122	0.061	0.098	**Cortex**
								x	0.201	0.126	0.216	0.003	0.024	0.012	0.019	**Elongation zone**
									x	0.975	0.235	0.607	0.003	0.756	0.04	**Meristem**
										x	0.59	0.737	0.369	0.553	0.724	**Lateral root**
											x	0.056	0.006	0.223	0.017	**Coleoptile (d)**
												x	0.063	0.784	0.15	**Coleoptile (l)**
													x	0.106	0.149	**Mesocotyl**
														x	0.134	**Coleopilar node**
															x	**Leaf**

	$p \leq 0.05$
	$p \leq 0.01$
	$p \leq 0.001$
N.D.	not detectable

ZmIAA29

Primary root 1-2 cm	Primary root 2-4 cm	Primary root 4-8 cm	Primary root 8-16 cm	Seminal root 1-4 cm	Crown root 0.5-4 cm	Stele	Cortex	Elongation zone	Meristem	Lateral root	Coleoptile (d)	Coleoptile (l)	Mesocotyl	Coleoptilar node	Leaf	
x	0.29	0.114	0.829	0.154	0.099	0.439	0.022	0.005	0.066	0.646	0.007	0.005	0.125	0.024	0.023	**Primary root 1-2 cm**
	x	0.815	0.289	0.535	0.05	0.51	0.034	0.006	0.026	0.221	0.013	0.007	0.094	0.024	0.016	**Primary root 2-4 cm**
		x	0.375	0.288	0.254	0.486	0.034	0.002	0.011	0.122	0.002	0.002	0.011	0.003	0.005	**Primary root 4-8 cm**
			x	0.295	0.102	0.406	0.034	0.001	0.011	0.157	0.002	0.001	0.035	0.003	0.001	**Primary root 8-16 cm**
				x	0.937	0.711	0.036	0.039	0.1	0.084	0.041	0.041	0.098	0.062	0.065	**Seminal root 1-4 cm**
					x	0.708	0.041	0.012	0.031	0.263	0.016	0.011	0.062	0.027	0.021	**Crown root 0.5-4 cm**
						x	0.416	0.215	0.291	0.502	0.23	0.221	0.323	0.259	0.252	**Stele**
							x	0.016	0.024	0.341	0.017	0.016	0.025	0.021	0.02	**Cortex**
								x	0.001	0.012	0.075	0.051	0.003	0.005	0.003	**Elongation zone**
									x	0.321	0.01	0.002	0.222	0.035	0.007	**Meristem**
										x	0.05	0.006	0.59	0.181	0.139	**Lateral root**
											x	0.157	0.001	0.007	0.021	**Coleoptile (d)**
												x	0.005	0.01	0.007	**Coleoptile (l)**
													x	0.004	0.011	**Mesocotyl**
														x	0.232	**Coleopilar node**
															x	**Leaf**

ZmIAA30

Primary root 1-2 cm	Primary root 2-4 cm	Primary root 4-8 cm	Primary root 8-16 cm	Seminal root 1-4 cm	Crown root 0.5-4 cm	Stele	Cortex	Elongation zone	Meristem	Lateral root	Coleoptile (d)	Coleoptile (l)	Mesocotyl	Coleoptilar node	Leaf	
x	0.099	0.656	0.07	0.04	0.001	0.086	0.732	0.07	0.087	0.169	N.D.	N.D.	N.D.	N.D.	N.D.	**Primary root 1-2 cm**
	x	0.31	0.421	0.028	4E-04	0.592	0.29	3E-04	0.023	0.379	N.D.	N.D.	N.D.	N.D.	N.D.	**Primary root 2-4 cm**
		x	0.313	0.254	0.01	0.418	0.554	0.208	0.231	0.451	N.D.	N.D.	N.D.	N.D.	N.D.	**Primary root 4-8 cm**
			x	0.02	3E-04	0.207	0.289	0.143	0.231	0.326	N.D.	N.D.	N.D.	N.D.	N.D.	**Primary root 8-16 cm**
				x	8E-04	0.028	0.274	0.022	0.026	0.108	N.D.	N.D.	N.D.	N.D.	N.D.	**Seminal root 1-4 cm**
					x	6E-04	0.011	4E-04	5E-04	0.022	N.D.	N.D.	N.D.	N.D.	N.D.	**Crown root 0.5-4 cm**
						x	0.381	0.134	0.221	0.722	N.D.	N.D.	N.D.	N.D.	N.D.	**Stele**
							x	0.203	0.226	0.529	N.D.	N.D.	N.D.	N.D.	N.D.	**Cortex**
								x	0.163	0.18	N.D.	N.D.	N.D.	N.D.	N.D.	**Elongation zone**
									x	0.134	N.D.	N.D.	N.D.	N.D.	N.D.	**Meristem**
										x	N.D.	N.D.	N.D.	N.D.	N.D.	**Lateral root**
											x	N.D.	N.D.	N.D.	N.D.	**Coleoptile (d)**
												x	N.D.	N.D.	N.D.	**Coleoptile (l)**
													x	N.D.	N.D.	**Mesocotyl**
														x	N.D.	**Coleopilar node**
															x	**Leaf**

ZmIAA32

Primary root 1-2 cm	Primary root 2-4 cm	Primary root 4-8 cm	Primary root 8-16 cm	Seminal root 1-4 cm	Crown root 0.5-4 cm	Stele	Cortex	Elongation zone	Meristem	Lateral root	Coleoptile (d)	Coleoptile (l)	Mesocotyl	Coleoptilar node	Leaf	
x	0.028	0.163	0.031	0.061	0.075	0.143	0.06	0.009	0.007	0.17	0.004	0.004	0.004	0.004	0.004	**Primary root 1-2 cm**
	x	0.759	0.506	0.599	0.438	0.722	0.077	0.005	0.019	0.074	0.001	0.001	0.002	0.001	0.001	**Primary root 2-4 cm**
		x	0.386	0.851	0.103	0.99	0.144	0.003	0.028	0.077	0.002	0.002	0.002	0.002	0.002	**Primary root 4-8 cm**
			x	0.231	0.836	0.289	0.069	0.003	0.028	0.005	0.002	0.002	0.002	0.002	0.002	**Primary root 8-16 cm**
				x	0.377	0.862	0.025	0.009	0.003	0.162	0.003	0.003	0.003	0.002	0.002	**Seminal root 1-4 cm**
					x	0.057	0.32	0.002	0.069	0.122	0.002	0.003	0.002	0.002	0.002	**Crown root 0.5-4 cm**
						x	0.142	0.002	0.026	0.13	0.002	0.003	0.002	0.002	0.002	**Stele**
							x	0.036	0.027	0.151	0.002	0.002	0.003	0.002	0.002	**Cortex**
								x	0.076	0.157	0.005	0.009	0.007	0.004	0.004	**Elongation zone**
									x	0.246	0.005	0.006	0.006	0.005	0.005	**Meristem**
										x	0.201	0.256	0.233	0.187	0.189	**Lateral root**
											x	0.237	0.255	0.005	0.008	**Coleoptile (d)**
												x	0.013	0.002	0.005	**Coleoptile (l)**
													x	0.095	0.226	**Mesocotyl**
														x	0.034	**Coleopilar node**
															x	**Leaf**

	$p \leq 0.05$
	$p \leq 0.01$
	$p \leq 0.001$
N.D.	not detectable

ZmIAA33

Primary root 1-2 cm	Primary root 2-4 cm	Primary root 4-8 cm	Primary root 8-16 cm	Seminal root 1-4 cm	Crown root 0.5-4 cm	Stele	Cortex	Elongation zone	Meristem	Lateral root	Coleoptile (d)	Coleoptile (l)	Mesocotyl	Coleoptilar node	Leaf	
x	0.066	0.006	0.002	0.143	0.005	0.139	0.14	0.326	0.305	0.181	0.137	0.127	0.003	0.934	0.142	**Primary root 1-2 cm**
	x	0.024	9E-04	0.188	6E-05	0.171	0.435	0.024	0.006	0.608	0.003	0.003	0.03	0.015	0.004	**Primary root 2-4 cm**
		x	0.008	0.346	0.264	0.311	0.124	0.037	0.009	0.354	0.007	0.006	0.557	0.009	0.007	**Primary root 4-8 cm**
			x	0.791	0.003	0.62	0.016	0.008	0.009	0.117	0.001	0.001	0.035	0.001	0.001	**Primary root 8-16 cm**
				x	0.271	0.862	0.289	0.032	0.134	0.149	0.129	0.129	0.386	0.146	0.13	**Seminal root 1-4 cm**
					x	0.239	0.672	0.005	5E-04	0.18	3E-04	3E-04	0.203	9E-04	3E-04	**Crown root 0.5-4 cm**
						x	0.263	0.194	0.123	0.425	0.121	0.121	0.301	0.134	0.121	**Stele**
							x	0.177	0.14	0.766	0.115	0.113	0.164	0.17	0.116	**Cortex**
								x	0.137	0.131	0.314	0.242	0.024	0.015	0.92	**Elongation zone**
									x	0.097	0.05	0.04	0.006	0.013	0.048	**Meristem**
										x	0.136	0.131	0.049	0.187	0.128	**Lateral root**
											x	0.092	0.005	0.001	0.288	**Coleoptile (d)**
												x	0.005	7E-04	0.024	**Coleoptile (l)**
													x	0.006	0.005	**Mesocotyl**
														x	7E-04	**Coleopilar node**
															x	**Leaf**

ZmIAA34

Primary root 1-2 cm	Primary root 2-4 cm	Primary root 4-8 cm	Primary root 8-16 cm	Seminal root 1-4 cm	Crown root 0.5-4 cm	Stele	Cortex	Elongation zone	Meristem	Lateral root	Coleoptile (d)	Coleoptile (l)	Mesocotyl	Coleoptilar node	Leaf	
x	0.985	0.868	0.577	0.233	0.148	0.646	0.016	0.008	0.043	0.028	0.007	0.008	0.007	0.007	0.007	**Primary root 1-2 cm**
	x	0.9	0.425	0.4	0.019	0.632	0.004	0.019	0.008	0.077	0.002	0.016	0.002	0.003	0.002	**Primary root 2-4 cm**
		x	0.23	0.23	0.073	0.62	7E-04	0.005	0.02	0.046	1E-04	0.002	1E-04	8E-05	9E-05	**Primary root 4-8 cm**
			x	0.175	0.038	0.573	0.002	0.033	0.02	0.034	6E-04	0.002	6E-04	8E-04	5E-04	**Primary root 8-16 cm**
				x	0.573	0.835	0.031	0.042	0.081	0.013	0.016	0.074	0.016	0.016	0.016	**Seminal root 1-4 cm**
					x	0.959	0.005	0.012	0.011	0.153	0.004	0.02	0.004	0.004	0.004	**Crown root 0.5-4 cm**
						x	0.345	0.395	0.407	0.503	0.278	0.374	0.279	0.292	0.28	**Stele**
							x	0.157	0.093	0.084	4E-04	0.006	2E-04	0.002	9E-04	**Cortex**
								x	0.426	0.126	0.014	0.009	0.014	0.018	0.017	**Elongation zone**
									x	0.089	0.017	0.065	0.016	0.025	0.019	**Meristem**
										x	0.017	0.017	0.025	0.002	0.075	**Lateral root**
											x	0.003	0.303	0.01	0.032	**Coleoptile (d)**
												x	0.076	0.028	0.04	**Coleoptile (l)**
													x	0.013	0.239	**Mesocotyl**
														x	0.027	**Coleopilar node**
															x	**Leaf**

Supplemental Figure 4 Summary of pairwise Student´s t-tests of *Aux/IAA* gene expression comparisons in root and shoot tissues. Pairwise comparison of differential gene expression patterns between the various roots and soot tissues by a two-sided Student´s t-test. Different significance levels are highlighted in color. Red: $p \leq 0.05$; yellow: $p \leq 0.01$; green: $p \leq 0.001$. N.D. expression was not detected in one of these tissues.

Supplemental Figure 5

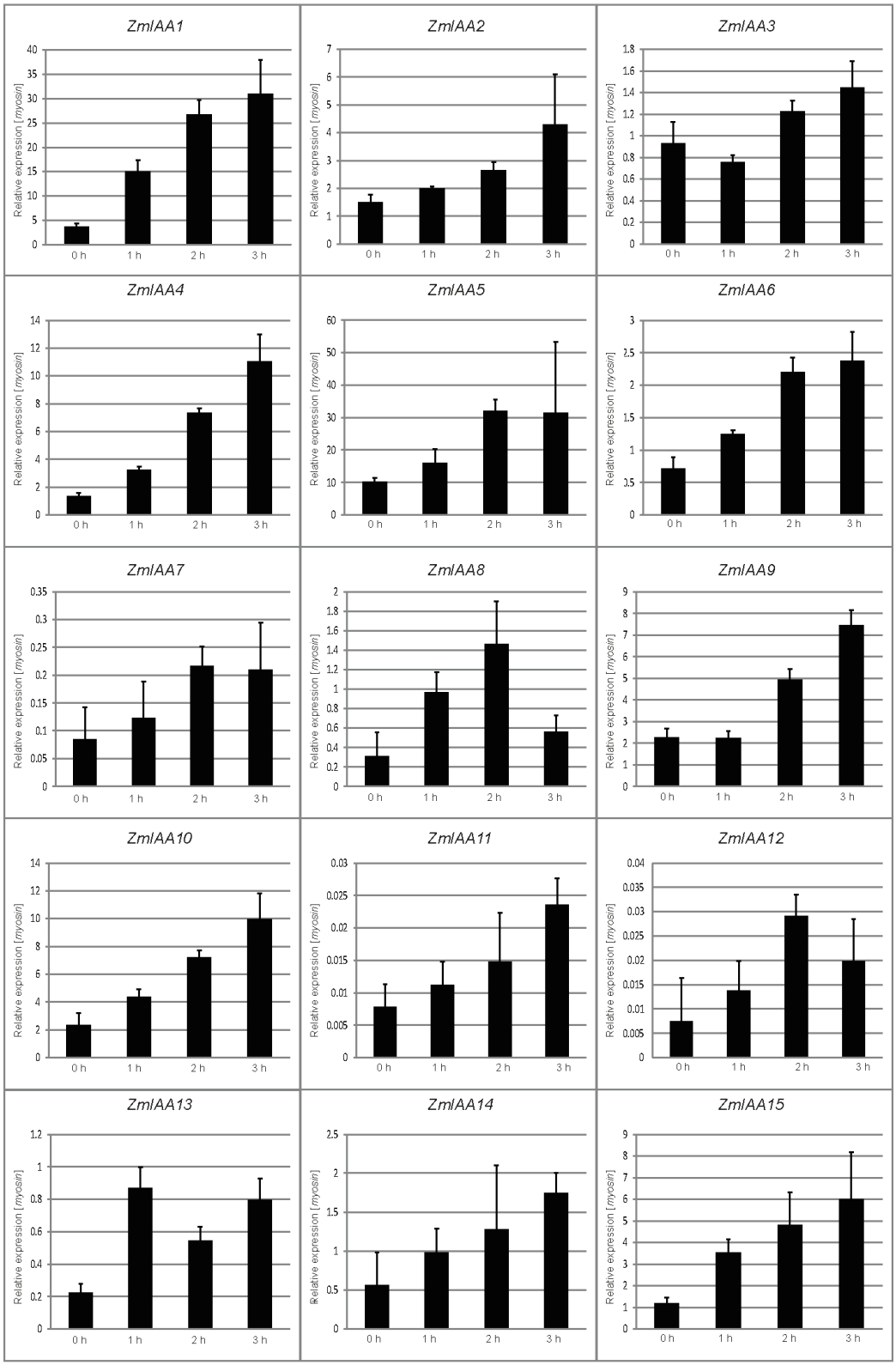

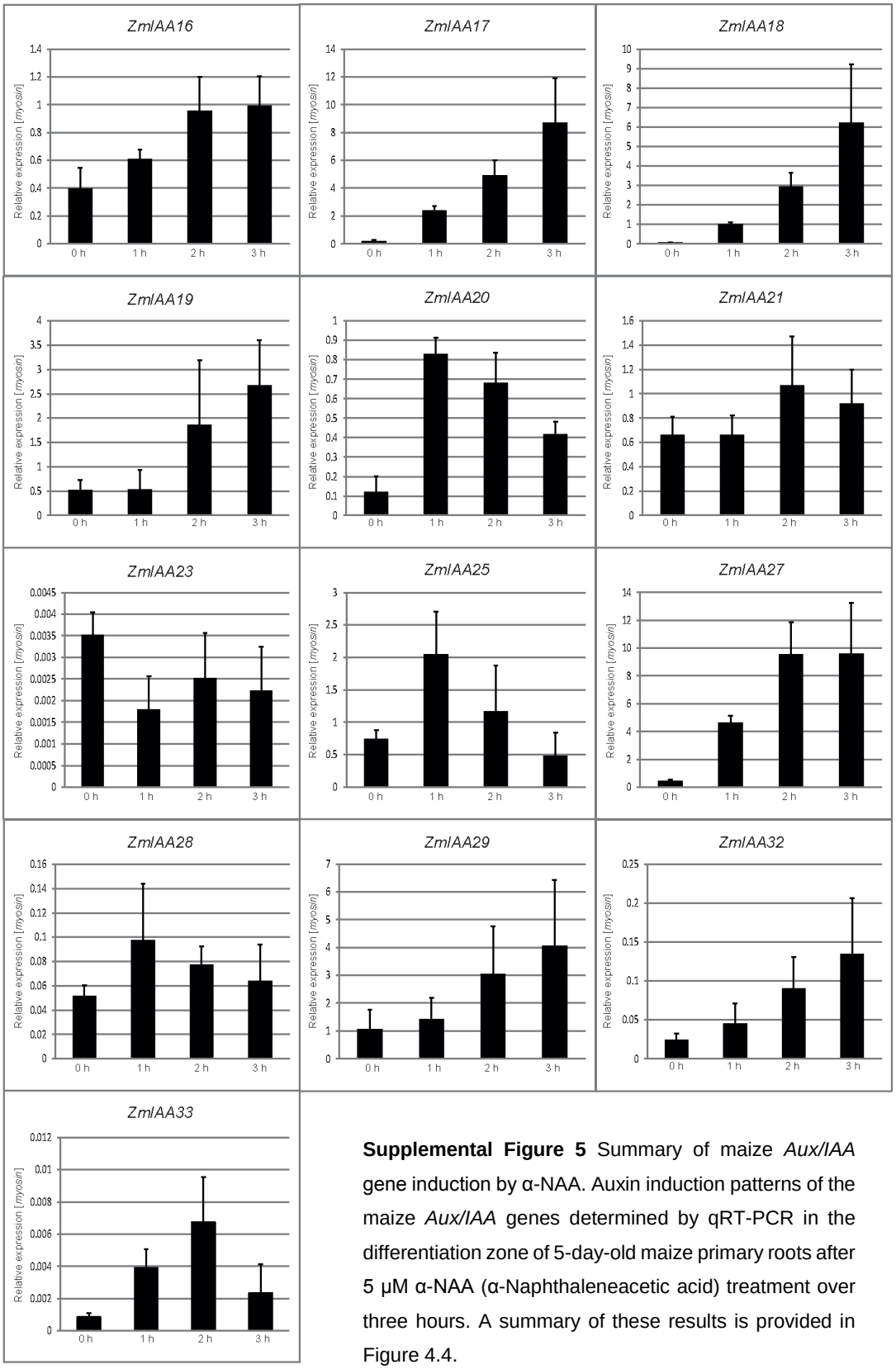

Supplemental Figure 5 Summary of maize *Aux/IAA* gene induction by α-NAA. Auxin induction patterns of the maize *Aux/IAA* genes determined by qRT-PCR in the differentiation zone of 5-day-old maize primary roots after 5 µM α-NAA (α-Naphthaleneacetic acid) treatment over three hours. A summary of these results is provided in Figure 4.4.

Supplemental Figure 6

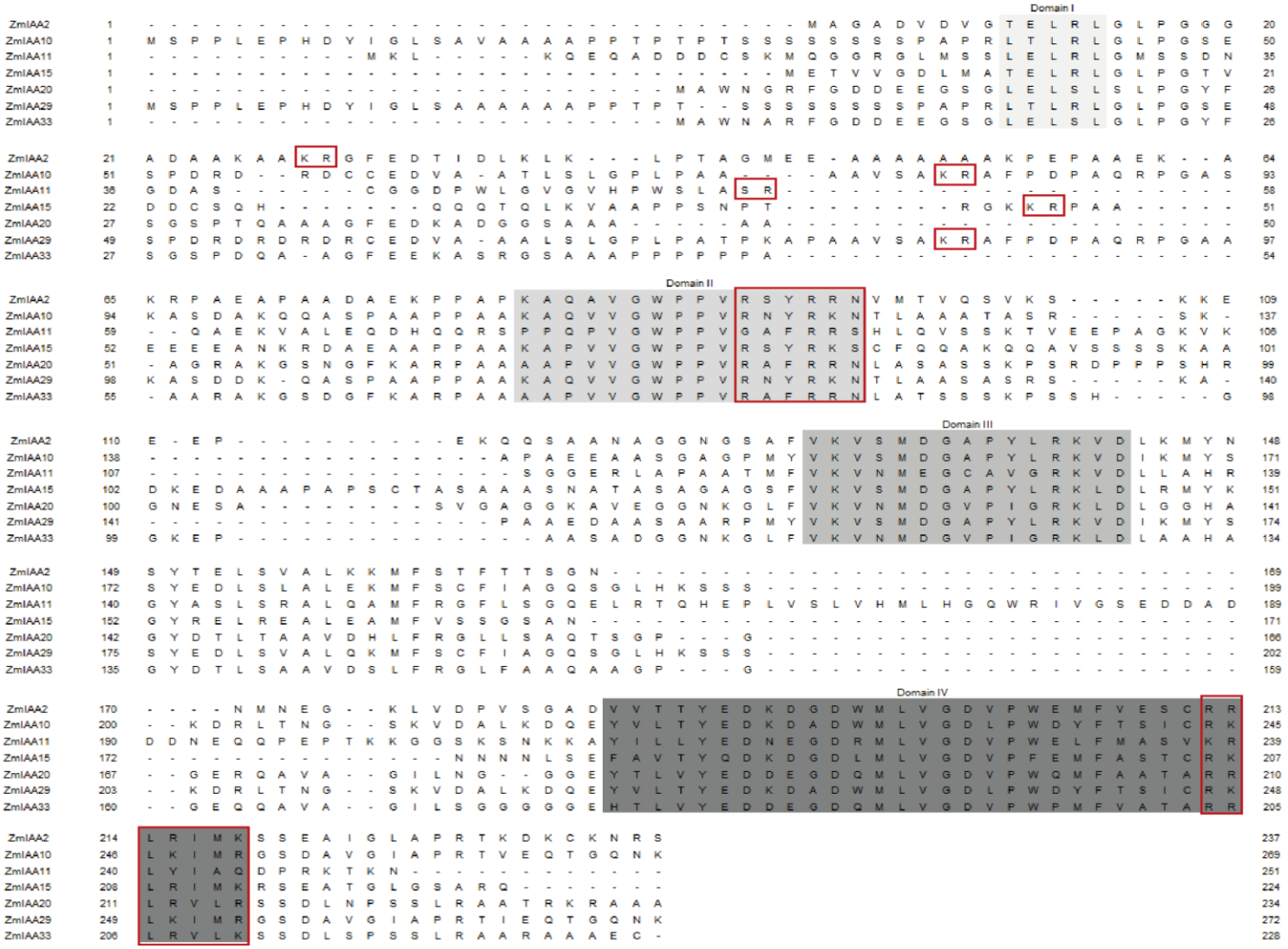

Supplemental Figure 6 Alignment of the sequences of Aux/IAA proteins analyzed in this study, including RUM1 (ZmIAA10) and RUL1 (ZmIAA29). The protein sequences were compared by multiple alignments with ClustalOmega. The four conserved domains are highlighted by grey. The bipartite nuclear localization signal is boxed in red.

Supplemental Figure 7

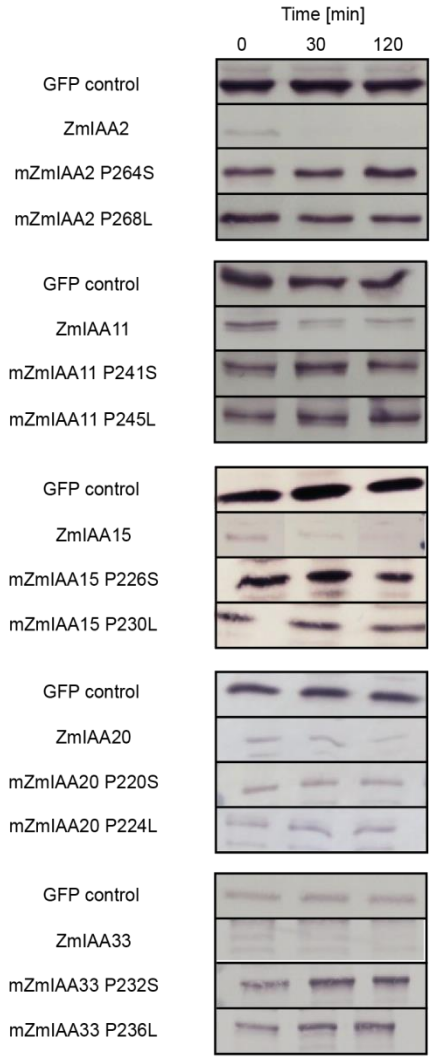

Supplemental Figure 7 Confirmation of Aux/IAA degradation by Western Blot experiments. Western Blot analysis of Aux/IAA-GFP constructs after α-NAA and cycloheximide treatment using an anti-HA antibody. Protein abundance was quantified at three different time points (0, 30 and 120 min). For ZmIAA15 the order of the three lanes was rearranged for the figure because of an error during gel loading.

Supplemental Figure 8

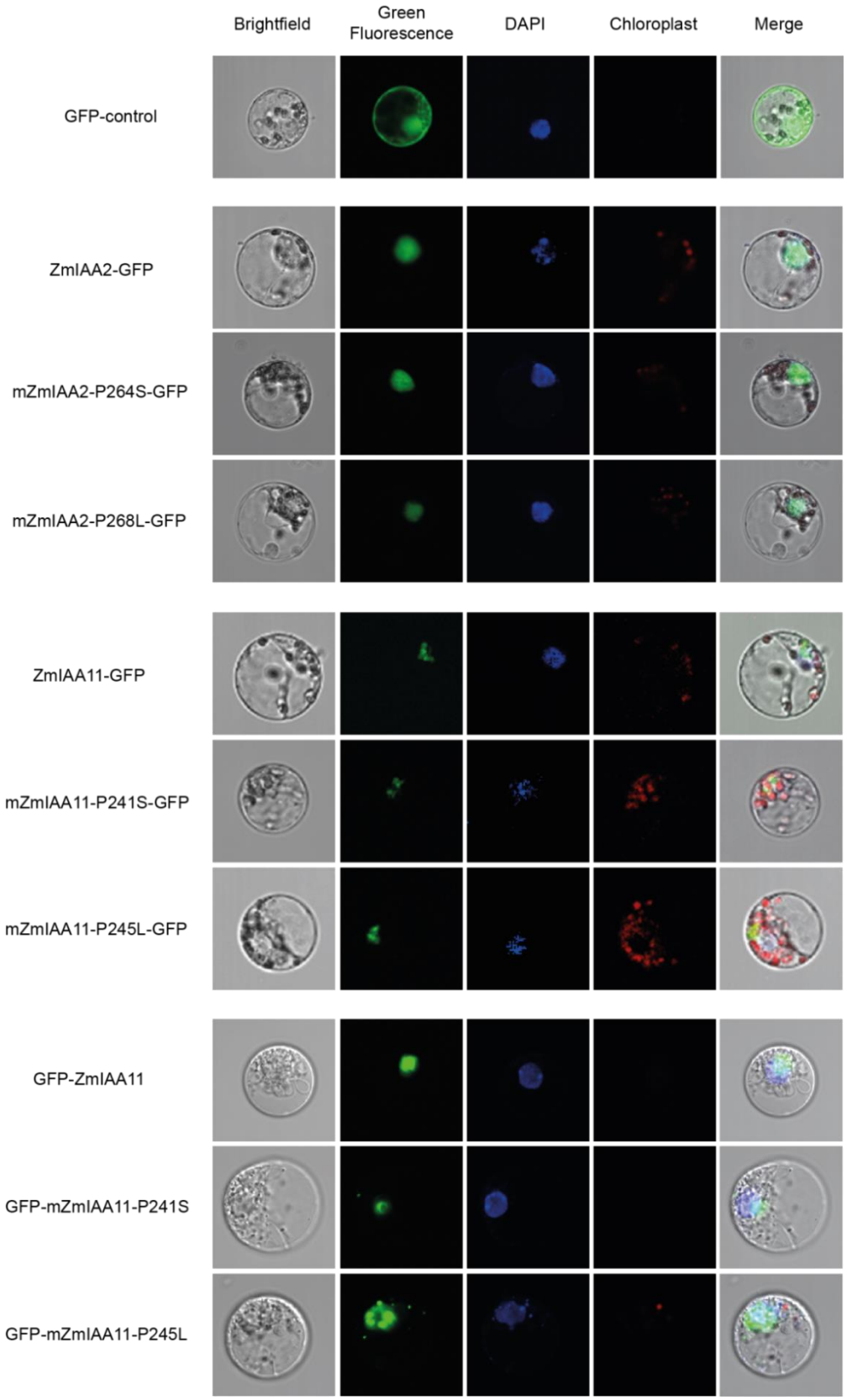

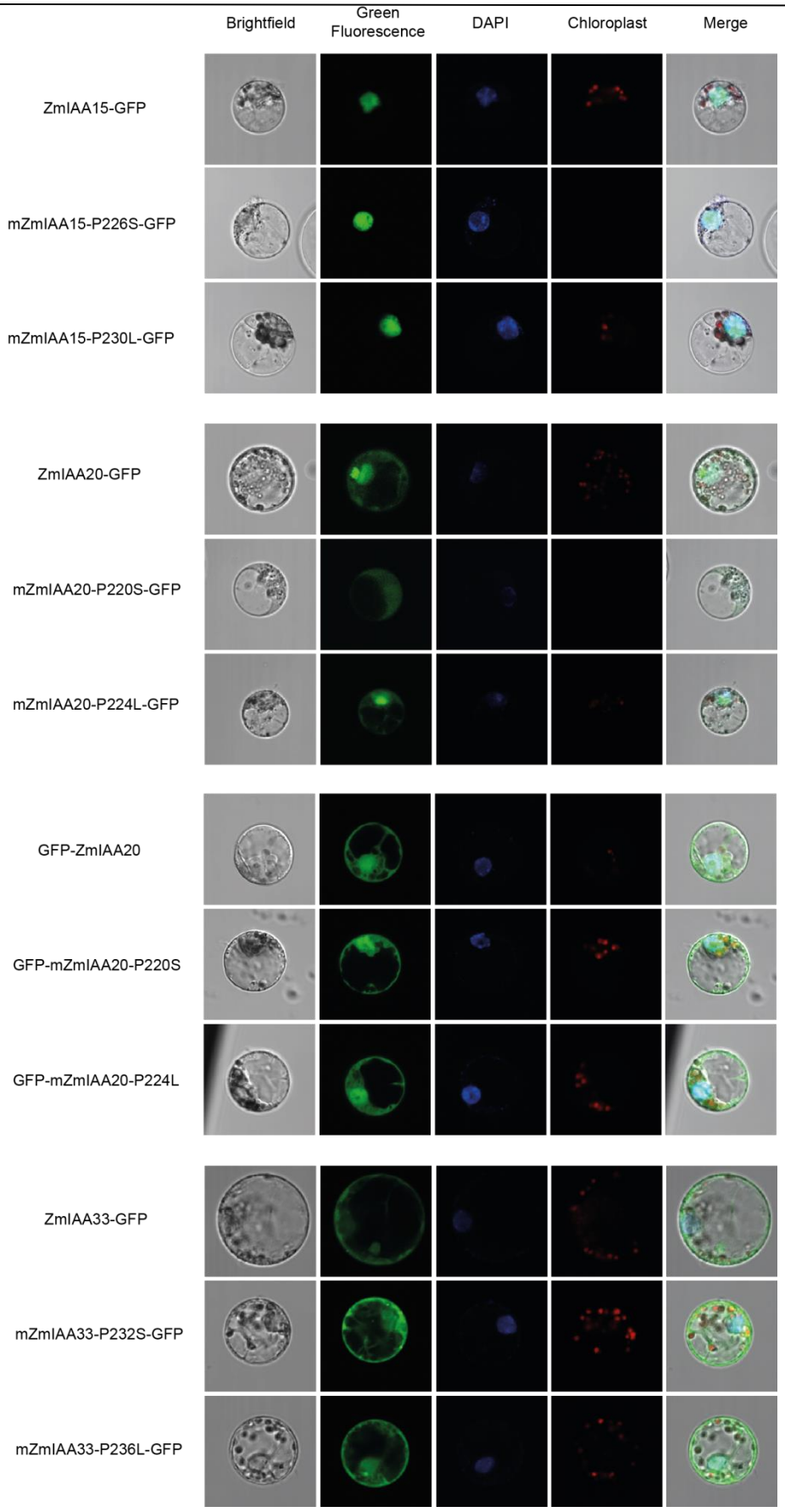
Brightfield
Green Fluorescence
DAPI
Chloroplast
Merge
ZmIAA15-GFP
mZmIAA15-P226S-GFP
mZmIAA15-P230L-GFP
ZmIAA20-GFP
mZmIAA20-P220S-GFP
mZmIAA20-P224L-GFP
GFP-ZmIAA20
GFP-mZmIAA20-P220S
GFP-mZmIAA20-P224L
ZmIAA33-GFP
mZmIAA33-P232S-GFP
mZmIAA33-P236L-GFP

Supplemental Figure 8. Summary of the subcellular localization of maize Aux/IAA wild-type proteins and two mutated protein forms of each protein in maize protoplasts. As a control, constitutively expressed free GFP, was localized in the cytosol and nucleus. ZmIAA2, ZmIAA11 and ZmIAA15 were exclusively located in the nucleus. The specific point-mutations in the degron-sequence did not affect the localization. For ZmIAA20 and ZmIAA33, wild-type and mutated proteins were localized in both, the cytosol and the nucleus. To investigate if the compartmentalization of the GFP signal is a result of C-terminal GFP fusion, N-terminal GFP fusion constructs of ZmIAA11 and ZmIAA20 with their mutated forms were also tested. Wild-type and mutated N-terminal GFP fusion constructs of ZmIAA11 and ZmIAA20 were also compartmentalized in the nucleus. Green: GFP fluorescence, red: auto fluorescence of chloroplast, blue: DAPI counterstaining.

Supplemental Figure 9

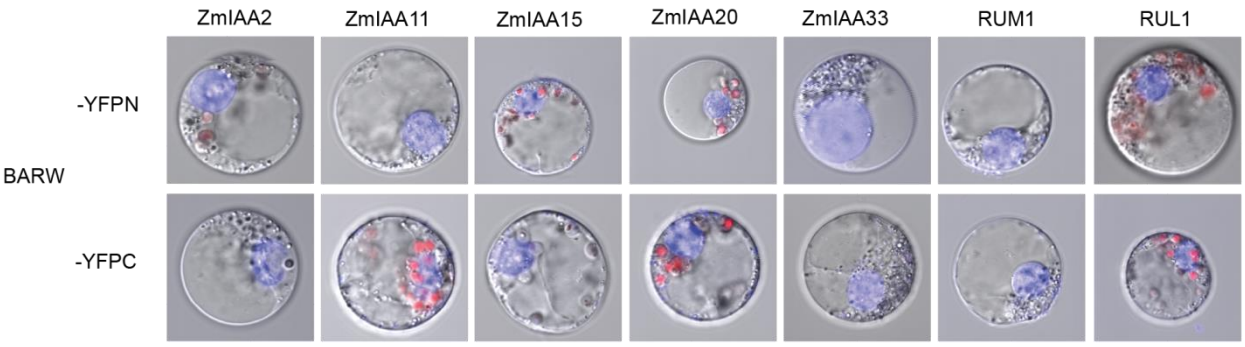

Supplemental Figure 9 Negative controls for protein-protein interaction studies in maize protoplasts (see Figure 4.8). Split-YFP experiments were conducted in maize protoplasts to demonstrate that Aux/IAA proteins do not interact with the control protein BARW. Red: auto fluorescence of chloroplast, blue: DAPI counterstaining

Supplemental Figure 10

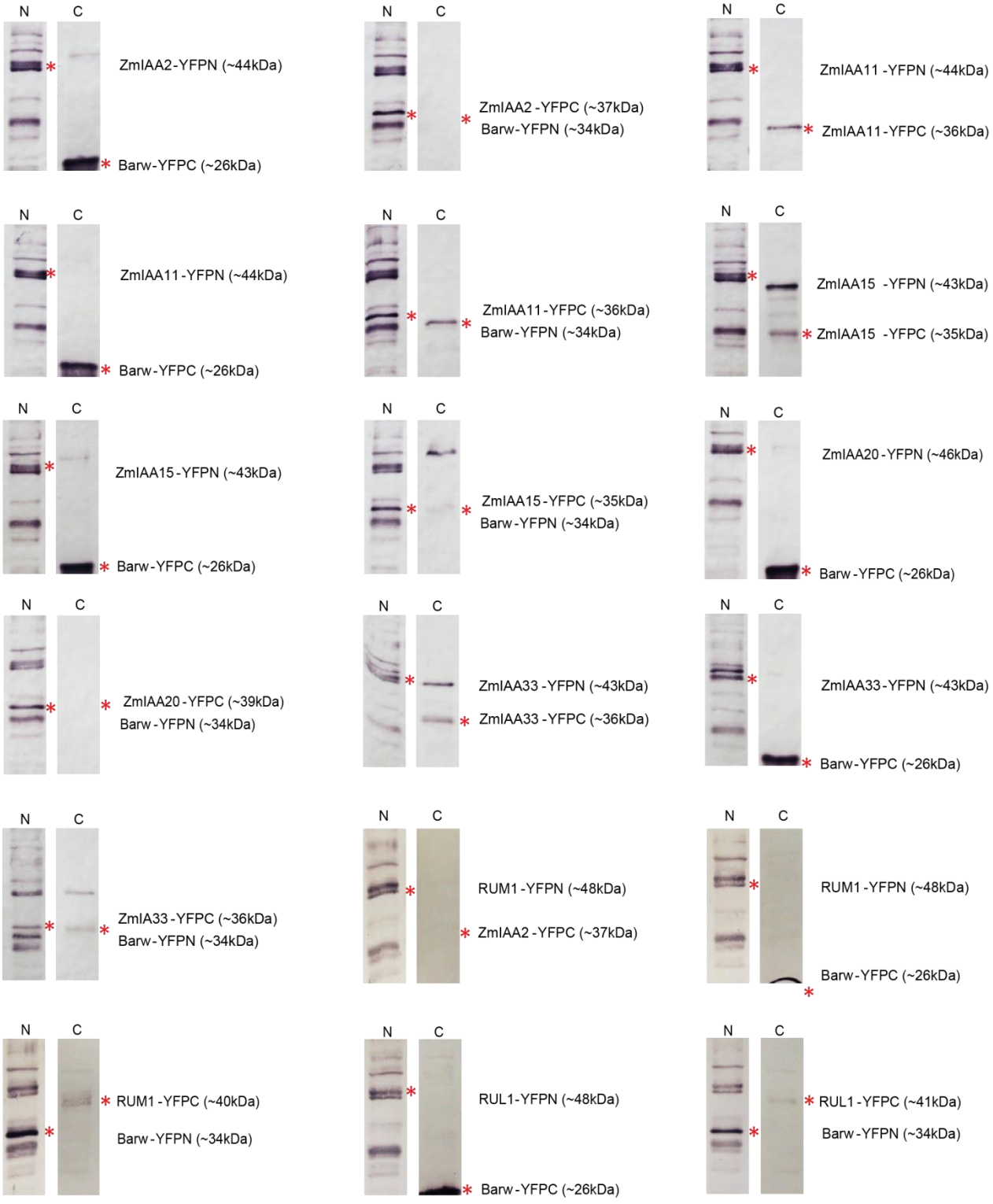

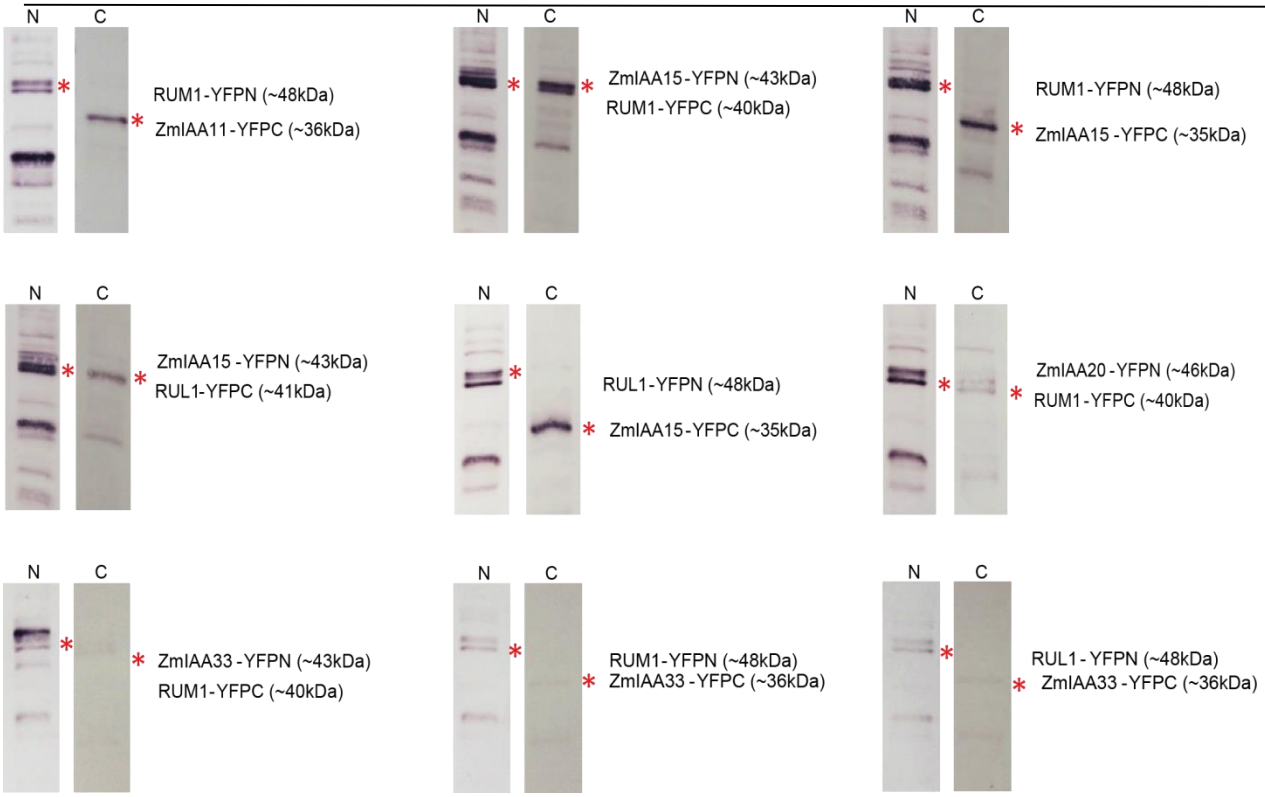

Supplemental Figure 10 Confirmation of fusion protein expression in protein-protein interactions studies by Western Blot experiments. The positions of the expressed proteins are indicated with red stars to the right of the corresponding lane. Anti-Myc antibodies were used for the detection of YFPN-152 and anti-HA for the detection of YFPC.

7.2 Supplemental Table

Supplemental Table 1 Promoter analyses of 3 kb upstream of the ATG start codon of maize *Aux/IAA* genes

Gene	Canonical AuxRE		AuxRE core	
	TGTCTC	GACACA	TGTC	GACA
ZmIAA1	1	1	16	7
ZmIAA2	1		11	15
ZmIAA3	2		11	7
ZmIAA4	1	1	8	10
ZmIAA5			6	8
ZmIAA6	1	3	14	9
ZmIAA7	2		10	9
ZmIAA8			10	14
ZmIAA9			10	11
ZmIAA10	1	2	6	3
ZmIAA11	1		12	17
ZmIAA12	1	1	9	13
ZmIAA13	2	2	7	13
ZmIAA14		1	11	15
ZmIAA15	1	1	5	7
ZmIAA16	1	3	11	9
ZmIAA17	2	1	13	17
ZmIAA18			7	15
ZmIAA19	1	1	13	
ZmIAA20		2	6	11
ZmIAA21			18	16
ZmIAA22		1	11	5
ZmIAA23			7	7
ZmIAA24		1	7	10
ZmIAA25	1		15	7
ZmIAA26		1	11	11
ZmIAA27		6	9	9
ZmIAA28	1		12	8
ZmIAA29	1	2	7	14
ZmIAA30		1	19	19
ZmIAA31		1	9	9
ZmIAA32	1		12	14
ZmIAA33	1	1	10	9
ZmIAA34		1	7	7

8 Acknowledgment

First of all I would like to thank my supervisor Prof. Dr. Frank Hochholdinger for giving me the opportunity to work on the exciting project of genetic dissection of the maize *Aux/IAA* gene family. Furthermore I appreciate that he always had a sympathetic ear for any scientific problem. Moreover, I am grateful for his valuable advice, thoughtful comments and scientific support in any way.

Many thanks to Kenneth W. Berendzen without his help I could not have handled that FACS machine. I would like to thank Caterina Brancato, my *Arabidopsis* protoplast specialist, for her support with the isolation and transformation of protoplasts as well as the nice entertainment in the long hours in Tübingen.

I am grateful to Prof. Dr. Andreas Meyer and Dr. Isabel Aller for their support in managing the CLSM. Likewise many thanks to Dr. Markus Schwarzländer for his help and discussion concerning protein assays. In particular, I would like to thank them for their critical discussion in the progress seminar. As well as many thanks to the whole working group Meyer which made the working environment a lot more comfortable with theirs breeziness.

Many thanks to my old and new colleagues Josefine, Changzheng, Yanxiang, Stefan, Nina, Huanhuan, Peng, Marine, Philipp, Eva, Caro and Anja who made the lab atmosphere so friendly and familiar. Also I would like to thank Christa, Helmut, Ute and Tanja who took care of the lab matters and the maize plants. Christine Jessen and Sonja Skamel I would like to thanks for theirs support with any kind of private and business issues.

Finally but most important I would like to say thanks to my family which always supported me in my aim of being a PhD as well as many thanks to my boyfriend Shalabh who always was my tower of strength and listened to all my little and big problems.